IEA
SOLAR R&D

INTERNATIONAL ENERGY AGENCY
solar heating and
cooling programme

Detailed Modeling of Evacuated Collector Systems

A Report of Task VI: The Performance of Solar Heating, Cooling, and Hot Water Systems Using Evacuated Collectors

December 1986

Detailed Modeling of Evacuated Collector Systems

A Report of Task VI: The Performance of Solar Heating, Cooling, and Hot Water Systems Using Evacuated Collectors

W. L. Gemmell
University of Waterloo
Canada

Professor M. Chandrashekar
University of Waterloo
Canada

Dr. K. H. Vanoli
IST Energietechnik GmbH
Federal Republic of Germany

Contents Finalized: August 1987

Table of Contents

List of Figures

List of Tables

Detailed Modelling Report for IEA Task VI

Introduction

This report describes several numerical models developed for the detailed simulation of solar energy systems by several member countries of the International Energy Agency (IEA) Task VI, namely Australia, Canada, the Netherlands, the U.S.A. and West Germany. The intended use for these models varies depending on topics of interest to the individual members and this is reflected in the capabilities of each model. Some of the models are restricted to simulating particular systems of subsystems whereas others are more general in their application. Between them, they cover a wide range of possible solar applications, namely; space heating/cooling, domestic hot water (DHW), industrial process heating (IPH) and district heating systems. The purposes of this report are documentation of these various models and validation of the models against measured results. A detailed characterization of each of the evacuated collectors and detailed models may be found in [1.1]. The scope of this effort was limited to each country's model development and comparisons with its measured results.

Regarding the need for detailed simulation models, we note that numerical performance predictions have become an accepted part of the design process for a wide range of applications since they provide a means of analyzing the behaviour of a specified system in response to selected inputs and allow the designer to test a variety of components, system configurations and control strategies without resorting to costly and time consuming physical experiments. Generally, the problem might be solved experimentally; but only a small fraction of the multitude of different solutions to be considered could be analyzed within reasonable time; moreover, the mutual comparison of the different experiments would be impossible because of both the stochastically changing meteorological conditions and the unreproducible load pattern of real-load systems.

Before simulation results can be confidently accepted it is necessary to validate the simulation program by establishing that the simulation results conform well with physical reality for the range of systems likely to be encountered. Therefore, in addition to describing the various models, this report will present the results of validation studies whereby the models were tested against measured results from monitored systems. Results of validation studies are given for four of the member countries. No material was available for the Netherlands.

Lastly, the validated models are applied to specific problems concerning the sensitivity of solar systems to a variety of factors which influence collector/system long-term performance. The factors investigated in these studies are listed briefly as follows:

Australia
- non-linear collector thermal behaviour
- incident angle modifier
- array capacitance and pipe losses
- collector pump control strategy

Canada
- system configuration
- collector flow rate
- storage tank mixing/stratification

Netherlands
- collector and load flow rates
- control strategy
- storage tank mixing/stratification

W. Germany
- system configuration
- storage size
- heat exchanger type/location/exchange rate
- radiation thresholds for collector pump control

All of the above with the exception of Australia also investigated the effect of collector type (flat plate - FPC or evacuated tubular - ETC) for a range of values of other factors. Unfortunately, no results were available from an American study since the DAYSIM model has only recently been validated.

2.0 Model Descriptions

The focus of research of Australia and the Netherlands led to the development of new subsystem models (collector and storage respectively) and for these cases the supporting simulation software will be described briefly or not at all. Similarly, the Canadian simulation program (WATSUN) has been in use for some time and is well documented [2.1]. Only the more recent developments in component modelling and simulation methods will be described in detail. The U.S.A. and West Germany however have developed complete new simulation programs which will be described more thoroughly.

2.1 Australia

A number of factors were studied which influence the performance of the Sydney University (S.U.) Evacuated Tubular Collector and may be important for the accurate modelling of the performance of other evacuated tubular collectors of similar design. To this end, a detailed collector model was created which considers the influence of factors such as non-linear thermal behaviour, incidence angle modifier effects, array capacitance, array pipe losses and collector pump controller effects on collector performance.

The characterization of S.U. Evacuated Tubular Collectors includes determination of properties of the selective surface [1.2], behaviour of S.U. evacuated tubes if assembled in different optical configurations [1.3,1.4] and thermal characterisation of a collector incorporating different types of heat extraction manifolds [1.5]. These factors, subject to the assumptions described below, have been incorporated into a detailed simulation of the array with a time step of one hour.

2.1.1 Model of single panel thermal behaviour

Based on results of Harding et al [1.5] the response of the Sydney University Evacuated Tubular Collector to normally incident beam radiation can be written as

$$\psi = \psi_{opt} - \kappa_1(T_m - T_a)/I - 12\kappa_2(T_s - T_a)/I - 12\varepsilon_s\kappa_4(T_s^4 - T_a^4)/I \qquad (2.1.1)$$

where the last three terms refer to conduction losses from the header fluid, conduction losses from the selective surface and radiation losses from the selective surface. The constant 12 refers to the twelve tubes per square meter of collector area.

The emissivity, ε_s, depends on the selective surface temperature T_s and is approximately given by $0.00012\ T_s + 0.015$. The selective surface temperature is known to be about 21°C above the mean fluid temperature when 575 W/m^2 is being collected. By presuming the thermal resistance between selective surface and fluid to be constant, T_s can be expressed as $T_m + 0.0365\,\psi I$.

Equation (2.1.1) can be converted in the standard form of a collector equation using the collector parameters $F'(\tau a)$ and $F'U_L$. The collector thermal behaviour then becomes

$$\psi = F'(\tau a) - F'U_L \left| \frac{T_c - T_a}{I} \right| - B(T_c - T_a) \qquad (2.1.2)$$

2.1.2 Model of single panel optical behaviour

The S.U. Evacuated Collector has a curved collecting surface and there is therefore no reason to expect incidence angle modifier effects to be minor or to be independent of the direction from which the beam is incident. Optical efficiency is thus potentially a function of four variables:

1. total collector plane radiation
2. diffuse fraction on the collector plane
3. incidence angle in the plane normal to the collector axis (which we will call the *east-west incidence angle)*
4. incidence angle in the plane along the collector axis, but normal to the collector plane (which we will call the *north-south incidence angle*)

An early ray-tracing study [1.4] showed that optical efficiencies for diffuse and normally incident beam radiation are very similar, diffuse being higher by 4%. The east-west incidence angle is significant (optical efficiency being increased) but the north-south incidence angle is not (optical efficiency being only slightly below the normal value).

The east-west incidence angle modifier will only apply to the beam portion of radiation. The optical efficiency with which diffuse is collected is independent of the direction from which the beam is incident.

Equation (2.1.3) states the expression for the optical efficiency of S.U. Evacuated Tubes. The optical efficiency is given as a function of the east-west incident angle modifier $M(\eta)$ and depends on the efficiencies for beam and diffuse radiation ψ_n and ψ_d respectively and the diffuse fraction f_d.

$$\psi_{opt} = \psi_d f_d + (1-f_d)\psi_n M(\eta) = 0.635F_d + (1-f_d)0.595M(\eta) \qquad (2.1.3)$$

The constants 0.635 and 0.595 are slightly above the theoretical values obtained from ray-tracing simulations - they have been derived to match experimental results at $\Delta T/I = 0$.

2.1.3 Pipe Losses

The model had to account for changing pipe loss values. Losses were found to vary within each month, the insulation drying out at high temperatures and becoming wet again with rain.

2.1.4 Array Capacitance

The thermal capacitance of an array reduces its performance since energy required to raise the array to its operating temperature, is still stored within the array at the end of energy collection and is lost overnight. It may appear at first sight that the amount of energy involved is $C\ \Delta T$ where C is the capacitance, but this is only approximately correct because of two factors:

(i) There may be some preheating of the array due to radiation collected before energy is extracted from it.

(ii) The average collector temperature changes during the day with energy collected and (possibly) changes in inlet temperature.

Both of these factors are dealt with in the model.

(i) Modelling of collector temperature when energy is not being extracted from the collector

This model is applied when the collector is preheating or at any other time when the pump is not running. Rapid stop-start collector pump operation within timesteps (collector cycling) is dealt with separately so we consider here periods when the average hourly conditions are such that the collector is below the threshold.

From an energy balance of the collector we obtain

$$\frac{dT_c}{dt} = \frac{\text{energy-in} - \text{energy-out}}{C}$$

$$= \frac{\psi_{opt} - U_L(T_c - T_a)}{C}$$

If T_{init} is the collector temperature at the beginning of the hour we obtain a solution

$$T_c = \frac{\psi_{opt} I}{U_L} + T_a + \left| T_{init} - \frac{\psi_{opt} I}{U_L} - T_a \right| e^{-\left[\frac{U_L t}{C}\right]}$$

$$= \begin{bmatrix}\text{Stagnation} \\ \text{Temperature}\end{bmatrix} + \left| \begin{bmatrix}\text{Initial} \\ \text{Temperature}\end{bmatrix} - \begin{bmatrix}\text{Stagnation} \\ \text{Temperature}\end{bmatrix} \right| e^{-\left[\frac{U_L t}{C}\right]}$$

Taking t = 1 hour, a value of T_c at the end of the hourly timestep is obtained.

(ii) Modelling of capacitive correction when energy is being extracted from the collector

When energy is being collected, this usually occurs in much larger quantities than the change in the amount of energy stored in the collector capacitance. It is therefore assumed that the average collector temperature is determined independently of the collector capacitance; that is it is equal to fluid inlet temperature plus half the temperature rise in the collector. The energy collected during the hour is corrected for the change in the average collector temperature [i.e., by an amount $(T_{\text{final}} - T_{\text{init}})C$].

2.1.5 Controller Cycling

The collector pump is controlled by a differential ON/OFF controller; that is the collector pump begins operation when a temperature difference of more that T_{ON} is detected across the collector and stops when the temperature drops below T_{OFF}.

Examination of some hourly data for similar conditions with and without cycling confirmed that the effect on overall energy collection is negligible and this factor has been ignored in the model.

2.2 Canada

The WATSUN [2.1,2.2] program was developed as a means of predicting the performance of residential alternate energy systems including solar collectors and heat pumps. Versions capable of modelling industrial process heat (IPH) systems, swimming pools, as well as domestic hot water applications are being used extensively in Canada by engineering firms, research organizations, and government agencies for purposes of design evaluation and sizing.

WATSUN can be described as a quasi-steady state simulation program since it assumes constant driving forces (radiation, temperatures, flows, etc.) for the duration of a simulation time step (usually one hour). These are used in conjunction with component and control parameters in the system model to sequentially compute predicted energy flows and temperature changes for each time step.

This program is written in FORTRAN and consists of a number of modular subroutines which contain solar component models (e.g., flat plate collectors, storage, exchanger, etc.) and overall simulation loops.

Simulations are carried out using hourly meteorological and load data. Hourly simulated energy quantities, (e.g., collected energy, energy delivered to storage and purchased energy) are accumulated and can be displayed on an hourly, monthly and yearly basis. Performance indices, such as solar fraction, collector efficiencies, are computed and displayed on monthly and yearly

basis. Detailed hourly values for temperatures, energies and other indices can also be obtained for detailed analysis purposes.

WATSUN contains models of fixed system configurations, however, all the system parameters can be varied by the user. The program can be accessed interactively from a remote terminal or on a microcomputer which greatly reduces the setup and execution time. Annual simulation for a typical system (DHW) can be carried out on hourly basis in a matter of seconds. The structure of the program is very modular thus allowing addition of new component and system models.

Many of the WATSUN component models have been described in an earlier paper [2.2] including collector, storages, load. New or revised components are described briefly below.

2.2.1 Exchangers

Three exchanger models are available: constant effectiveness external exchanger, wrap around exchanger and immersed coil exchanger. Models based on free convective heat transfer have been developed for the immersed coil and wrap around exchangers. In the present study, only external exchangers are used, which are given by

$$Q_x = E^* (\overset{o}{m}C_p)_{\min} * (T_{hi} - T_{ci}) \tag{2.1}$$

where E is the effectiveness, $(\overset{o}{m}C_p)_{\min}$ is lesser of the hot side and cold side capacitance flow rates and T_{hi}, T_{ci} refer to hot inlet and cold inlet temperatures to the exchanger. The collector and the exchanger models are solved simultaneously for configurations in which there is an exchanger between the collector array and storage.

2.2.2 Pipes

Pipes are modelled in terms of a heat loss coefficient UA and a pipe thermal capacitance MC_p using

$$\dot{m}C_p * (T_i - T_f) = UA * (T_f - T_{env}) + MC_p * (dT_f/dt) \tag{2.2.2}$$

where T_f is solved using known T_i for the time step. An analytical solution to (2.2.2) as in TRNSYS pipe and duct routine can also be used.

2.2.3 Storage

WATSUN contains models for a variety of common storage schemes such as water tank or rock-bed storage and incorporates features for dealing with stratification and auxiliary energy sources. In the course of the validation exercise however, it was found necessary to modify these models to incorporate some of the control functions regarding auxiliary energy input, collector and load side flow rates.

Stratified Storage

A new model was created in order to investigate the effect of stratification in fluid based storage. Briefly, the model considers volumes of fluid entering the tank from collector (at the top of the tank) and load (bottom of tank) as new segments at the beginning of the timestep. These volumes are then treated according to the stratification strategy being used: If stratification is temperature-elevation (T-E) dependent, they will mix with warmer layers below or cooler layers above; if no mixing is to take place (T-E independent), the new volumes are inserted between warmer and cooler layers; and if the tank is to be fully mixed (M), a single tank temperature is calculated based on the additional volumes and their respective temperatures added to the volume of fluid in the tank at its former temperature.

After calculating new temperatures to account for energy losses to the environment from the tank sides and ends (tank is assumed to be cylindrical) and for elevated temperatures above the heating element (if present), energy flows from the source and to the load are calculated. This is done by calculating the average temperature of the segments exiting from the top (to the load) and from the bottom of the tank (to the collector) and using these temperatures in conjunction with their respective inlet temperatures and capacitance flow rates.

Also computed for each timestep is the change in internal energy for the tank (based on the change in average tank temperature) and an energy balance based on the quantities mentioned above (which is reported if its absolute value exceeds a preset maximum error - in this case 5J, for the timestep). In order to limit the number of segments in the tank the user specifies a maximum (<39) and minimum (>0) number for the simulation (15 and 10 were used here). If and when the maximum number is exceeded, adjacent tank segments closest in temperature are mixed until the minimum number of segments is attained.

Other noteworthy features of the model include the capability of extracting energy to the load at a specified rate (as required with a system which has no load flow per se) and the capability of extracting load fluid at a fixed temperature (tempering) whereby the load flow is reduced to a value which yields an energy flow to load equivalent to that produced by the nominal mass flow rate with a fixed temperature for fluid passing to the load.

2.2.4 Loads

Load is specified as a 24-hour profile which can change depending on the hour of the day, the day of the week (weekend or weekday) and the month. Alternatively it may be given as measured load (e.g., mains water flow rate and temperatures for each hour along with other inputs such as hourly meteorological data).

2.2.5 Meteorological Data

Measured or typical meteorological year (TMY) data comprised of radiation and ambient temperature are proved at 1 hour intervals. WATSUN has the capability of converting TMY radiation data from the horizontal to the tilted collector plane using an anisotropic sky model [2.5].

2.2.6 Overall Simulation Cycle and Input/Output

A system logic routine contains the daily and hourly simulation loops and controls the end-of-month and end-of-year calculations. In each hour of simulation, appropriate component models are accessed and an energy balance is performed on the system. At the end of the simulation period monthly energy tables and performance indices are calculated and displayed.

For a time step shorter than an hour, the system logic routine can repeat the simulation step several times using scaled parameters as appropriate while accumulating results for the hour. An overall simulation logic flow diagram is included in Figure 2.2.1.

2.3 Netherlands

In assessing the optimum flow control in a system it is necessary to use a so-called *register model* of the storage. In this model the storage is not viewed as a set of differential equations, but as a stack of registers with different temperature or a filing cabinet where packages of a certain temperature are stored and retrieved. Several models are in use, of which ZONERGIE and an extended version of the EEC model EMGP2, EMGP2/strat, are the most detailed ones.

2.3.1 Description of ZONERGIE

ZONERGIE (SUNERGY) is a quasi steady model incorporating the most important parts of a solar energy installation for both heating and hot water. The model of the stratified storage is a conventional segment model with a fast algorithm for the treatment of temperature inversions. Several controls for the delivery and supply flows are implemented, i.e. floating inlets and movable outlets. Heat can be delivered by a normal connection, floating inlets or internal heat

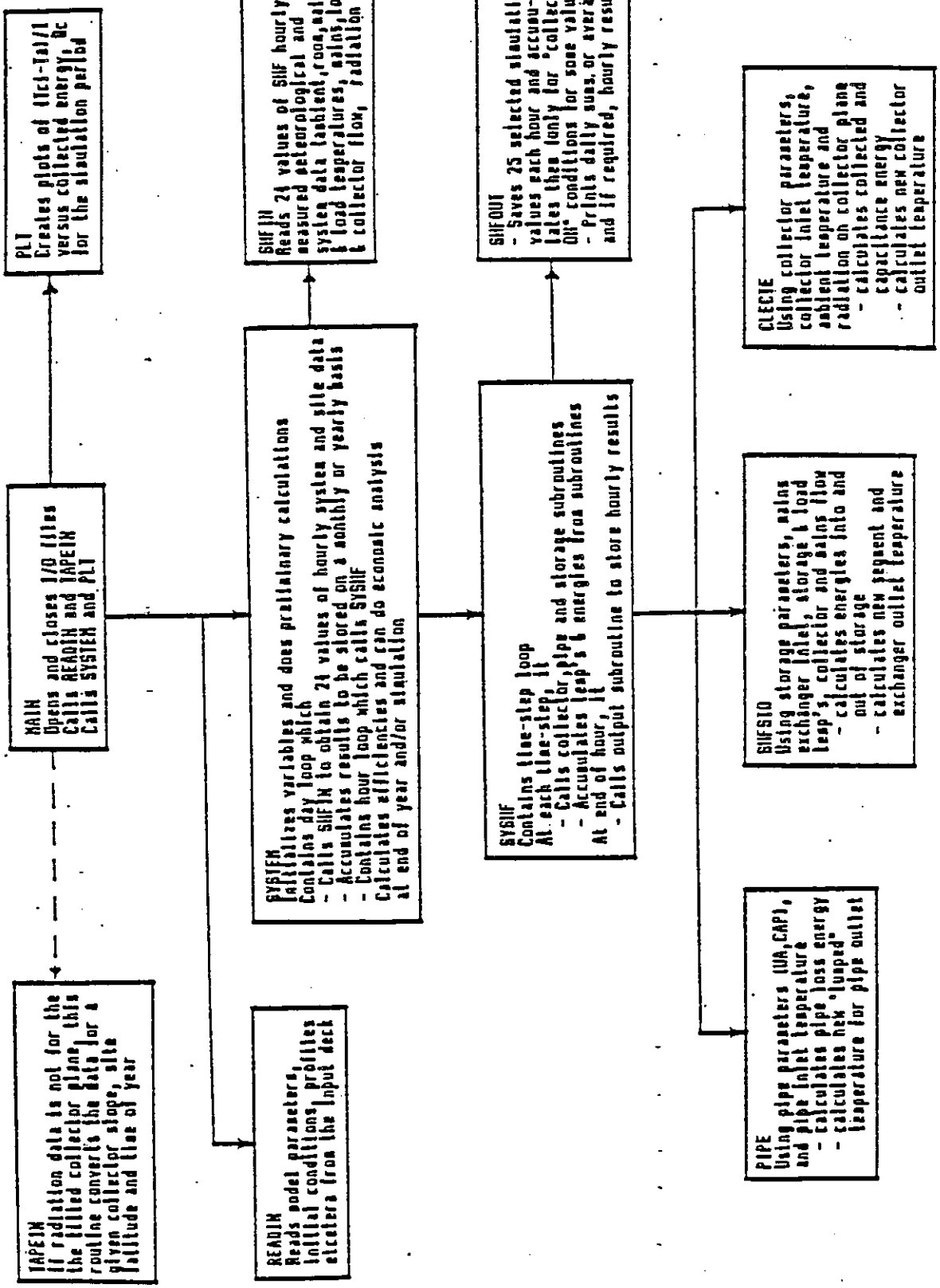

Figure 2.2.1 - Flowchart of WATSUN-SHF calling structure

exchangers. Hot water can be drawn directly from the store or via a coil. Several collector types including an evacuated tube are available, with flow dependent characteristics. For the collector flow several control strategies are available, ranging from a physically impossible dynamical optimisation to simple on-off control. Several load configurations are possible, parallel or series auxiliary heaters and air heaters or radiators. For the load flow several controls are available, the usual ones like constant or weather dependent temperature of the auxiliary heater, and more sophisticated ones, like a load dependent flow control.

The program is written in ALGOL and uses actual hourly values of meterological data. Wherever possible, analytical solutions for the subsystem equations are used and iterations avoided. Timestep and the number of storage segments can be adapted to the type of problem.

2.3.2 Description of EMGP2/strat

EMGP2 is a modularly structured simulation program for active solar systems and is designed as a research tool. It is, in principle, a continuous simulation program for one variable, viz. the temperature. Other variables like the flow, are of type boolean (on-off only). A system can be simulated by selecting an arbitrary number of components out of a restricted set of elements, which can be represented by differential equations or algebraic equations. Further, controllers can be specified to switch flows on or off. Several types of external functions, using time series can be applied. The elements obtain their input values from the preceeding element in the direction of the flow and from the on-off information in the actual operational mode. In some restricted cases, the flow of a preceeding element can be input to an element, but normally only the temperature is a continuous input variable. The slope of the temperature rise with time of each element is calculated simultaneously and with a choice of integration routines, with variable time steps. The behaviour of the system is calculated within the specified accuracy limits. The input to the program is organized to accept integer parameters and the real parameters separately, and is strictly formatted.

2.3.3 Stratified Tank Model

In order to make EMGP2 suitable for simulation of optimum controlled stratified storages, the models of the Eindhoven University of Technology (EUT) are implemented. In these models the storage is treated as a virtually single element with as many outlet elements as necessary. Besides the classical spacially discretised *segment* model, the more correct thermally discretised *register* model of the EUT is implemented. The last model is necessary for control studies. The stratified storage register model is based on discretisation in temperature and not in height of the storage. The variable in this model is not the temperature as normal in EMGP2, but the content

of a temperature register or, equivalently, the thickness of a register of a certain temperature. Only part of the register model of the EUT is implemented in EMGP2. The features implemented are;

- floating inlets
- fixed outlets at the top and/or the bottom of the storage only
- heat exchangers anywhere in the storage
- heat conduction in the medium
- heat loss to the outside

In principle the model is quite simple; fluid entering the storage at a certain temperature is stored in a register with that temperature and fluid leaving the storage is retrieved from the highest or lowest filled register. Only the registers that are filled are treated, which reduces calculation time. In effect, the stratified storage is not calculated as a set of differential equations, coupled via the internal flows, but as though the internal flow is being followed. The result is that the internal flow effects present in the segment model vanish and strong temperature gradients are preserved. Especially the last feature is necessary for a correct optimisation of the flows in a system.

The program is written in FORTRAN and is well documented.

2.4 U.S.A.

A simulation program named DAYSIM for solar heating, cooling, hot water and IPH/district heating systems using event incremented time-steps has been developed at Colorado State University. It is based on the methods of Monaghan [4.2] and Bruno [4.3].

This approach yields a substantially compressed data representation and allows direct analytic solutions for the system of non-linear differential equations over long time-steps which do not occur at fixed intervals, but instead are determined by events such as collector pump turn-on time, domestic hot water withdrawal, or a switch from solar to auxiliary usage.

To obtain results of high accuracy most simulation models use fixed time-steps of an hour or less and require large amounts of data and computer time. The method of simulation presented in this report reduces the amount of computer time and data input required by the use of longer event incremented time-steps and a compression of data to an analytic form that is more easily handled. Data such as radiation, ambient temperature, and loads may be input as daily cosine waves or constants. This data compression allows for calculation of the exact time of occurrence of events such as collector pump turn-on or a switch from solar to auxiliary.

These events define the time-steps used by the day-by-day simulation.

For simulation of a year of heating, cooling and domestic hot water use DAYSIM currently requires about 50 seconds execution time on a CDC CYBER 170 of which a substantial part is required for output. The compilation of data necessary to obtain the cosine fittings takes less than 70 seconds, but only has to be done once for a given location and collector orientation. TRNSYS, with 15 minute time-steps, requires about 750 seconds or 15 times as much execution time.

The program has also been run on the IBM PC and requires about 50 seconds to run a simulation of 15 days on that machine.

A general discussion of the modelling is presented below with additional detail provided in Appendix B. Many of the assumptions indicated below are not mandated by the event increment approach but have been made to produce simpler models.

2.4.1 Collector

$F_R(\tau\alpha)$ of the collector is assumed constant for a simulation period. A subroutine has been added to calculate varying values for $F_R U_L$ if desired. Currently, the collector is assumed to have no capacitance. All parameters except plate temperature are input to the simulation. Plate temperature is calculated relative to fluid temperature as a function of radiation input and the conductance factor G_1.

2.4.2 Collector Loop Heat Exchanger

A correction factor is used to modify the energy equation if a heat exchanger is used.

2.4.3 Collector Piping

Some approximations have been made. Pipe losses inside the building are neglected. The temperature of the fluid exiting the collector is calculated without pipe losses. Pipe losses occurring outside the building are estimated using average fluid temperature.

2.4.4 Collector Pumps

The collector loop pump is assumed to be turned on before the storage loop pump so there are no problems with transients.

2.4.5 Storage Tank

A single fully-mixed (one node) storage tank has been modelled. Losses occur to the environment and are based on a UA parameter input by the user.

2.4.6 Controls

Energy distribution controls are used to specify if there is series or parallel auxiliary. For a parallel auxiliary, energy is supplied by either the storage or auxiliary. The storage supplies energy whenever its temperature is above a minimum set by the user. A dead band may be specified to avoid cycling. The minimum temperature specified should be larger than the minimum storage temperature determined from heat-exchanger effectiveness, room temperature and distribution characteristics.

For series auxiliary, the auxiliary makes up the load that cannot be provided by the solar source. Controls for this case are based on energy rates rather than on storage temperature.

2.4.7 Pressure Relief Valve

A pressure relief valve is required when the storage boils. The storage temperature is checked at the beginning of each time-step, if greater than the maximum allowed, excess energy is dumped.

2.4.8 Loads

If the user does not wish to input daily functional loads, a UA model or some other model of the user's choice may be utilized. The program includes the option of inputing two cosine waves for the load, one to be used when the collector is on and the other when it is off. Thus, direct heat gains through the windows may be better modelled. Internal heat generation and other gains, except tank losses, should be included in the load function as they are not modelled in the program.

An auxiliary heat source in series with the solar source is assumed to boost temperatures to the required DHW temperature.

Energy withdrawal for DHW is currently modelled as three point demands per day. The components of the DHW system are not currently modelled and DHW system losses are assumed to be part of those specified for storage.

Both the space heating and cooling loads may be input as daily cosine waves or constant similar to that used for radiation and temperature data. A UA model for load, or some other model supplied by the user may be incorporated.

The cooling subsystem is an absorption chiller. Its COP is calculated at the beginning of each time-step based on condenser and storage temperatures. The current calculation uses a curve fit of data from the TRNSYS absorption chiller. For any other chiller, the user may supply his own fit.

A solar-assisted heat pump may also be used to help meet heating requirements.

2.4.9 Data Input

Weather and load data, as well as system characteristics are input to the simulation. For ambient temperature, radiation, and heating and cooling loads, a cosine wave approximation has been chosen as the functional representation.

DAYSIM, as with other models, has the capability to transform horizontal radiation data to radiation on the tilted surface. The method used to to take the hourly TMY data for horizontal and direct normal radiation, translate them by curve fit into hourly values on the tilted surface, and then translate these values into daily cosine waves. The fit is chosen such that the total radiation over a day on the tilted surface with the cosine function is equal to that obtained from real data, and such that the day length is approximately the same. Bruno [4.4] suggests using a day-length reduction constant of 0.90-0.95 over a year to reduce the day length and increase maximum radiation value.

2.5 West Germany

2.5.1 Model Description

The principles of the component-model were developed and reported by Schreitmüller in 1980 [5.5]. In this model, the solar system (Fig. 3.5.1) is represented by the Primary Circuit (solar loop) and the Secondary Circuit (DHW-System), which on their part consist of several components. Each component m is characterized by

- the temperature T_m and the thermal capacity C_m, as well as

- the total energy flow into and out of the component $Q_{\text{in},m}$ and $Q_{\text{out},m}$

The energy balance of this component over the time increment dt

$$dt * \dot{Q}_{\text{in},m} = dt * \dot{Q}_{\text{out},m} + dQ_m ,$$

with dQ_m describing the change of the *internal energy* within dt, provides the characteristic differential equation of the m-th component:

$$C_m * dT_m = (Q_{\text{in},m} - Q_{\text{out},m}) * dt \,.$$

A flowing heat transfer medium establishes then a coupling between neighbouring components such that the outlet temperature of the m-th component equals the inlet temperature of the $(m+1)$-th component.

$$T_{\text{out},m} = T_{\text{in},m+1} \,.$$

When the interacting loops are coupled via a heat exchanger, the outlet temperature is calculated based on the specific heat exchange coefficient and the associated secondary temperature (or temperature-profile in the storage tank).

Figure 2.5.1 shows the sequential structure of the iterative calculation process. A fixed interval length of 300 sec. serves as synchronisation to the experimental climate and load data, which were taken as driving functions, and as reference for the validation procedure. Integration of the linear, first order differential equations is performed by Euler-Integration; a variable time-step algorithm automatically adapts to the varying dynamics of the system behaviour. By setting a maximum temperature variation of 0.5 K within one subinterval, its length is then determined by the maximum derivative of all component temperatures.

Control decisions may be taken between subintervals, (e.g., if the solar system operates in the bypass-mode) in order to accurately model control processes.

The overall structure of the two simulation programs used for the validation and for the sensitivity analysis is presented in Figure 2.5.2. Both programs have essentially the same structure. The Validation program has additional features for the comparison of experimental data with their corresponding simulated quantities.

3.0 Validation of Detailed Models

3.1. Australia

3.1.0 Systems & Models Used

Models describing the effects of the various factors on short-term behaviour are validated against detailed measurements, on both a daily and hourly basis. The data are obtained from an array of 40 m^2 of evacuated tubular collectors using Sydney University Evacuated Tubes, forming part of a solar heating and cooling system located at the Department of Mechanical Engineering, University of Sydney, Australia [1.1].

CALCULATION MODULE

1. Gain- and Loss-Terms for each Component

2. Calculation of Temperature-Gradients from Diff.-Equn's

3. Maximum of Temperature-Gradients

4. Determination of Sub-Interval-Length

5. Accumulation of Sub-Intervals

6. Euler-Integration provides Component-Temperatures

7. Convective Temperature Balance in Storage layers with inversed Temperature-Stratification

8. Calculation of Component - outlet temperatures

9. Accumulation of relevant Energy-flows

10. End of current Interval ?

no:
Bypass-Control between Subintervals and
Update of outlet-temperatures
Iteration continues with top 2.

yes:
Iteration reached end of current Interval:
Transfer of Results to printout- and graphic-modules

Figure 2.5.2 - Iterative Calculation of the Component-Temperatures

Programs for Model-Validation SY2VAL7	Programs for System-Analysis VARISIMP1
(1) Input of SHF-DHW System-Parameters	(1) Input of System-Parameters for the System to be analysed
(2) BEGIN OF LOOP FOR THE SIMULATION PERIOD	
(3) Input of measured Climate, Load and SHF-DHW-System Data	(3) Input of measured Climate and Load Data
(4) Initialisisation of Component-Temperatures with measured SHF-Data	(4) specific Initialisisation of Component-Temperatures
(5) BEGIN OF DAY-LOOP	
(6) Updating of Inhomogenities (radiation, ambient-, room-, and coldwater-temperature; warmwater-consumption)	
(7) Calculation of measured energy-flows	(7) not needed
(8) Control-Algorithm	
(9) Calculation-Module	
(10) Processing of simulated and measured results (hourly and daily averages and integrals; period integration of energy flows)	(10) Processing of simulated results
(11) END OF DAY-LOOP	
(12) Results printout, file handling and graphics	
(13) END OF LOOP FOR THE SIMULATION PERIOD	

Figure 2.5.3 - Overall Structure of the Simulation Programs

Figure 3.1.1 shows a diagram of the collector. Table 3.1.1 lists key parameters of the Sydney University Evacuated Tubular Collector and collector array information.

The non-linear thermal model uses values of

$$k_1 = 0.26 \pm 0.05 \ [W\ m^{-2}\ K^{-1}]$$

$$k_2 = 0.039 \pm 0.013 \ [W\ K^{-1}\ \text{tube}^{-1}]$$

$$k_4 = (8.5 \pm 1)10\text{–}9 \ [W\ K^{-4}\ \text{tube}^{-1}]$$

for equation (2.1.1) which correspond to H-W-B (2.1.2) values of

$$F'(\tau\alpha) = 0.575[\text{–}]$$

$$F'U_L = 1.14 + 0.0064(T_c - T_a)[W\ m^{-2}{}^{\circ}C^{-1}]$$

$$B = 2.78^{*}\ 10^{-4}[{}^{\circ}C^{-1}]$$

3.1.1 Model Setup & Validation Procedure

Models of short-term behaviour are used to obtain an indication of the influence of the various factors on long-term (i.e., monthly) performance. This is achieved by constructing a detailed simulation of the array and noting the sensitivity of predictions of energy collected to the removal of different factors from the simulation. The estimate of the significance of the variations is obtained for two sets of operating conditions and climatic data for a typical Sydney winter and summer months.

Pre-validation checks were made to ensure that hourly results were consistent with the final form of the instantaneous model. Approximate validation of the panel power curve (uncorrected for pipe losses) is shown in Figure 3.1.2 and was obtained using noon data to minimize incident angle modifier and capacitance effects. No correction was made for the increase in effective radiation under diffuse conditions. Validation for optical effects in the model involved two days of data (one very clear, one completely diffuse). The incident angle modifier (Figure 3.1.3) is taken as the ratio of measured radiation divided by the equivalent calculated level of normally incident beam radiation for the same collected energy.

The major part of the validation involved comparing predicted and measured values of the total energy collected over complete days. The simulation used measured hourly values of collector inlet temperature and collector plane radiation. Incidence angles were computed from the time of day and year. Because of the uncertainty, and sometimes variability of pipe losses within individual months two simulations were run, one with *theoretical* pipe losses and another

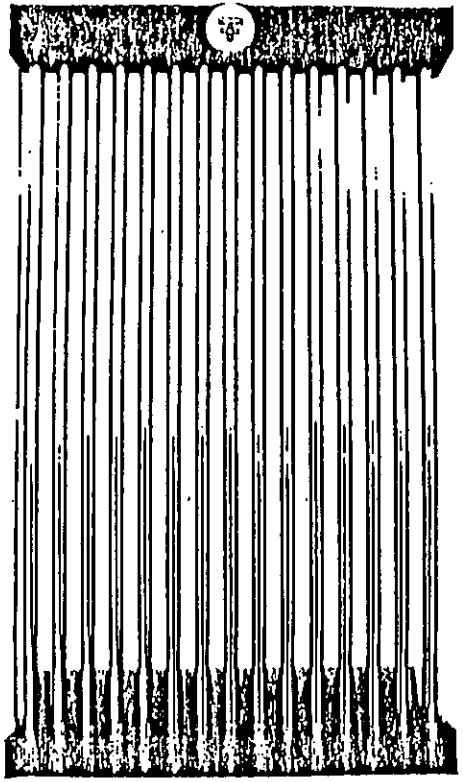

PHOTOGRAPH OF COLLECTOR PANEL

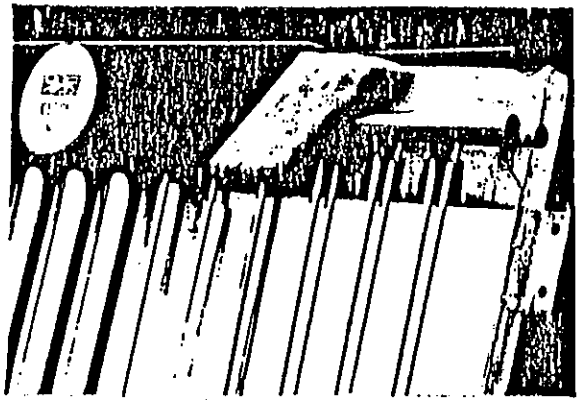

CLOSE-UP OF MANIFOLD

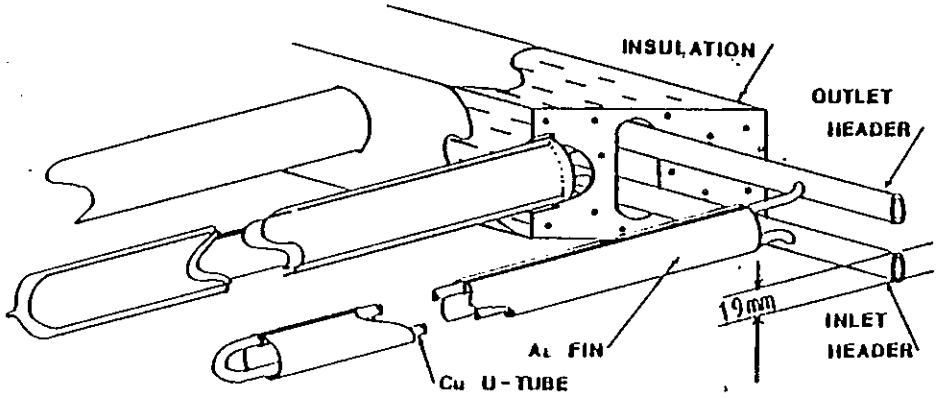

METHOD OF HEAT EXTRACTION

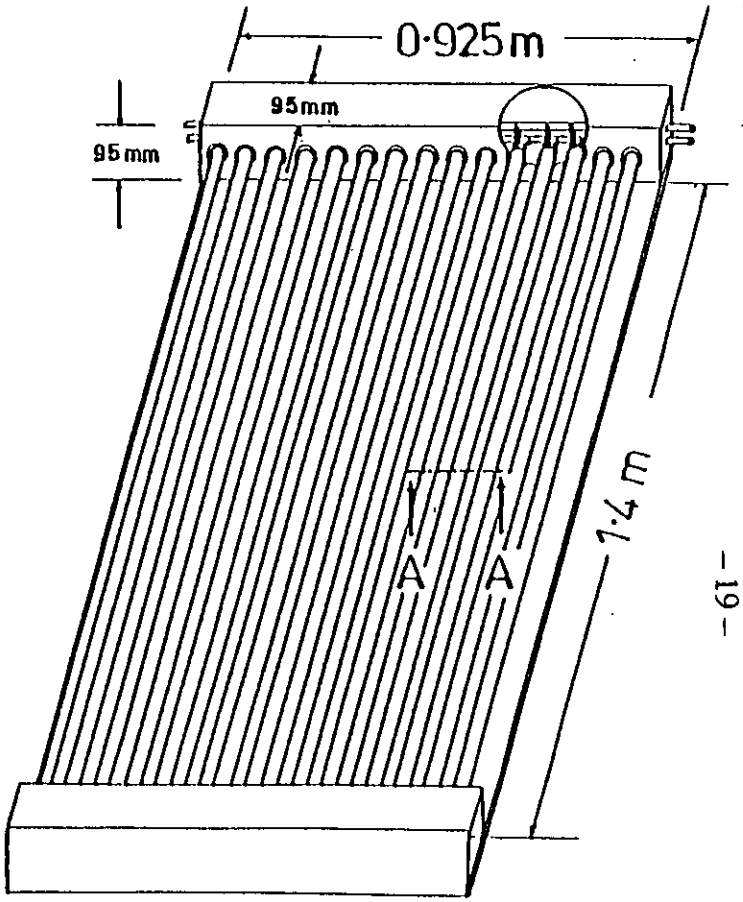

CROSS - SECTION A - A

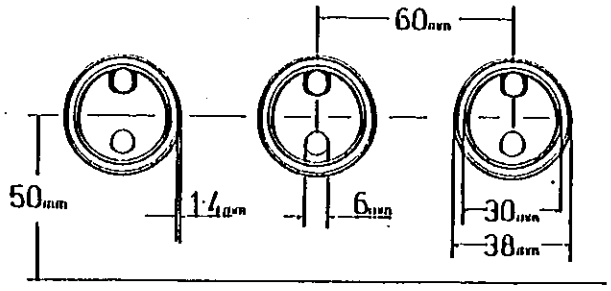

Figure 3.1.1 - Sydney University Evacuated Tubular Collector with a Cu U-Tube and Al-Fin Manifold

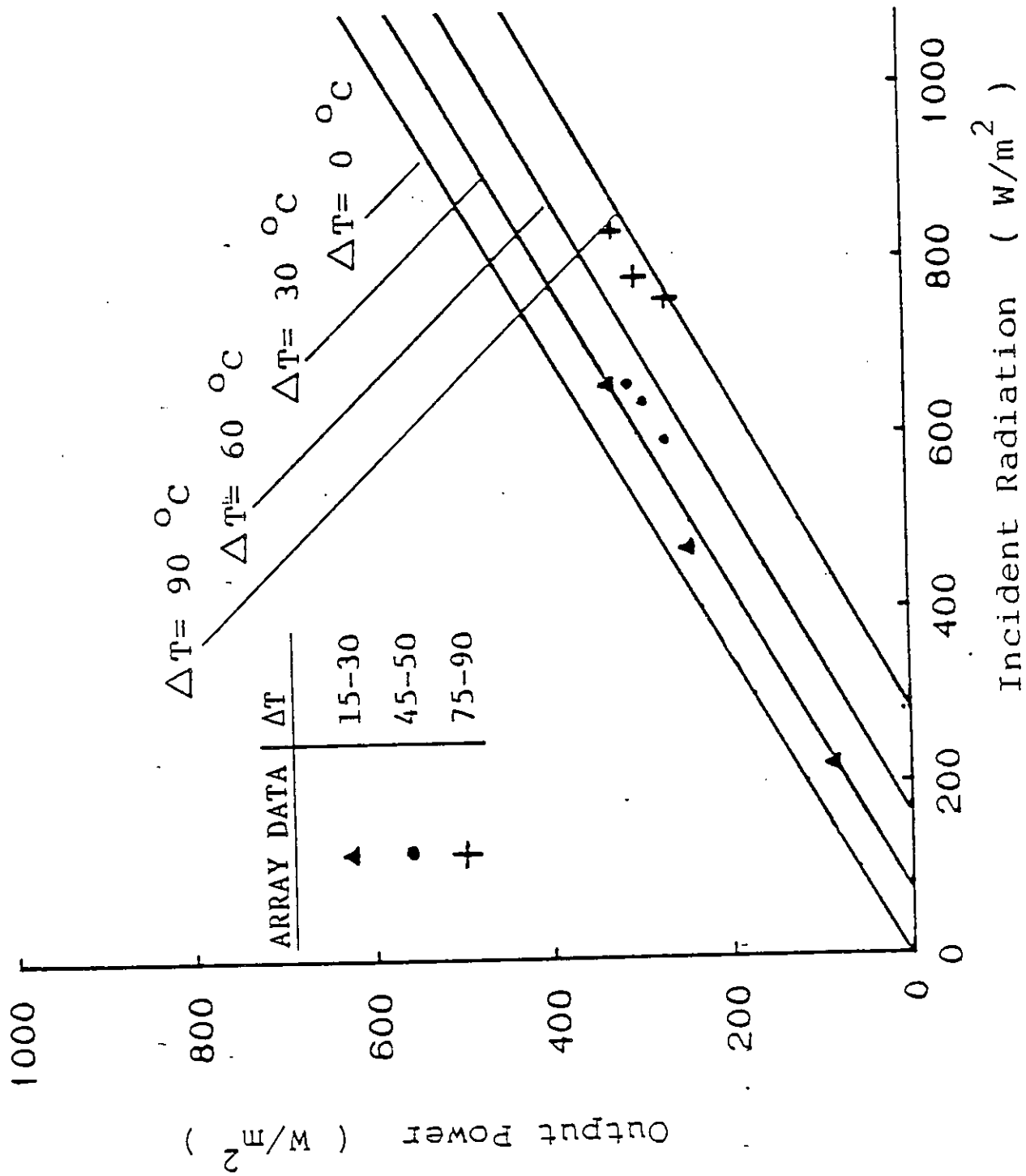

Figure 3.1.2 - Comparison between Model and Measured Array Data -

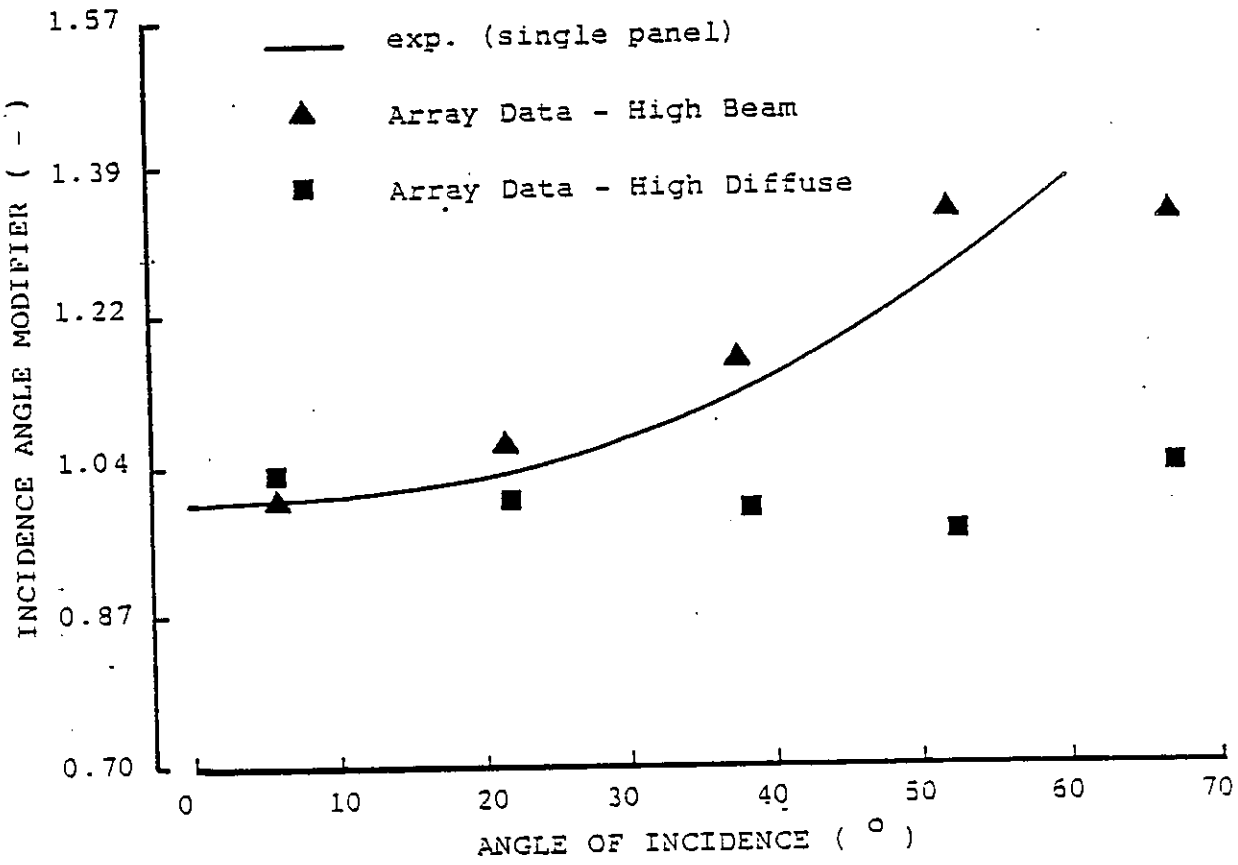

Figure 3.1.3 - Optical Behaviour of Sydney University Evacuated Tubular Collector under Beam and Diffuse Radiation Conditions

Table 3.1.1 - Specifications of Sydney University Evacuated Tubular Collector and Collector Array

	Parameter	Specifications
SINGLE MODULE	No. of tubes per module/pitch (mm)	15/60
	Incident angle modifier (E-W)	0° 15° 30° 45° 60° 1 1.03 1.08 1.20 1.38
	Characterisation of selective surface	dc reactive sputtered; copper/ graded metal carbide, absorptance = 93% emittence (Room temp) = 3-5%
	Collector parameters $F'(\tau\alpha)$	0.575
	$F'U_L$ [W/m²C]	1.74
	Collector capacitance [kJ/°C]	25.00
	Typical monthly temperature difference between absorber and fluid	20°C
	Absorber area [m²]	1.97
	Aperture area per module [m²]	1.25
	Collector fluid	
	a) type	water
	b) amount [ℓ/m²]	0.78
	Fluid flowrate [ℓ/m²min]	1
	Glass material	borosilicate glass
	Reflector.	flat, diffuse white
ARRAY	No. of modules	32
	No. of rows	4
	No. of tubes	480
	Total aperture area [m²]	40.0
	Collector array capacitance [kJ/h]	791
	Collector tilt [°]	13
	Collector orientation [°]	-180
	Total flow [ℓ/hr]	2500

with the maximum pipe losses estimated from August 1984 data. With the exception of pipe losses which are estimated from piping connecting the array to the tank, the model contains no parameters which are adjusted to improve the fit of data and model. All aspects of the model are based upon measurements which have been obtained from experiments independent of the array from which measurements for validation have been obtained.

3.1.2 Results

Two aspects of validation are considered:

(1) the absolute accuracy with which the model predicts the measured performance;

(2) the accuracy with which the model tracks the influence of conditions modifying the performance (i.e., the relative accuracy).

The absolute accuracy can be assessed by examining the overall errors in the results for the two months of data used for validation (January 1985 and June 1984). The results obtained for the two months and two different assumptions about pipe losses, as a percentage deviation from measured values are:

	Theoretical pipe Losses	Maximum pipe Losses
Jan 1985	-3.7%	-14.3%
Jun 1984	-0.9%	-12.5%

The relative accuracy can be assessed by examining the correlation between predicted and measured values. The comparison is made by plotting predicted daily values against measured ones for each month for which the comparison is made and computing the correlation coefficient and regression line. Perfect agreement would result in a regression line with a correlation coefficient and slope which were both 1, but any high correlation coefficient suggests a high level of consistency between the assumptions of the model and the measured behaviour. If the slope of the regression line is also close to 1 then this indicates that the response to factors which alter performance is also modelled reasonably well. The results obtained are:

	Regression Coefficient	Regression Line Slope
Jan 85, theoretical losses	.996	.987
Jan 85, maximum losses	.996	.971
Jun 84, theoretical losses	.991	.883
Jun 84, maximum losses	.992	.855

Results of the daily comparison of predicted and measurement are also given for June 1984 (Figure 3.1.4) and January 1985 (Figure 3.1.5).

3.1.3 Discussion & Conclusion

It is clear that on an overall basis the model underpredicts performance by several percent. The sources of these errors are not known but obvious possibilities are pyranometer errors, errors in measurement of the relatively small T's involved, errors in calculating the loss or gain of energy when temperatures are changing rapidly at start-up and, possibly, errors in the underlying equations under those conditions where they have not been checked experimentally.

The regression line deviates significantly from the expected value in June 1984. Given the high regression coefficient the errors are unlikely to be due to any fundamental problem with the assumptions about the nature of the array's behaviour but due to errors in data or in model coefficients.

3.2 Canada

3.2.0 Systems & Models Used

A range of different types of solar heating system types were used for the validation study. The solar installations involved were simulated as part of a study for International Energy Agency (IEA) Task VI on Evacuated Tubular Collectors (ETC's) and the National Research Council (NRC) of Canada. They are summarized in Table 3.2.1.

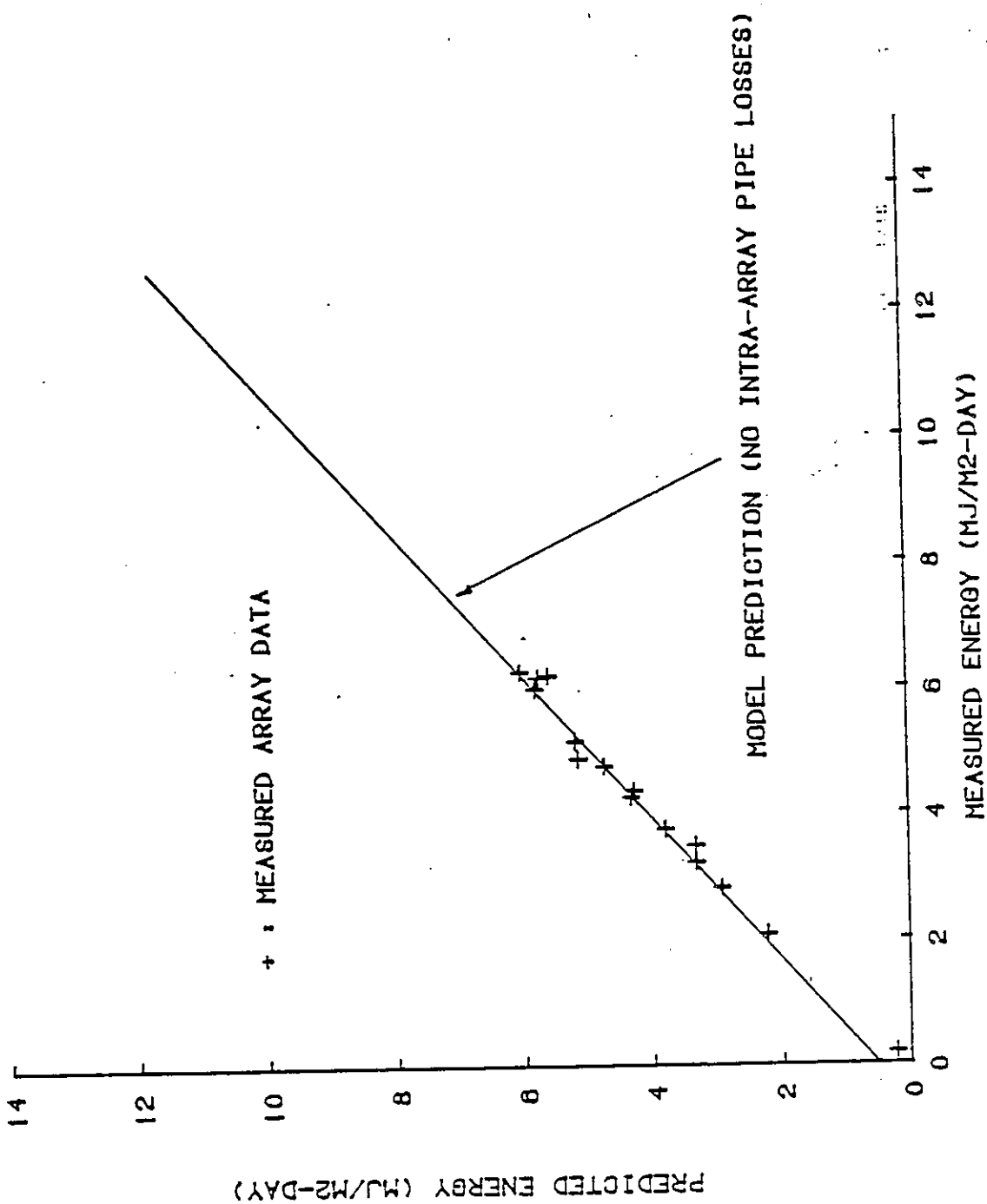

Figure 3.1.4 - Predicted and Measured Energies for Sydney University Evacuated Tubular Collector During June 1984

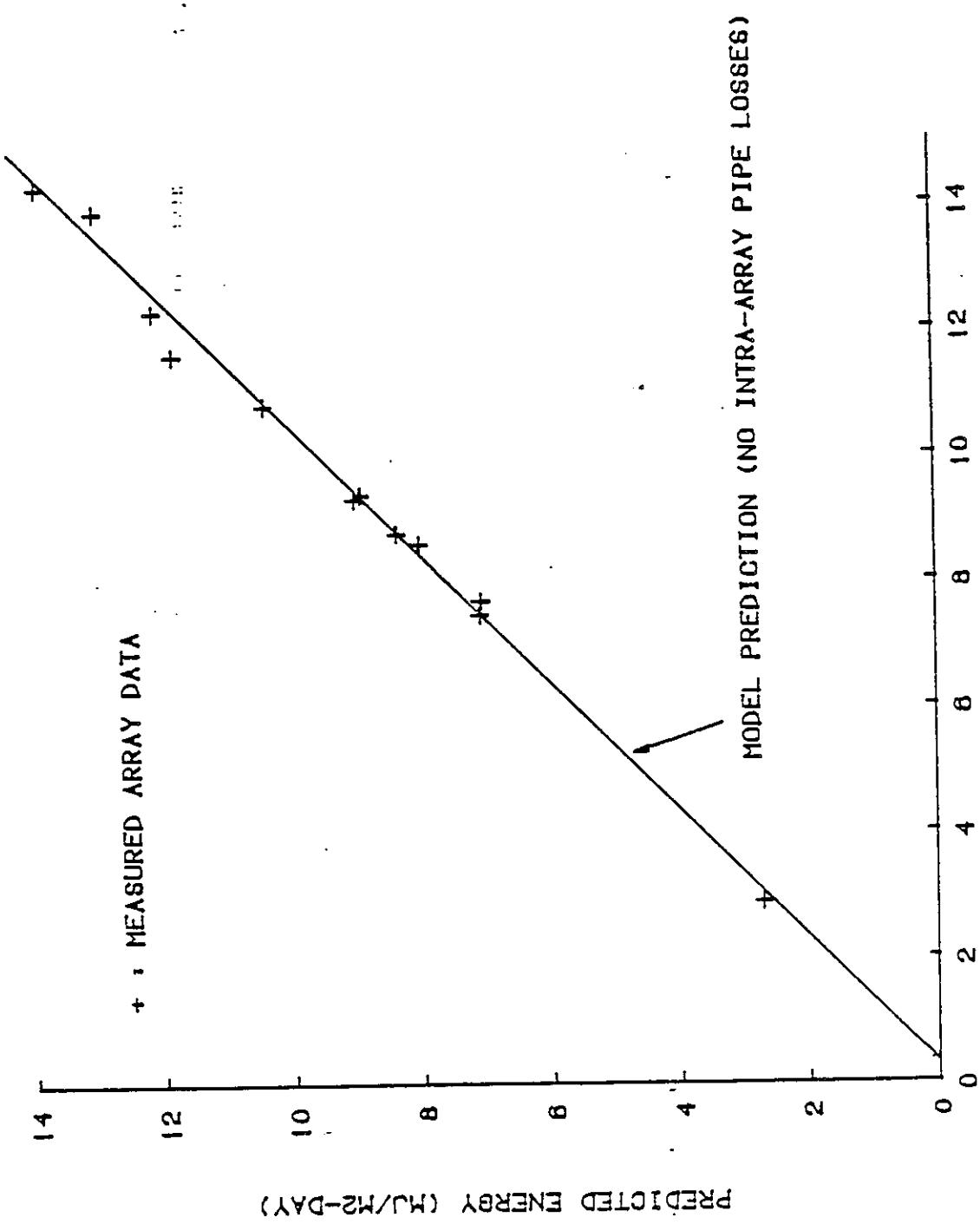

Figure 3.1.5 - Predicted and Measured Energies for Sydney University

Table 3.2.1 - Systems Characteristics

		Collector				Piping		Storage					
System Location	Configuration	Area (M2)	Type	FRUL (W/M2-C)	FRTA	UA (W/K)	CAP (KJ/C)	UA (W/K)	VOL (M3)	TSTOR (C)	Load (GJ/DAY)	Simulation (Month-Length)	Climate Latitude
1. Mountain Spring Plant Edmonton, Alberta	IPH Open Collector Loop 2-Tank	281.6	ETC Sun-master TRS-81	1.39	0.42	10.	1700	4.4 490	4.2 14.8	60-80 50-70	2.5 6: to 15: (Weekday)	08,09/83 - 21 days	Continental 53.55 N.
2. Colorado Solar House Ft. Collins, Colorado	DHW, Space Htg. Closed Collector Loop 2-Tank & Brick-Work Furnace	59.6	ETC Philips VTR-141	0.85	0.49	45.	220	6.1 5.5	4.4 3.0	50-60	.08 DHW (Peaks at 6:, 10:,21:) .15 to .26 Space Htg.	11/80 to 03/81 - 138 days	Steppe or Semi Arid 40.60 N.
3. Solarhaus Frieburg Freiburg, West Germany	DHW Closed Collector Loop 2-Tank	33.3	ETC Corning	1.37	0.66	28.	850	6. 9.	1.0 1.5	25-50 40-50	0.2 DHW	09,10/80 - 17 days	Meso-Thermal Forest 47.58 N.
4. Les Provost Montreal, Quebec	IPH Open Collector Loop 2-Tank	497.4	F.P. Petro Sun Cim-2	4.75	0.73	29.	2750	29.	19.1 13.	50-60	15 6 Days/Wk	10,11/83 - 61 Days	Continental 45.5 N.

System schematics for the four systems simulated are given in Figure 3.2.1 and correspond to those listed in Table 3.2.1. All are two-tank systems using a pre-heat (PH) or a small accumulator tank along with a second special purpose tank. For the IPH systems (Figure 3.2.1(a), (d)) load requirements were such that this second tank was much larger and held at a pre-set minimum temperature during load periods by injecting auxiliary energy. In the residential systems the second tank provided domestic hot water (DHW) at a pre-set temperature using electric resistive heating.

The Colorado system was the only one for which space heating was simulated. The energy was drawn from the PH tank and supplemented by auxiliary energy to a boiler.

Mountain Spring Plant (MSP)

The MSP system uses solar IPH for washing soda-pop bottles in a long shallow (approx. 1m × 3m) *soaker tank* which contains a continuously circulating 4% caustic soda solution. The fluid temperature is maintained at a minimum of 63 to 65.5°C from the weekday hours of 3:00 to 16:00 which bracket the load period (approximately 6:00 to 15:00). The bottle load had to be approximated from monitored data consisting of fluid flowrates and temperatures for the soaker loop and auxiliary energy inputs.

The collector subsystem includes a set of three arrays of Sunmaster evacuated tubular collectors (ETC's) with a total aperture area of 282 square meters. It is a drain-back type system requiring about 25 minutes for full drain-back. Residence or fill time for nominal full flow is about 15 minutes. Unique features of collector subsystem include a minimum *ON* time of 30 minutes followed by a minimum *OFF* time of 5 minutes to prevent uncontrolled cycling. The system has large capacitance values for the collector piping and a second capacitance with *long time constant* associated with the thermal insulation on the pipes.

Colorado Solar House (CSH)

The array provided space heating and DHW to an office building. The collector has Philips VTR141 ETC. The DHW-load and internal heat gain were also specified. The system is essentially the same as the U.S. space heating system used to validate the American detailed model (see below).

Solarhaus Freiburg (SHF)

The DHW portion of the system provided hot water to a 20-unit apartment building via a piping network which continuously circulated water during a maximum load period from 7:00 to 22:00 local time. The collector (Philips and Corning ETC) loop was closed, containing a

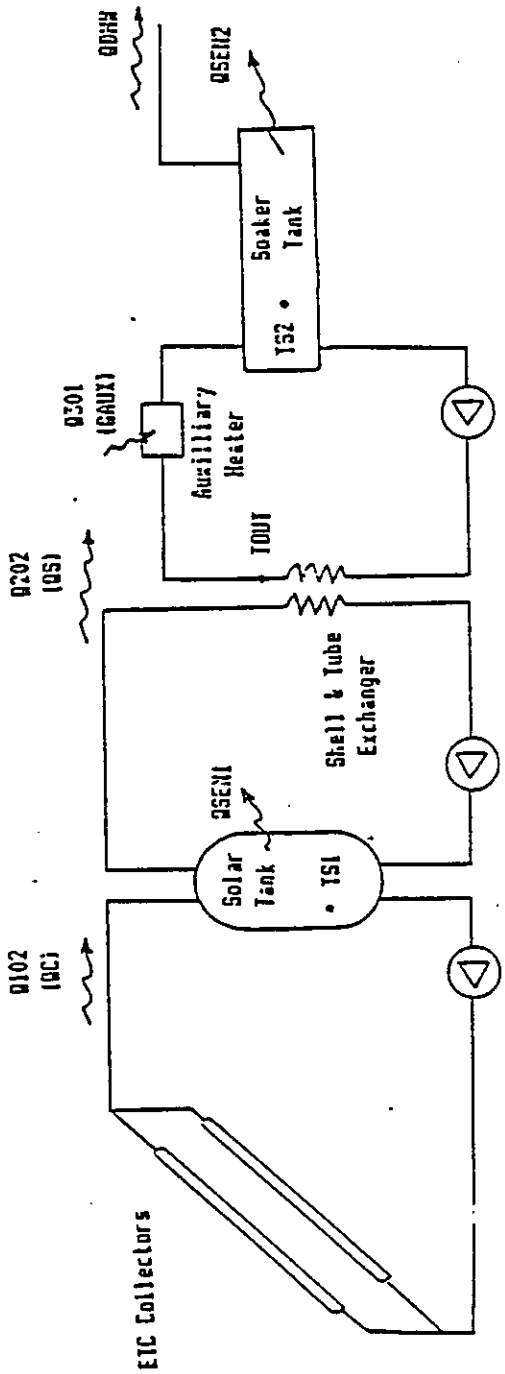

Figure 3.2.1.a - Mountain Spring Plant in Edmonton, Alberta, Canada

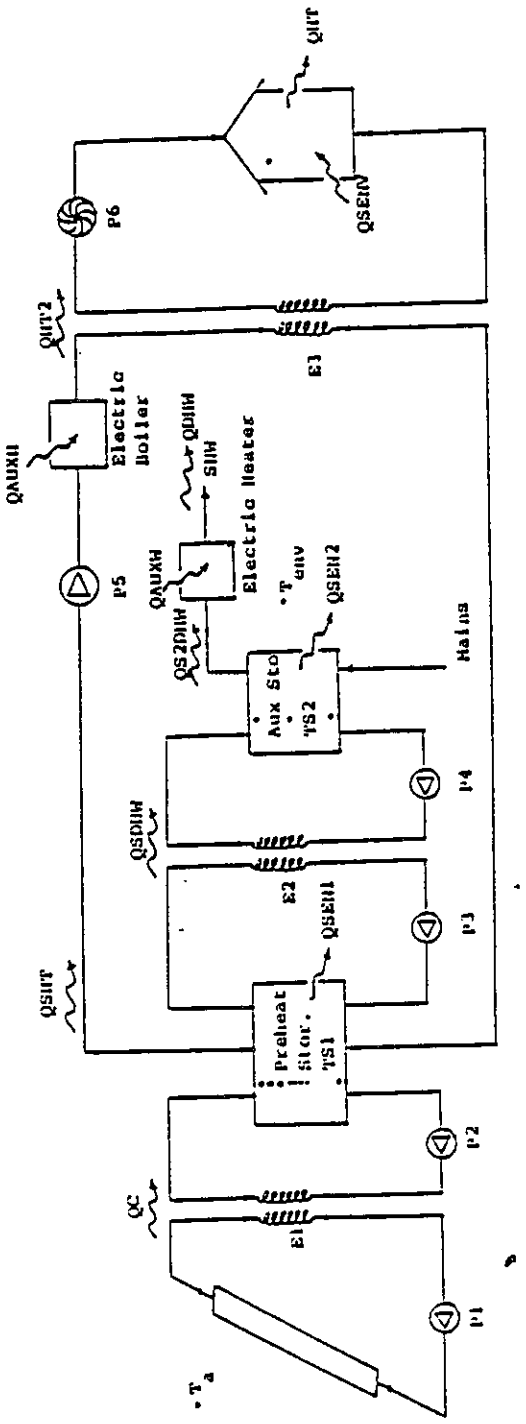

Figure 3.2.1.b - Colorado State University Solar House in Ft. Collins, U.S.A.

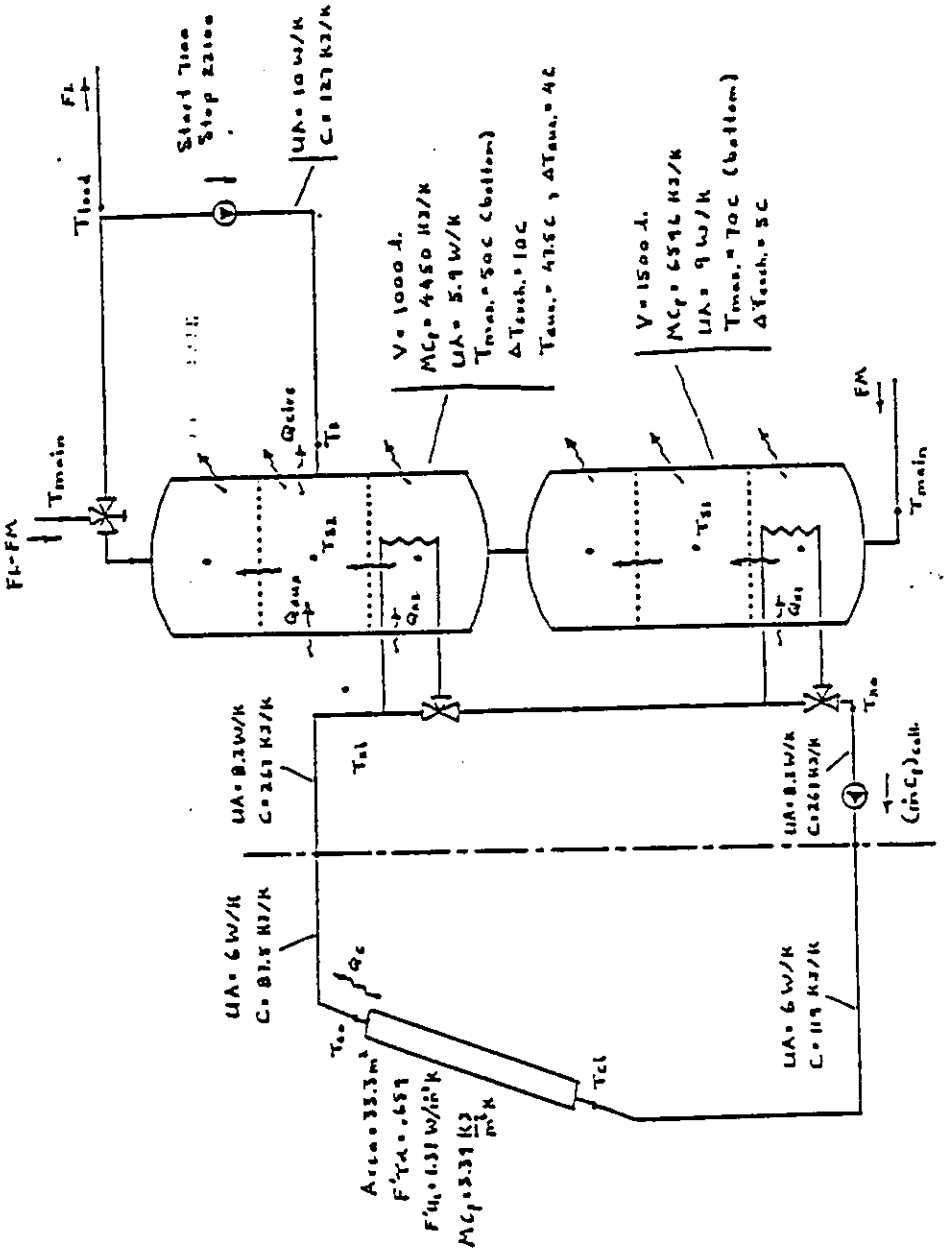

Figure 3.2.1.c - Solar Haus Freiburg, West Germany

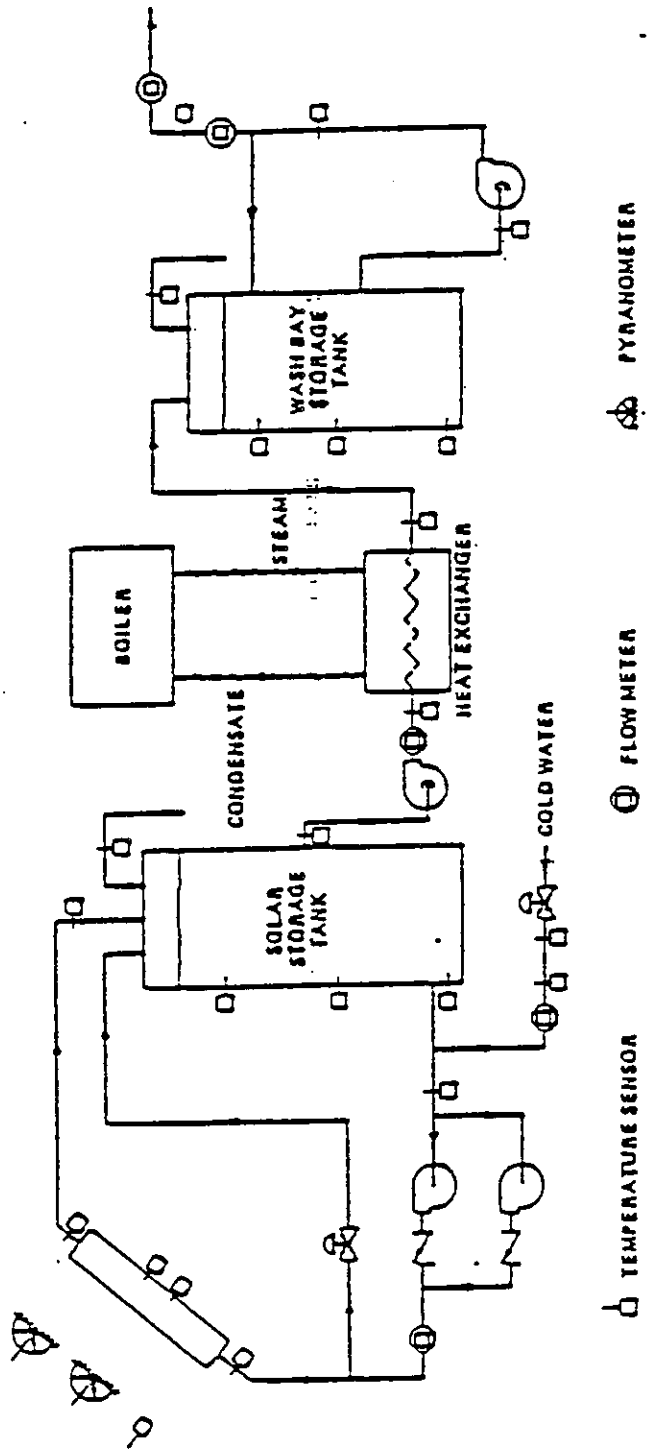

Figure 3.2.1.d - Provost System in Montreal, Canada

propylene glycol - water solution which circulated through immersed coil exchangers of either or both storage tanks depending on the tank temperatures, the collector outlet temperature and an operating strategy set in advance for a given day's operation. The collector pump flowrate was relatively large (with respect to the volume of fluid in the loop) so that the cycle time for the collector loop was of the order of five minutes. The system is identical to that used in the validation study of West Germany below.

Les Provost (PRV)

The Provost truck washing facility is the only non-IEA system simulated. The portion of the system downstream of the heat exchanger inlet was excluded from the model. Due to the *flow through* nature of the solar subsystem however, excluding the he load had little or no effect on the validity of the simulation results. The Provost system, unlike the other systems, has flat plate collectors. Due to the climate the collectors are plumbed for drain-back.

3.2.1 Model Setup and Validation Procedure

Simulations were performed for periods given in Table 3.2.1 with initial temperatures based on measured data which are provided as input to the program on an hourly basis. Load data are provided from daily profiles based on average hourly measured data. For the IPH systems which have a different weekend load, a second load profile is supplied.

All of the simulations used a one hour timestep except for the SHF System. Due to a short (5 minute) collector loop cycle time this system was simulated using a 5 minute timestep. A 30 minute timestep was also used in order to test the applicability of a flow correction factor (for derivation see Appendix A) which allows the use of longer simulation timesteps for such systems.

Parameter values for components and control were calculated from measured values. In some cases this involved short duration (several hours) WATSUN simulations in order to assist in incorporating dependent effects and to minimize timestep induced errors during transients.

Changes to the simulation program which were required to model the different systems mainly involved the storage subroutine since it was used to control solar and auxiliary energy supplied to the load(s). In the case of CSH the system configuration seen in the schematic in Figure 3.2.1(b) was valid for the first month and a half of the simulation period but was changed in the middle of January, 1981 with the electric water heater being replaced by a heating element in the top of the DHW tank. In February, the electric boiler in the space heating loop was replaced by an off-peak electric heater which charged a brickwork core overnight to a temperature sufficient to meet the next day's heating demand. These changes are also incorporated into

the WATSUN storage model.

A fully mixed (one node) storage model was used for all of the systems except SHF which used a 3 node segmented model. The WATSUN collector model for all systems was based on the H-W-B equation corrected for thermal capacitance and accounting for pipe losses and capacitance.

The method of validation for WATSUN mainly involves comparison of simulation results with measured results, which include both raw data and energies calculated directly from the measured data but which may incorporate corrections for transport lag and/or thermal capacitance effects.

For the Mountain Spring plant in Edmonton, Alberta, model to model comparisons were made using the results of TRNSYS simulations in addition to WATSUN and measured results. The TRNSYS simulations used a five minute timestep and hourly measured loads for the simulation period. The TRNSYS collector subroutine modelled the cycling during startup/shutdown periods, the thermal capacitance of the piping insulation and the temperature dependence of the collector loss factor, $F_R U_L$.

3.2.2 Results of the Validation

Mountain Spring Plant

Comparisons are given in Figure 3.2.2 of simulated (symbols) and measured (solid curve) tank temperature in the form of time profiles for a four day period from August 17 to 21, 1983. Corresponding TRNSYS results are shown in Figure 3.2.3.

Measured results are plotted against the simulated results for the solar and soaker tank temperatures in Figure 3.2.4(a) and 3.2.4(b) corresponding to the WATSUN results of Figure 3.2.2 and in Figures 3.2.5(a) and 3.2.5(b) for the TRNSYS results.

The 45 degree line represents perfect agreement between simulated and measured results with solid lines representing error bands of ±2K and ±5K. Note that the TRNSYS and WATSUN results are of comparable accuracy. The vertical row of points in Figure 3.2.4(b) are caused by the 65°C set point temperature since auxiliary energy input is assumed to maintain this temperature for each hour of the load period whereas the real system cycles between auxiliary heater ON and OFF in 1.5 to 2 hours.

Energy comparisons are given in Table 3.2.2 for simulation period and 3 separate days for various levels of insolation levels (7401, 5519, 2799 MJ). The most striking feature of this table is the consistent overprediction of energies by the TRNSYS simulations even though tank

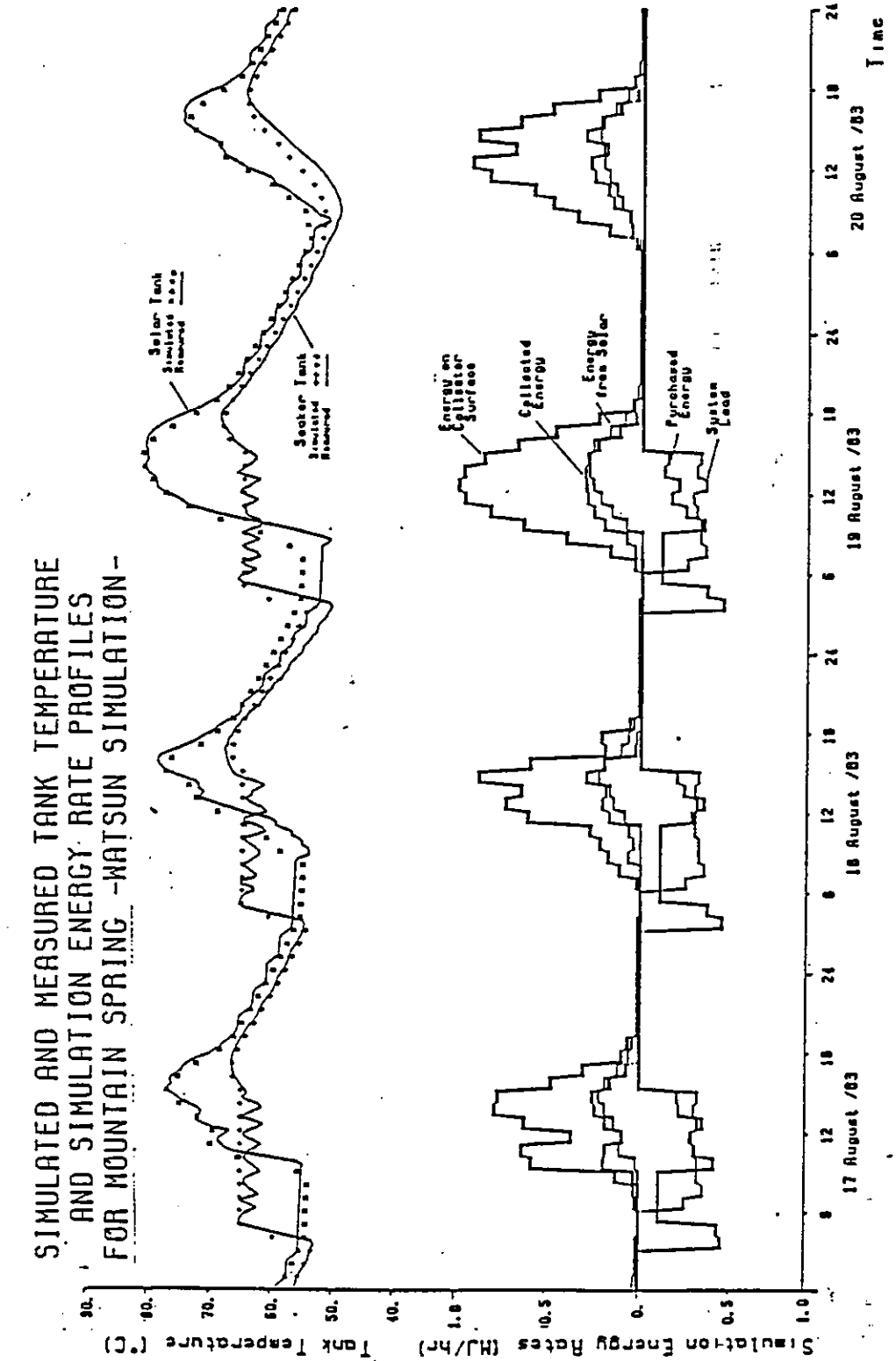

Figure 3.2.2 - WATSUN Simulation Profiles - Aug. 17 through Aug. 20, '83

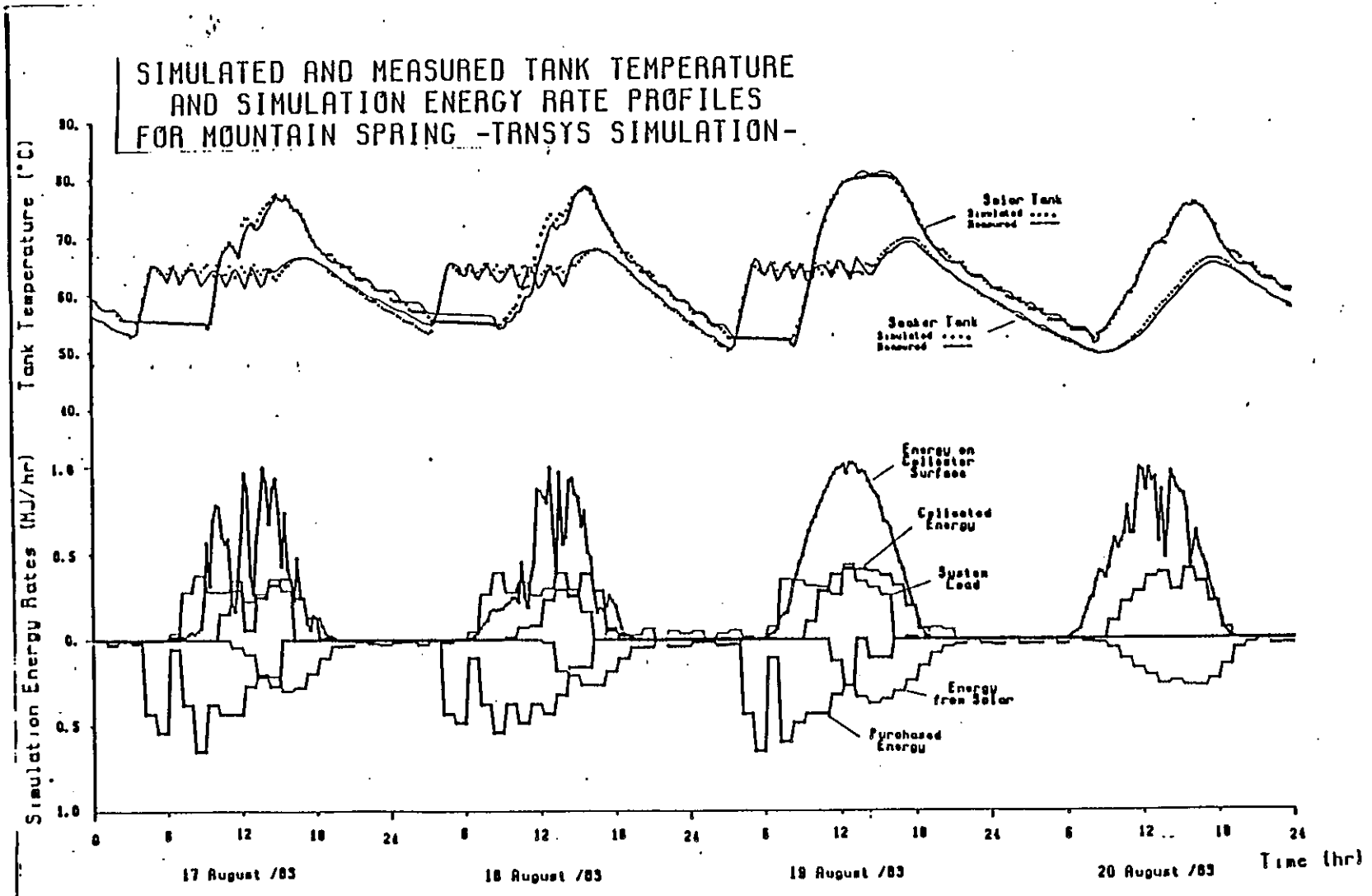

Figure 3.2.3 - TRNSYS Simulation Profiles - Aug. 17 through Aug. 20, '83

Figure 3.2.4 - WATSUN Comparison of Temperatures - Aug. 17 - 20

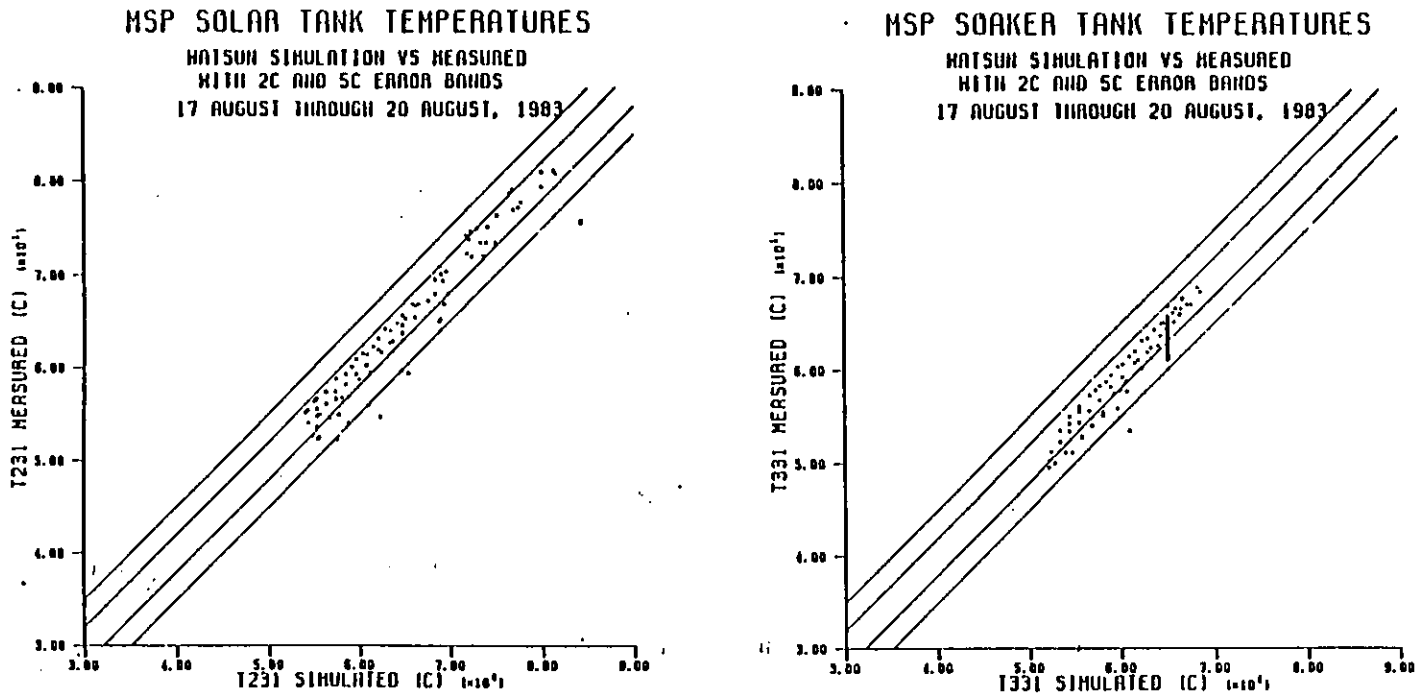

(a) (b)

Figure 3.2.5 - TRNSYS Comparison of Temperatures - Aug. 17 - 20

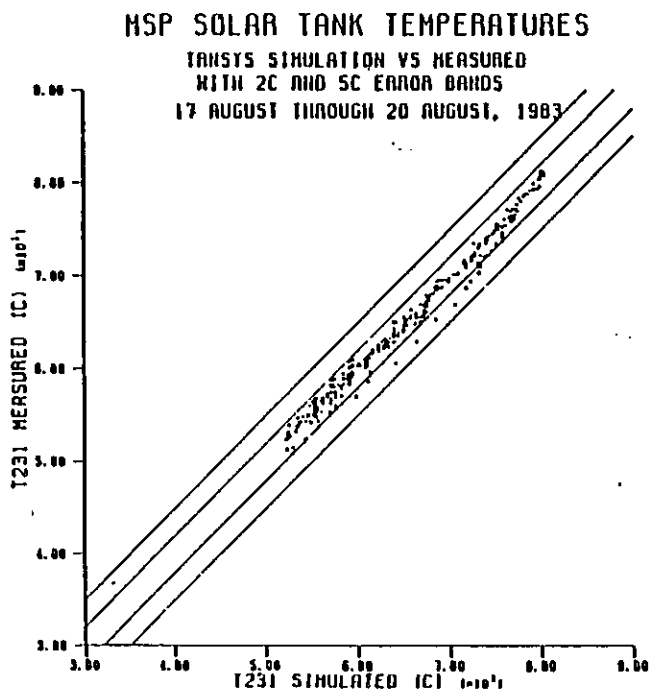

(a)

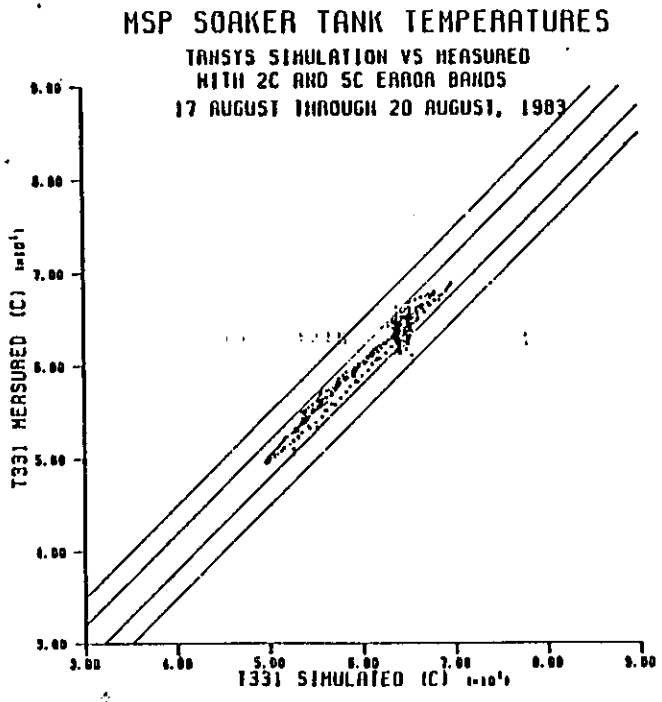

(b)

temperature tracking was quite good. We feel that this may be the result of the option chosen for calculating the measured energies, since the *calculated* hourly radiation is less than the raw data as the insolation level rises and more as it falls. Furthermore, there is considerable difference between measured and simulated values of the auxiliary energy use for both models: while WATSUN underpredicts in most cases, TRNYS overpredicts in all the cases. We believe the measured data are not very reliable, in this case, as well as there are inaccuracies introduced due to the assumption of a constant efficiency for the heater in WATSUN. In fact, heat losses, burner efficiency and make-up air temperatures change constantly, making it difficult to model in either of the simulation programs. In other words, total energy delivered to the load (sum of the last two columns for each model and the measured values in Table 3.2.2) is not a reliable figure for comparison purposes.

Colorado Solar House

Energy results from the simulation are compared with measured values in Table 3.2.3. This table shows monthly values of solar energy collected and delivered for space heating and hot water. The difference between simulated and measured results for delivered solar energies averaged about 10% and 15% for space heating and hot water respectively and were somewhat larger than expected. The error is partly due to error in collected energy values (3.5 to 5%) but mostly due to changes in tank internal energies over the course of a month (5.5 to 7.5% of collected energy). Also, space heating and hot water demand deviated from reported values by an average 1.5 to 2%.

Simulated and measured pre-heat tank temperatures are plotted against time in Figure 3.2.6 for a nine day period chosen at random. The shift between measured and simulated temperature curves is due to accumulated error over a three month period. The error in internal tank energy as of March 1, 1980 is about 110MJ based on a temperature error of 5.8k. This error is about 0.4% of measured useful collected energy for the period. If the curves are superimposed, an average absolute deviation of 2.6K is obtained for the period. This is very good considering the fact that the measured data vary by more than 25K over the interval.

Solarhaus Freiburg

Simulation results are given as comparisons of measured (solid lines) and simulated (solid lines with symbols) average tank temperatures in Figure 3.2.7 and energies in Table 3.2.4. Table 3.2.4 covers the last nine days of a seventeen day simulation period from 27 September, 1980 to 13 October, 1980. Comparing simulated and measured values of collected energy, delivered energy from the DHW tank for a range of insolation values (average hourly available radiation of

Table 3.2.2 - Comparison of Simulated and Measured Energies for Mountain Spring Project

TIME	Radiation (MJ)		Solar Energy (MJ) Delivered to Storage			Solar Energy (MJ) Delivered to Load			Auxiliary Energy (MJ)		
1983	Meas.	Simu.	Meas.	WATSUN	TRNSYS	Meas.	WATSUN	TRNSYS	Meas.	WATSUN	TRNSYS
Aug 19	7401	7380	2346	2231	2704	2171	2140	2560	3469	2450	3952
% error		-0.3		-4.9	+15.0		-1.0	+18.0		-27.0	+14.0
Aug 29	5519	5522	1531	1476	1605	1167	1170	1365	1630	2010	2058
% error		+0.1		-3.6	+ 5.0		0	+17.0		+23.0	+26.0
Sep 4	2799	2788	729	787	860	820	890	961	-159	0	0
% error		-0.4		+7.4	+18.0		+9.0	+17.0		(no-load day)	
Aug 17 to Sep 6	103612	103269	29731	29109	35069	27785	28090	34102	40778	34720	47576
% error		-0.3		-2.1	+18.0		+1.1	+22.7		-14.9	+16.6

Table 3.2.3 - Comparison of Simulated and Measured Energies for Colorado Solar House

TIME	Radiation (MJ) on Collectors (H001)		Solar Energy (MJ) Collected (Q112)			Solar Energy (MJ) to (Space Heat) & DHW			Auxiliary (Purchased) Energy (MJ)		
	Meas.	WATSUN	Meas.	WATSUN	Error	Meas.	WATSUN	Error	Meas.	WATSUN	Error
Dec /80	23460	23200	7575	6865	-9.4%	7010	6865	-2.1%	3010	3330	+10.6%
% error		(-1.1%)				(5400)	(5085)	(-5.8%)			
Jan /81	31530	31725	10150	10970	+8.1%	11300	11000	-2.7%	990	1715	+73.2%
% error		(-0.6%)				(8540)	(8070)	(-5.5%)			
Feb /81	31870	31975	9480	9575	+1.0%	8960	8420	-6.0%	1880	2860	+52.1%
% error		(+0.3%)				(6720)	(5650)	(-15.9%)			
Mar /81 (23 days)	25630	25600	7910	7540	-4.7%	7450	7520	+0.9%	230	385	+67.4%
% error		(-0.1%)				(5680)	(5360)	(-5.6%)			

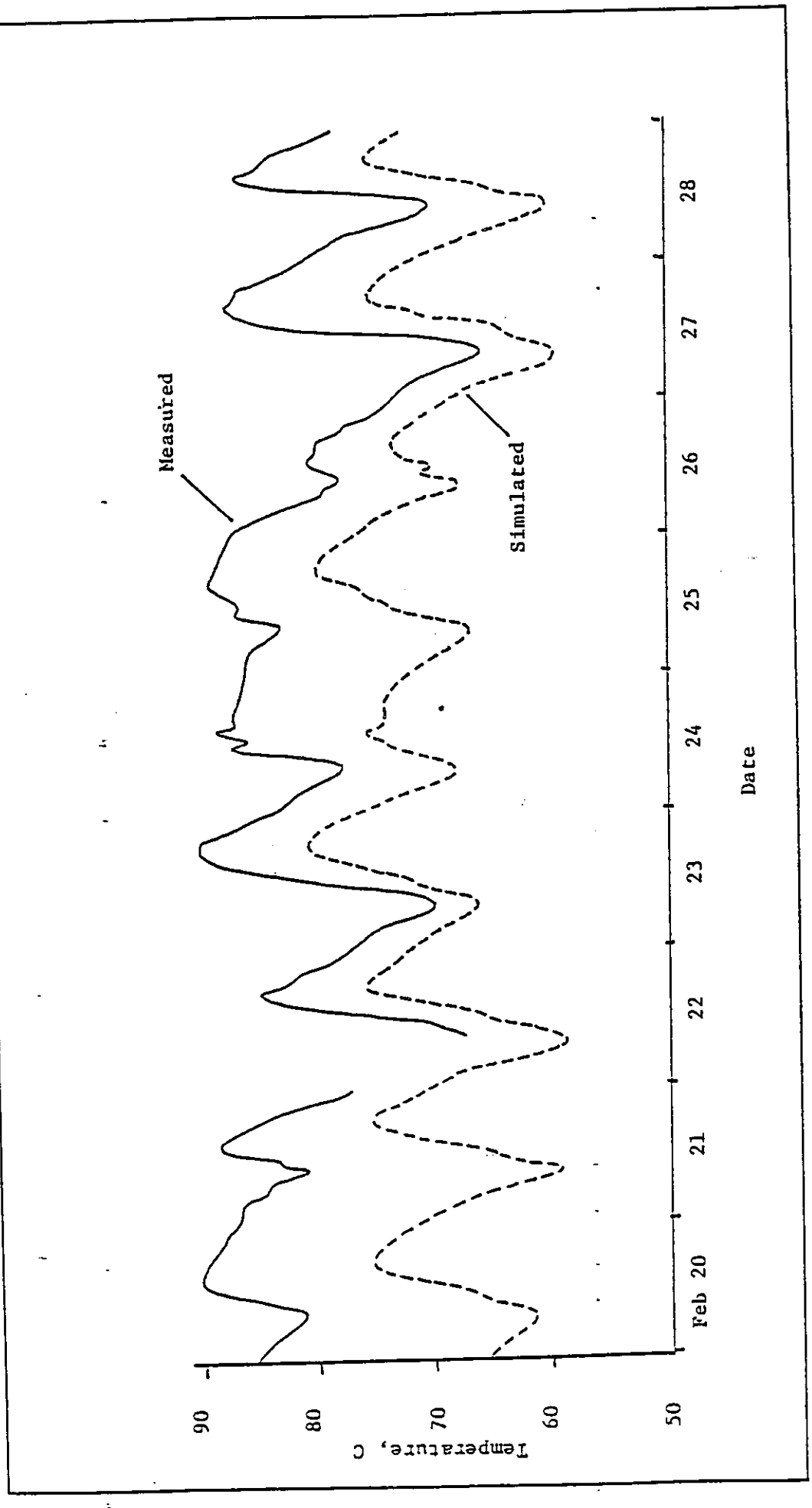

Figure 3.2.6 - Simulation Versus measured values of storage tank average temperatures - Colorado Solar House

22.2, 15.9, 7.3 kWh on the 14th, 4th and 12th day of the simulation period) and for the totals over the simulation period.

The major energy quantities (collected, exchanged to PH, delivered from storage) showed relative errors of less than 9% and the storage tank average temperatures had mean RMS errors of about 3K for 5 minute timestep and 3.5 to 4K for the 30 minute timestep simulations. Collector ON time was 112 hours for the 5 minute timestep and 109 hours for the 30 minute timestep simulations which compares well with the 111 hours of collector operation observed for the 17 day period. Mean RMS deviation from measured collector inlet and outlet temperatures was less than 2K for the 5 minute timestep and less than 5K for the 30 minute timestep simulations.

Results from simulations using a 30 minute timestep and mass flow correction factor of 0.65 compared well with measured results. The simulated energy exchange rates were within 10% above the measured data.

Provost

Figure 3.2.8 shows a comparison of simulated (dashed line) and measured tank temperatures and collected energy for a two day period. The predicted and measured energy start to deviate as the mixing process stops upon collector shut-down. This is because the load water is drawn from the tank at 60% elevation and leaves warm water in the top section undisturbed.

Predicted values for collected and delivered energies are compared with measured for the months of October and November in Table 3.2.5. The results show that collected energy is within 5% and the delivered energy is within 10% of the measured values. There is approximately 10% error in the recorded radiation data due to logging malfunctions. The correct value of 180.6 GJ was used.

3.2.3 Discussion & Conclusions

WATSUN simulation results in terms of predicted temperatures and energies agree quite well with monitored results; in most situations, the simulated values are within 5 to 10%. In view of the range of systems (domestic hot water systems to process heating systems) with complex configurations and operating strategies, the results presented show that the WATSUN program has the potential to be a useful tool for the analysis and design of solar thermal energy systems. As in the case of Freiburg house, it is shown that WATSUN can be used for detailed simulation using short timesteps of five minutes to thirty minutes.

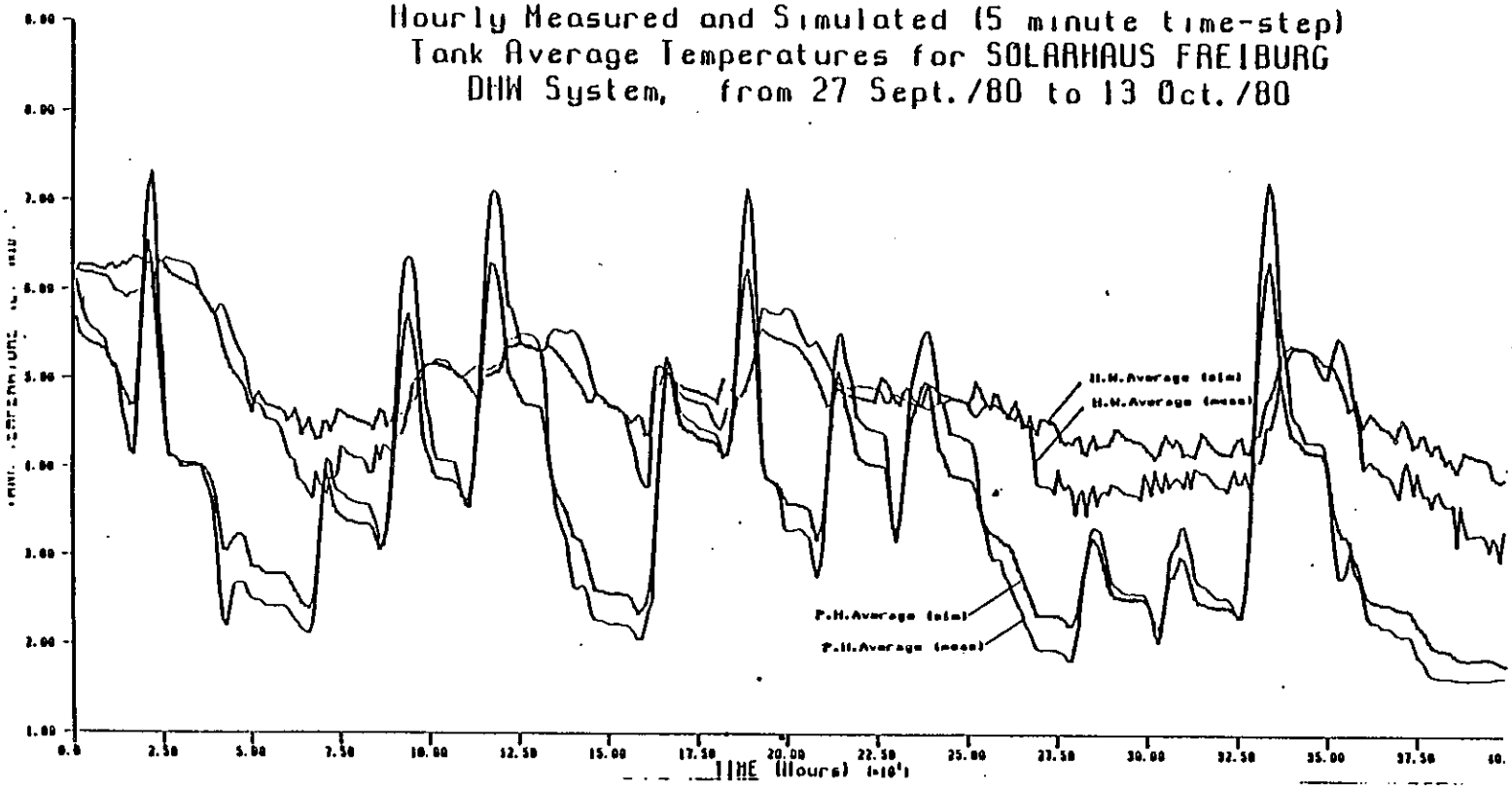

Figure 3.2.7 - WATSUN Simulation - Temperature Profiles
Sept. 27 - Oct. 13, 1980

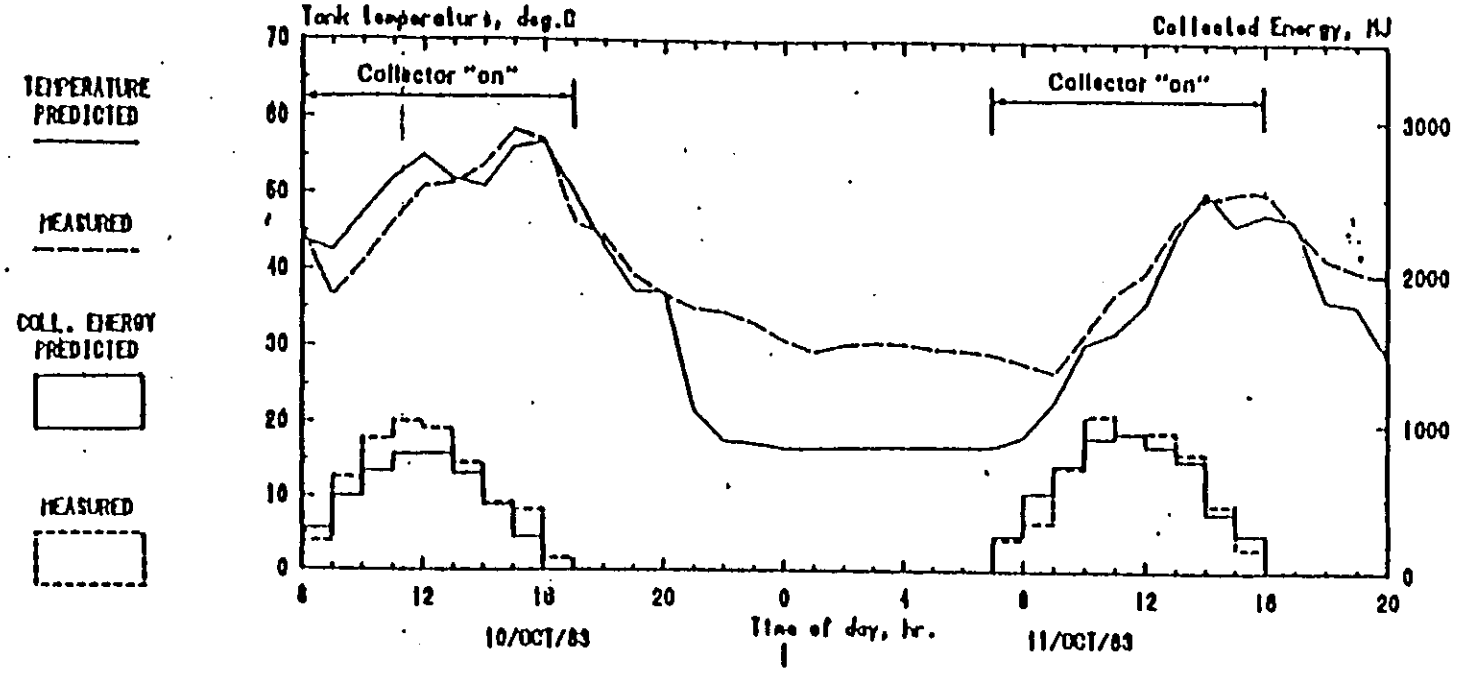

Comparison between measured and predicted collected energy and solar tank temperatures.

Figure 3.2.8 - WATSUN Simulation - Temperature Profile for Provost Oct. 10-11, 1983

Table 3.2.4 - Comparison of Simulated and Measured Energies for Solar Haus Freiburg

TIME	Average Hourly Radiation (kW_h) on Collectors (while operating) (H001)		Solar Energy (kW_h) Collected (Q112)			Solar Energy (kW_h) Delivered to Storage			Energy (kW_h) from Auxiliary		
1980	Meas.	WATSUN (Total)	Meas.	WATSUN	Error	Meas.	WATSUN	Error	Meas.	WATSUN	Error
10 Oct	(18.5)	22.4	106.3	114.6	+7.8%	92.9	96.8	+4.2%	28.3	30.7	+8.5%
30 Sep	(14.2)	15.9	75.2	81.3	+8.1%	65.2	68.0	+4.3%	21.8	23.3	+6.9%
8 Oct	(5.9)	7.3	28.5	31.3	+9.8%	27.9	26.6	-4.7%	32.6	39.4	+20.9%
27 Sep to 14 Oct	(9.5)	10.7	739.5	802.4	+8.5%	681.7	681.7	0%	236.6	301.9	+27.6%

Table 3.2.5 - Comparison of Simulated and Measured Energies for Provost

TIME	Incident Energy (GJ)		Solar Energy Collected (GJ)			Delivered Energy (GJ)		
	Meas.	WATSUN	Meas.	WATSUN	Error	Meas.	WATSUN	Error
Oct /83	202.0 (logging malfunc-tion)	180.6	92.9	89.5	-3.7%	89.3	89.4	+0.1%
Nov /83	88.8	87.4	40.5	42.5	+4.9%	44.3	48.7	+9.9%
Total	290.8	268.0	133.4	132.0	-1.0%	133.6	138.1	+3.4%

Differences between actual and predicted results occur mainly due to two factors: (a) differences between actual and modelled behaviour, and (b) differences between parameters and inputs in the actual and modelled system. The first concerns with the modelling philosophy while the second is generally due to either lack of data or changes brought about during construction phase of a system.

Table 3.2.6 shows some of the key parameters which were subject to alterations during modelling and simulation processes. It is evident that in order to have some confidence in the results of simulation studies it is highly desirable to perform sensitivity studies on a number of key parameters. This would allow one to consider a subset of parameters for detailed modelling and evaluation.

In terms of comparison between WATSUN and TRNSYS, the results show that in spite of simplicity of modelling technique used in WATSUN the results were quite comparable to a considerably more complex model using finer timesteps. This may be due to the very nature of the physical processes being simulated which are relatively slow in time and due to the fact that on a cyclical basis (daily and yearly) over and under predictions cancel each other. The speed of calculations and simplicity of user interface, particularly in the case of standard prepackaged systems (such as domestic hot water heating systems and industrial process heating systems) make WATSUN a useful tool in design sizing and sensitivity studies. However, it should be noted that for more detailed studies involving shorter time steps and other system configurations, TRNSYS provides greater versatility.

3.4 U.S.A.

3.4.0 Systems & Models Used

System types currently implemented in DAYSIM are used for comparison. One space heating and DHW system, Figure 3.4.1, and one space cooling and DHW system, Figure 3.4.2, are modelled for the validation. Both systems are liquid heat transfer fluids in the collector with a double loop arrangement. An ethylene glycol-water mixture is the fluid in the collector loop and a counter flow heat exchanger is used to transfer heat to the main storage tank. Energy in the main storage is then distributed to either space conditioning or DHW load.

The system parameters used in these simulations are listed in Table 3.4.1. These particular parameters were chosen to be representative of those in systems actually used in Colorado State University Solar House 1. This selection was made to facilitate the eventual comparison of TRNSYS and DAYSIM predictions with measured results.

Table 3.2.6 - List of Key Parameters

Collector Loop	Tank
Collector Parameters, $F'U_L$	Heat Loss Coefficients, UA
Capacitance, C	Stratification Factor
Temperature Settings, ΔT - on, off	
Mass Flow Rate	
Pipes	Exchanger
Loss Factor, UA	Effectiveness, ϵ
Capacitance	
Electrical Auxiliary Heating	Load
On-Off Control	Mass Flow Rate and Set Point Temperature

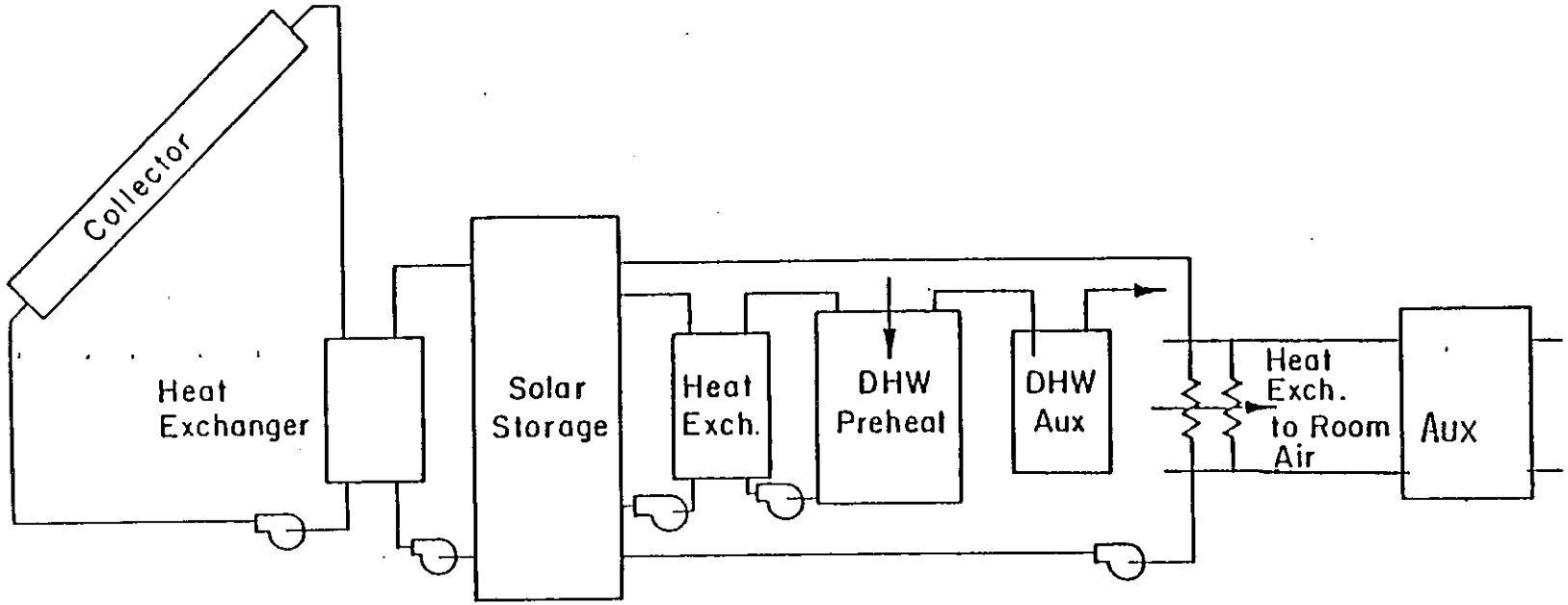

Figure 3.4.1 - Space and Service Water Heating System with Series Auxiliary

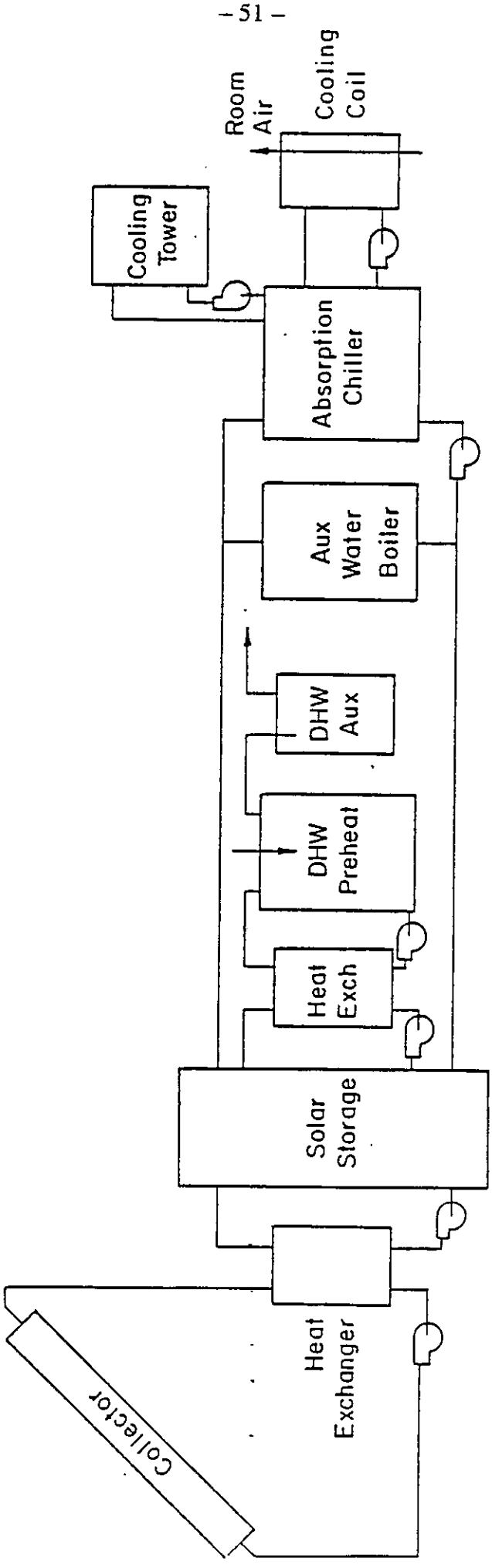

Figure 3.4.2 - Solar Cooling System

Table 3.4.1 - System Parameters

Collector

Area = 44.7 m^2
$F_R(\tau\alpha)$ = .77
$F_R U_L$ = 7 kJ/hmr^2
collector flow rate = 400 kg/hr
collector fluid C_p = 3.9 kJ/kg°C

Slope = 45°
Azimuth = 0°
piping UA = 50 kJ/hr°C

Heat Exchanger

UA = 21,000 kJ/hr°C
flow rate to storage = 1500 kg/hr

Storage

Volume = 4.35 m^3
C_p = 4.19 kJ/kg°C
UA = 23 kJ/hr°C
no stratification, one node
initial temperature = 25°C

Loads

$UA_{house,\ heating}$ = 1000 kJ/hr°C T_{house} = 20°C
$UA_{house,\ cooling}$ = 2000 kJ/hr°C T_{house} = 23°C
no solar gain or internal heat generation
main storage tank losses are to conditioned space
heating auxiliary: series
cooling auxiliary: series

Domestic Hot Water

300 kg per day at 60°C
3 instantaneous withdrawals per day
preheat tank volume = .300 m^3
main water temperature = 10°C

Both TRNSYS and DAYSIM are capable of a more sophisticated simulation of more detailed systems, in at least some respects. The objective here was not to test every capability, but to maintain strict comparability.

3.4.1 Model Setup & Validation Procedure

Several simplifying assumptions are made in these simulations so that a minimum number of changes to standard TRNSYS components and standard DAYSIM configurations need be made.

Collector	- liquid based with constant $F_R U_L$, $F_R(\tau\alpha)$ and no capacitance
Heat Exchanger	- specified by overall heat transfer coefficient
Storage Tank	- fully mixed with UA losses to the surrounding space
DHW Subsystem	- two tank with no heat exchangers or tank losses
DHW Load	- three equal energy draws daily
Heating/Cooling Load	- from UA model with no capacitance, internal heat generation with no capacitance
Absorption Chiller	- constant condensing water temperature

The energy distribution system is controlled so that solar energy is supplied to meet space heating or chiller demands until a minimum temperature of available solar energy is reached. After this point, auxiliary subsystems supply all energy demands.

The procedure followed in comparing DAYSIM with TRNSYS is illustrated in Figure 3.4.3. A detailed TRNSYS model using Typical Meteorological Year (TMY) weather data for input is used as a benchmark for comparison (TRNSYS, TMY). The TMY radiation and ambient temperature data are fit with daily cosine curves for use as input to DAYSIM. Hourly data are then recalculated from the cosine curves and used as input to another TRNSYS simulation otherwise identical to the first one (TRNYS, COSINE). Comparing the results of the two TRNSYS runs isolates the effects of using a particular cosine weather data fit versus using real hourly weather data. The comparison of results between DAYSIM and the second TRNSYS run, both of which use the same data, indicates differences that result primarily from the different simulation techniques. A further comparison can be made between DAYSIM and TRNSYS using TMY hourly data to show the bottom line differences of the combined effects of different simulation technique and different weather input representation.

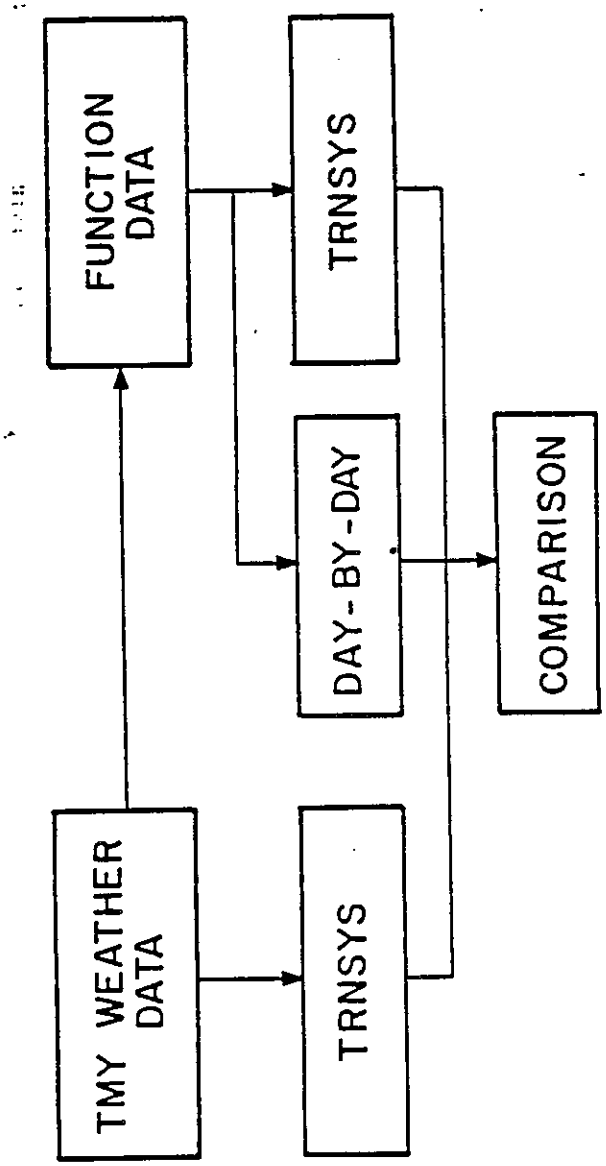

Figure 3.4.3 - Validation Procedure

The simulations described above were run for three locations. The space heating and domestic hot water system was run for three heating seasons using weather data from Madison, Washington, and Fort Worth. The space cooling and domestic hot water system was run for two cooling seasons using Fort Worth and Washington weather data.

3.4.2 Results of Validation Study

Table 3.4.2 presents the major results for TRNSYS using TMY, TRNSYS using cosine data and DAYSIM. The resulting fractional differences between TRNSYS, TMY and DAYSIM, and between TRNSYS Cosine and DAYSIM are also shown. The comparison of these fractional differences indicates the relative error induced by using functional representation of weather data and that induced by using an event dependent simulation technique.

The results in Table 3.4.2 indicate a moderate difference of 4.8% between DAYSIM and TRYSYS, TMY at Madison for energy collected. Of this total, a difference of about 1.7% appears to be attributable primarily to differences in radiation weather data. The observed difference in solar energy delivered to space heating and hot water loads appear to be due to the fact that more energy was collected in the DAYSIM simulation. The calculated space heating loads for all three simulations compare favourably, indicating that ambient temperature was satisfactorily represented by a cosine function. The differences induced by the poor fit to hourly radiation data can be corrected to a large extent by more sophisticated curve fitting techniques and should be treated in further work. The differences in energy collected that are not due to differences in weather data are more troublesome, however, since they appear to be due to the simulation technique.

Results for Fort Worth shown in Table 3.4.3 are even more accurate. Solar energy collected in DAYSIM is within 1.5% of that in TRNSYS, Cosine and within 0.5% of that in TRNSYS, TMY. Calculation of solar energy delivered to load is again within 1.5% in both cases.

Results in Table 3.4.4 for the Washington heating season show only a 1.5% difference in energy collected between DAYSIM and TRNSYS, TMY. This comparison is much closer than that shown for the Madison heating season, but differences due to the data fit are still over 3%. For this case, however, TRNSYS, Cosine has a lower value for energy collected than does TRNSYS, TMY, whereas for Madison it had a higher value. Once again the calculated space heating loads for all three are very close, confirming a good temperature fit.

Table 3.4.5 shows results for the cooling season in Washington. Results are good for solar collected, but not good for solar delivered. This is due to assumptions used in chiller performance in DAYSIM. The cooling load in Washington is not very large and little auxiliary is

Table 3.4.2 - Heating Season Performance Madison, Days 1-90, 274-365

	Incident Solar	Solar Collected	Total Heating Load	Solar to Heating Load	Storage Loss	Solar to DHW	Solar Dumped
TRNSYS, TMY	91.95	47.33	90.36	40.21	2.079	5.577	.2640
TRNSYS, Cosine	95.17	48.86	90.32	41.43	2.123	5.683	.2065
DAYSIM	95.17	49.70	90.19	42.41	2.192	6.277	.2122
$1 - \frac{\text{TRNSYS,TMY}}{\text{DAYSIM}}$	.034	.048	-.002	.052	.052	.111	-.244
$1 - \frac{\text{TRNSYS,Cosine}}{\text{DAYSIM}}$	0.	.017	.001	.023	.031	.097	.027

All quantities in Gigajoules

Table 3.4.3 - Cooling Season Performance Fort Worth, Days 152-243

	Incident Solar	Solar Collected	Total Cooling Load	Solar to Cooling Load	Storage Loss	Solar to DHW	Solar Dumped
TRNSYS, TMY	84.57	41.53	27.94	32.10	3.091	5.051	.3262
TRNSYS, Cosine	83.68	40.68	28.01	32.52	3.065	5.047	.3053
DAYSIM	84.09	41.27	28.68	32.56	3.237	5.520	.3010
$1 - \frac{TRNSYS,TMY}{DAYSIM}$	.006	-.006	.026	.014	.045	.085	-.084
$1 - \frac{TRNSYS,Cos}{DAYSIM}$	.005	.014	.023	.001	.053	.086	-.014

All quantities in Gigajoules

Table 3.4.4 - Heating Season Performance Washington, Days 1-90, 274-365

	Incident Solar	Solar Collected	Total Heating Load	Solar to Heating Load	Storage Loss	Solar to DHW	Solar Dumped
TRNSYS, TMY	98.38	50.00	62.32	38.77	3.030	6.630	2.230
TRNSYS, Cosine	98.97	48.13	62.49	37.73	2.905	6.526	1.670
DAYSIM	99.01	49.25	62.13	37.97	2.968	7.079	1.663
$1 - \frac{\text{TRNSYS,TMY}}{\text{DAYSIM}}$	.006	-.015	-.003	-.021	-.021	.063	-.341
$1 - \frac{\text{TRNSYS, Cosine}}{\text{DAYSIM}}$	0.	.023	-.006	.006	.021	.078	-.004

All quantities in Gigajoules

required. The current chiller model is adequate when much more cooling is required, as in the case of Fort Worth. More work is needed on the chiller model.

Table 3.4.6 shows heating season performance in Fort Worth, and compares results for two different day-length constants. Results seem substantially better for a day-length constant of 0.9 than for 1.0 for solar collected, solar delivered, storage loss and energy dumped. This is because the use of a day-length constant allows better fit to radiation in the middle of the day.

Daily performance comparisons between TRNSYS using TMY and DAYSIM for the Washington heating season and the Fort Worth cooling season are presented in Figures 3.4.4 through 3.4.7. Figures 3.4.4 and 3.4.5 show that the maximum differences in solar energy collected are on the order of one percent or less of the 300 to 450 MJ average daily values for both cities. The differences are also fairly symmetric about the mean difference, more so for Washington and less so for Fort Worth. The greater central clustering and greater skewness of the Washington differences may be due to the overly simplistic chiller model and its consequent effect on storage tank temperature histories.

Figures 3.4.6 and 3.5.7 indicate that there is a less close agreement for solar energy to load than for solar energy collected. The high degree of central clustering in Washington does not indicate a close match for TRNSY using TMY and DAYSIM predictions of within a few percent for most days. However, the natural tendency for any two models' storage temperature predictions to lead or lag with consequent variation in the capability of storage to meet each day's load, and the chiller model simplicity may account for the greater variation in the remaining daily difference.

3.4.3 Discussion and Conclusions

The basic simulation structures for DAYSIM and TRNSYS are quite different. TRNSYS achieves high accuracy only by using small timesteps. DAYSIM achieves high accuracy by functional representation of the data and directly solving system equations. Compared to TRNSYS, DAYSIM has short running times, short data input, no problems with convergence, no tolerance settings, exact solution to the equations, and it is relatively easy to use. In fact, for such information as collector turn-on time, or time of switch from solar to auxiliary DAYSIM may be more accurate due to the exact calculation permitted by the analytic nature of the data. Accuracy of this information in TRNSYS depends on the timestep chosen.

Results from DAYSIM demonstrate that day-by-day simulation can be a good alternative to simulations requiring great amounts of computer time and hourly data, especially for long term analysis. Functional representation of the data is a powerful technique for maintaining high accuracies while reducing computer time. This is accomplished by the use of event-determined

Table 3.4.5 - Cooling Season Performance, Washington, Days 152-243

	Incident Solar	Solar Collected	Total Cooling Load	Solar to Cooling Load	Storage Loss	Solar to DHW	Solar Dumped
TRNSYS, TMY	73.58	30.48	10.65	17.51	3.452	5.071	4.454
TRNSYS, Cosine	73.40	29.35	10.79	17.17	3.424	5.066	3.679
DAYSIM	73.26	28.96	12.13	14.82	3.671	5.520	4.969
$1 - \frac{\text{TRNSYS,TMY}}{\text{DAYSIM}}$	-.004	-.052	.122	-.182	.060	.081	.104
$1 - \frac{\text{TRNSYS, Cosine}}{\text{DAYSIM}}$	-.002	-.013	.110	-.158	.067	.082	.260

All quantities in Gigajoules

Table 3.4.6 - Heating Season Performance Fort Worth, Days 1-90, 274-365

	Incident Solar	Solar Collected	Total Heating Load	Solar to Heating Load	Storage Loss	Solar to DHW	Solar Dumped
TRNSYS, TMY	130.0	62.49	34.06	30.40	5.955	9.344	16.93
TRNSYS, Cosine, DLC = 1	130.1	59.59	34.15	30.20	5.834	9.275	14.28
DAYSIM, DLC = 1. (DLC=.9)	130.5	(62.86) 60.34	32.69	(30.18) 30.04	(5.960) 5.866	(10.12) 10.07	(16.05) 13.86
$1 - \frac{\text{TRNSYS, TMY}}{\text{DAYSIM}}$ DLC = 1.(DLC=.9)	.004	(.006) -.036	-.042	(-.007) -.012	(.001) -.015	(.077) .072	(-.054) -.222
$1 - \frac{\text{TRNSYS, Cosine}}{\text{DAYSIM}}$ DLC=1.	.003	.012	-.045	-.005	.005	.079	-.030

All quantities in Gigajoules

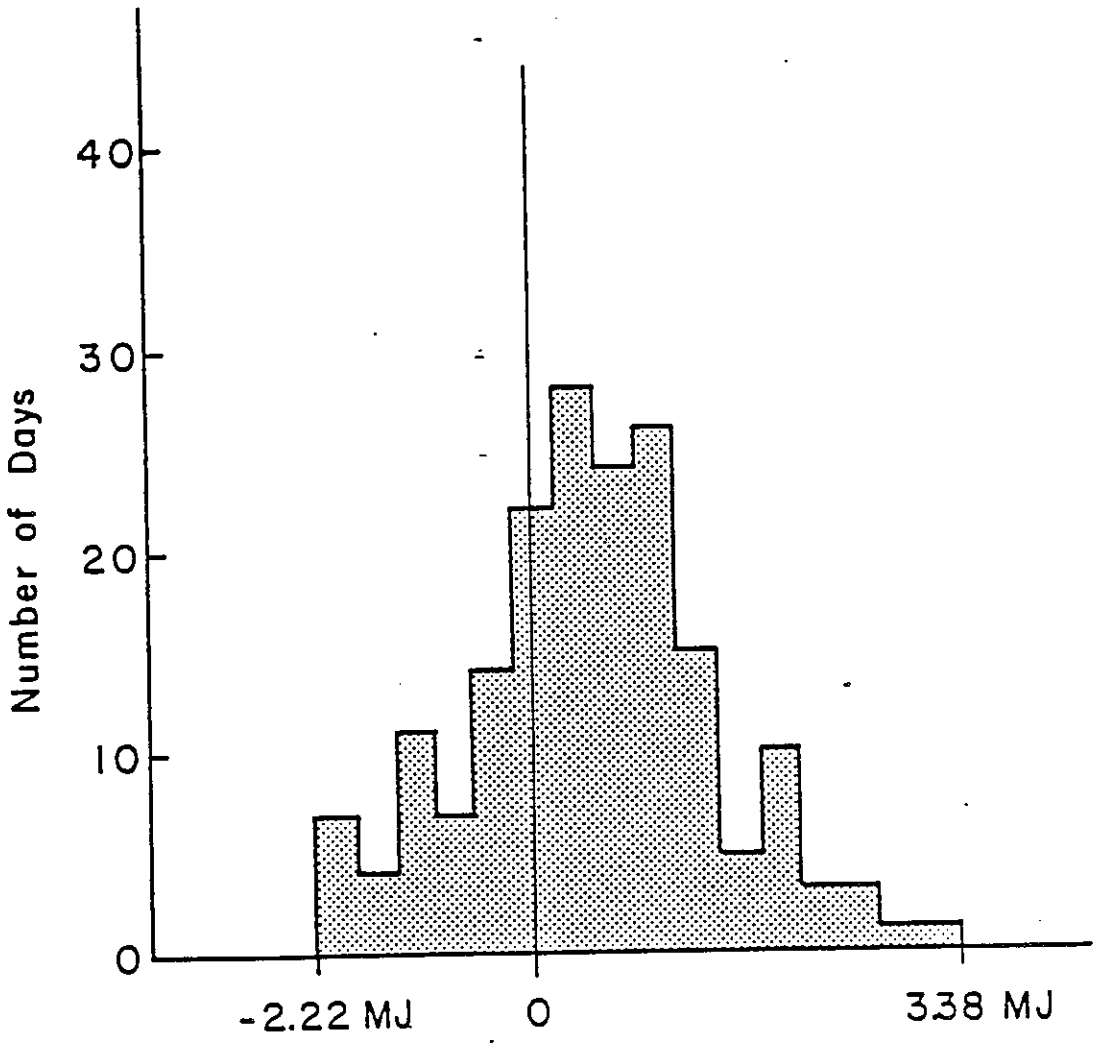

Figure 3.4.4 - Washington Heating Season Differences in Daily Solar Collected between TRNSYS Using TMY and DAYSIM

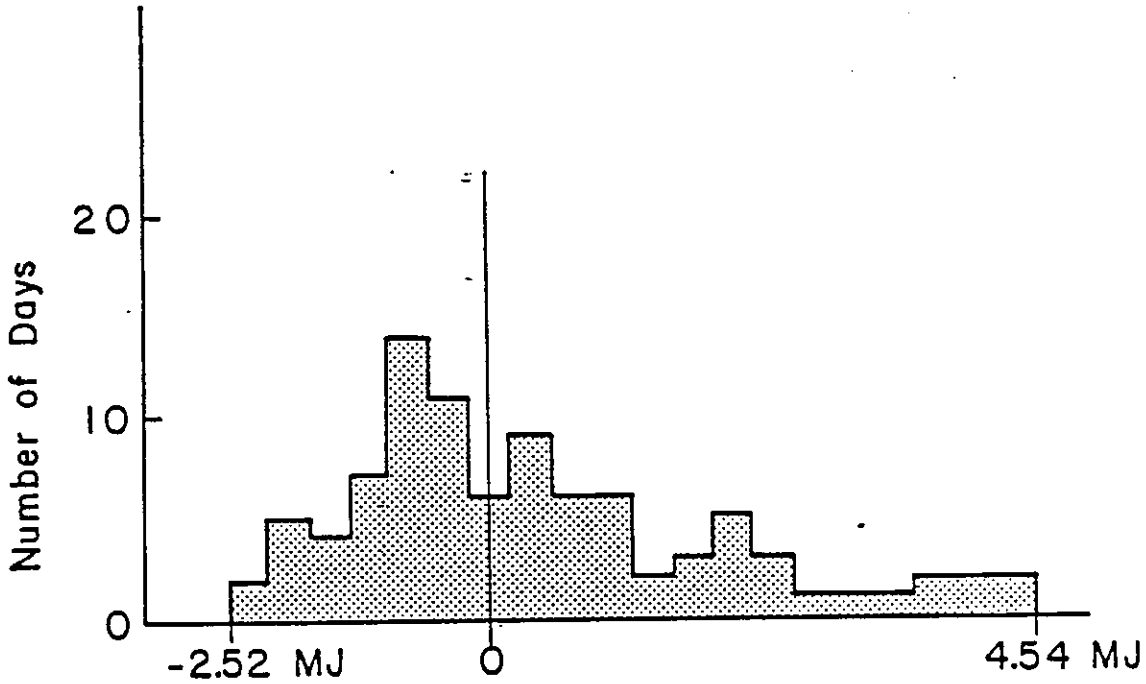

Figure 3.4.5 - Fort Worth Cooling Season Differences in Daily Solar Collected between TRNSYS using TMY and DAYSIM

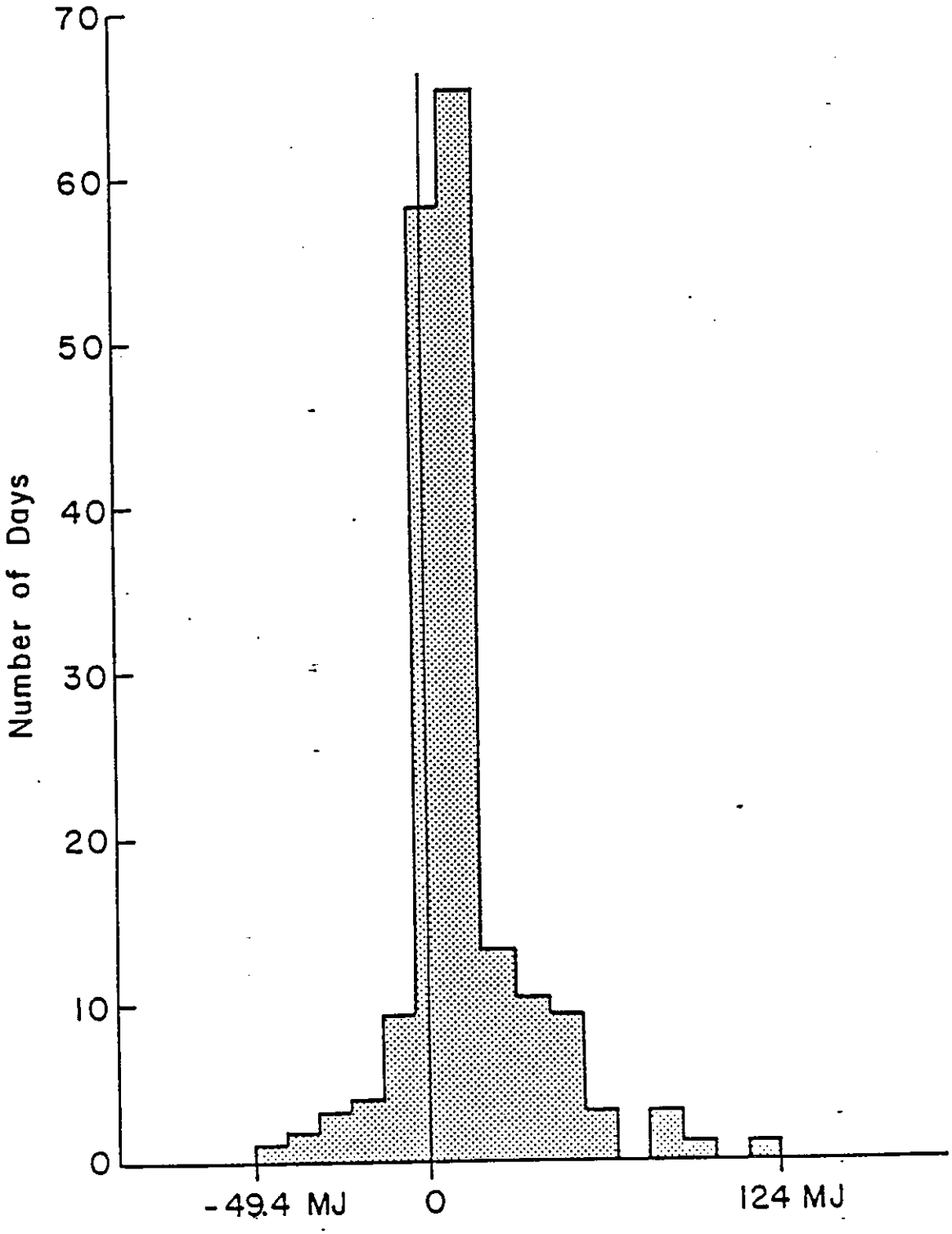

Figure 3.4.6 - Washington Heating Season Differences in Daily Solar to Load between TRNSYS Using TMY and DAYSIM

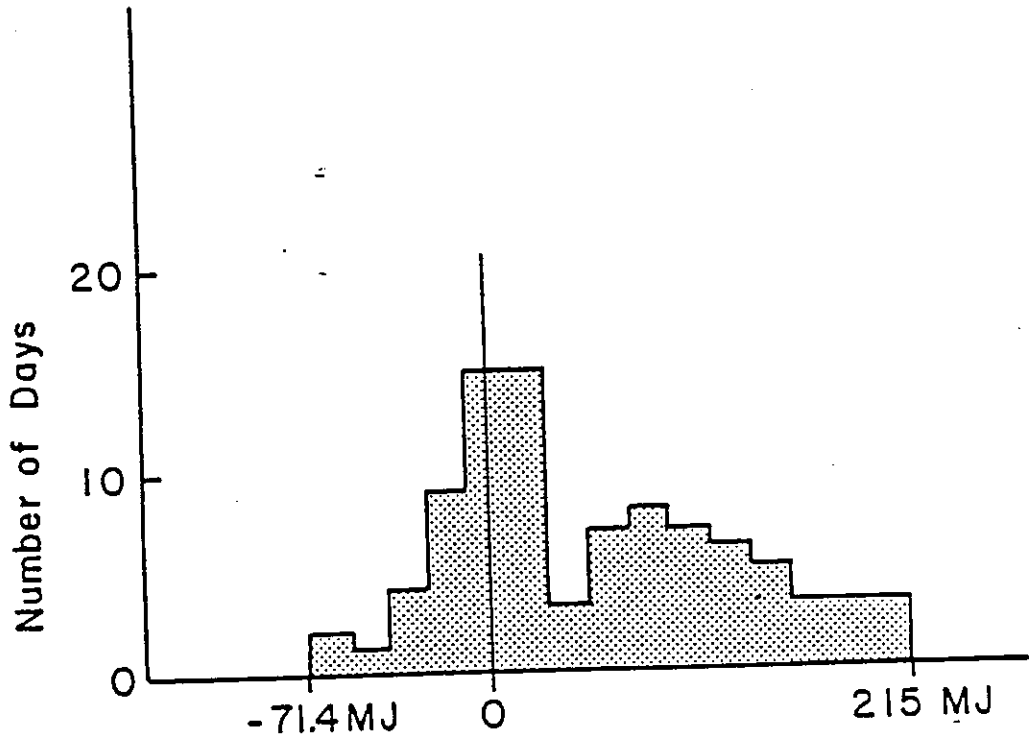

Figure 3.4.7 - Fort Worth Cooling Season Differences in Solar to Load between TRNSYS Using TMY and DAYSIM

timesteps which may be calculated exactly from the functional form of the data. DAYSIM seems particularly well-suited to uses where accurate long term results and moderate levels of detail are needed. Where greater levels of detail are sought, use of TRNSYS may be preferable; once TRNSYS has been set up for a particular system then some changes to the system are more readily accomplished with TRNSYS.

3.5 West Germany

3.5.0 Solar System Description

Figure 3.5.1 shows the SOLARHAUS FREIBURG DHW-System with the location of temperature and flow sensors. The indicated principal energy quantities have been used for the validation against measured data.

Figure 3.5.2 shows the control characteristics of the collector pump, the heat-exchanger operation and of the electric auxiliary heater in the hot water storage. The definitions of the component parameters are given in Figure 3.5.3.

3.5.1 Model Setup and Validation Procedure

Numerical values of the component parameters are listed in Table 3.5.1.

The initial temperatures of all components are taken from the first data element of the simulation/validation period; after this initialisation, the only input-data to the validation program are the measured values of the incident radiation, the ambient temperature and the warm water consumption which are taken as driving functions. The validation can then be done in time steps of 5-minutes, hours or days.

3.5.2 Results of the Validation using SOLARHAUS FREIBURG DHW-System Data

Solar Circuit

The following three paragraphs describe some validation results of a continuous period of six days.

Figure 3.5.4 shows very good agreement between the measured and calculated solar energy (delivered by the collector array Q112 and supplied to the preheat storage tank Q200 for a typical day with extremely fluctuating incident radiation H100. The daily prediction accuracy is 2.1% for Q112 and -1.7% for Q200, which is only about 1/5 of the daily piping heat loss between collector array and storage tank. The scatter of the calculated instantaneous power

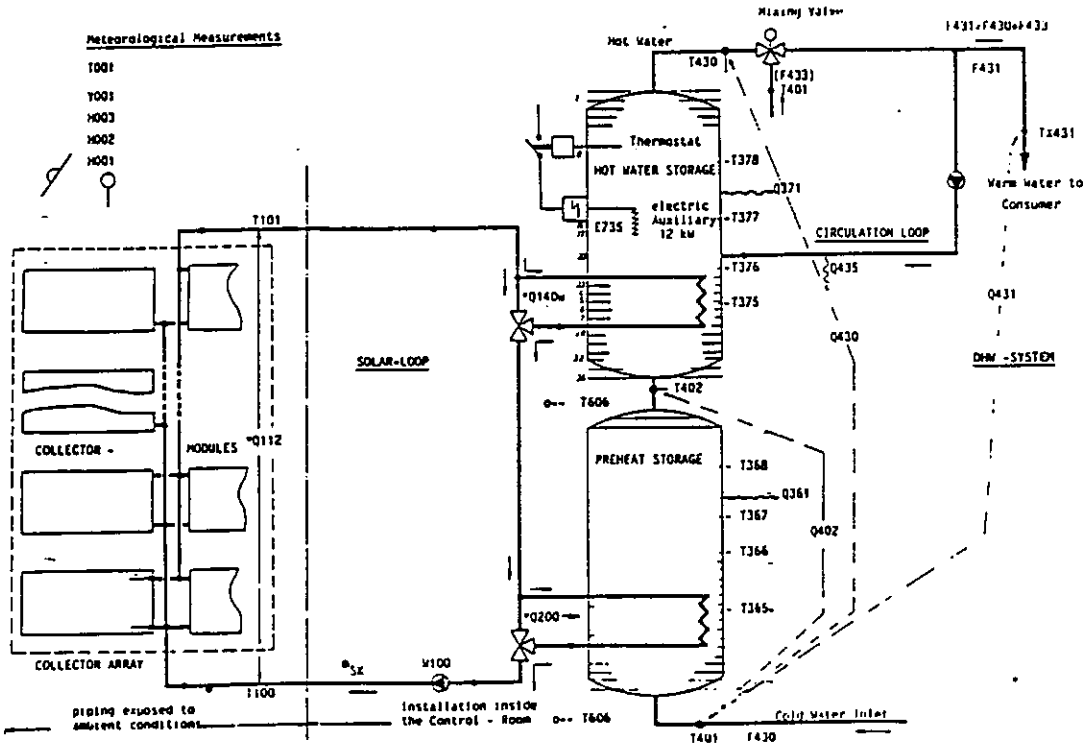

Figure 3.5.1 - Solarhaus Freiburg DHW-Systems Schematic

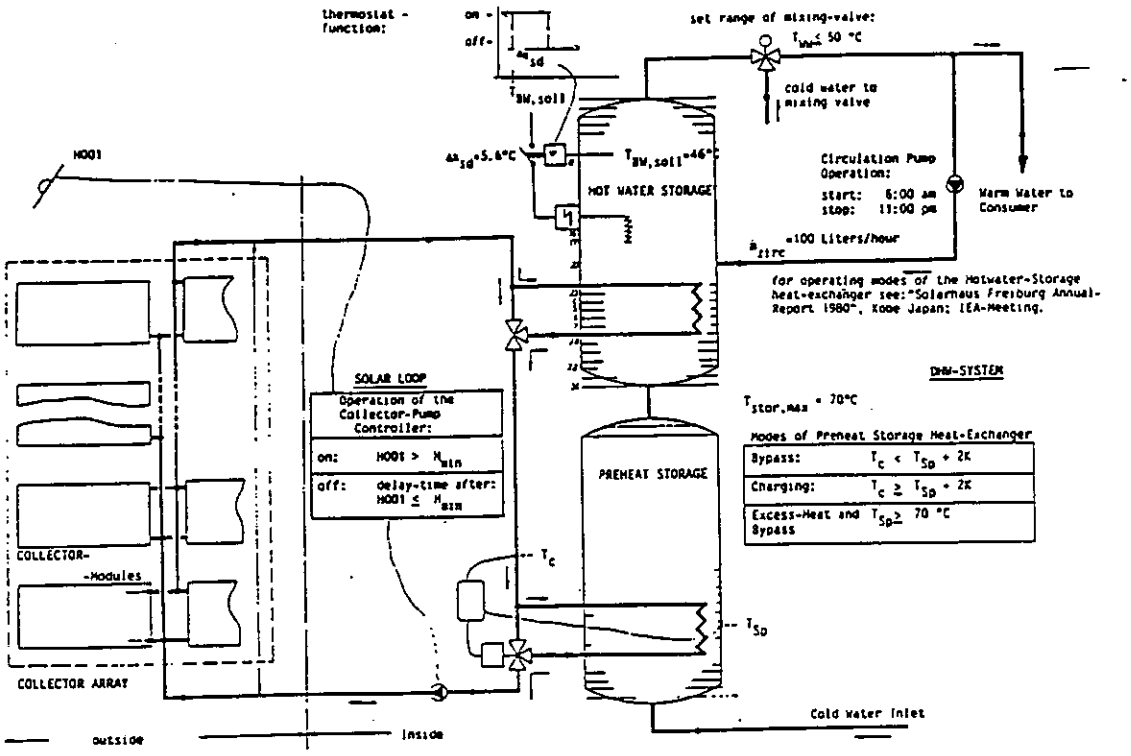

Figure 3.5.2 - Solarhaus Freiburg DHW - System Control Features

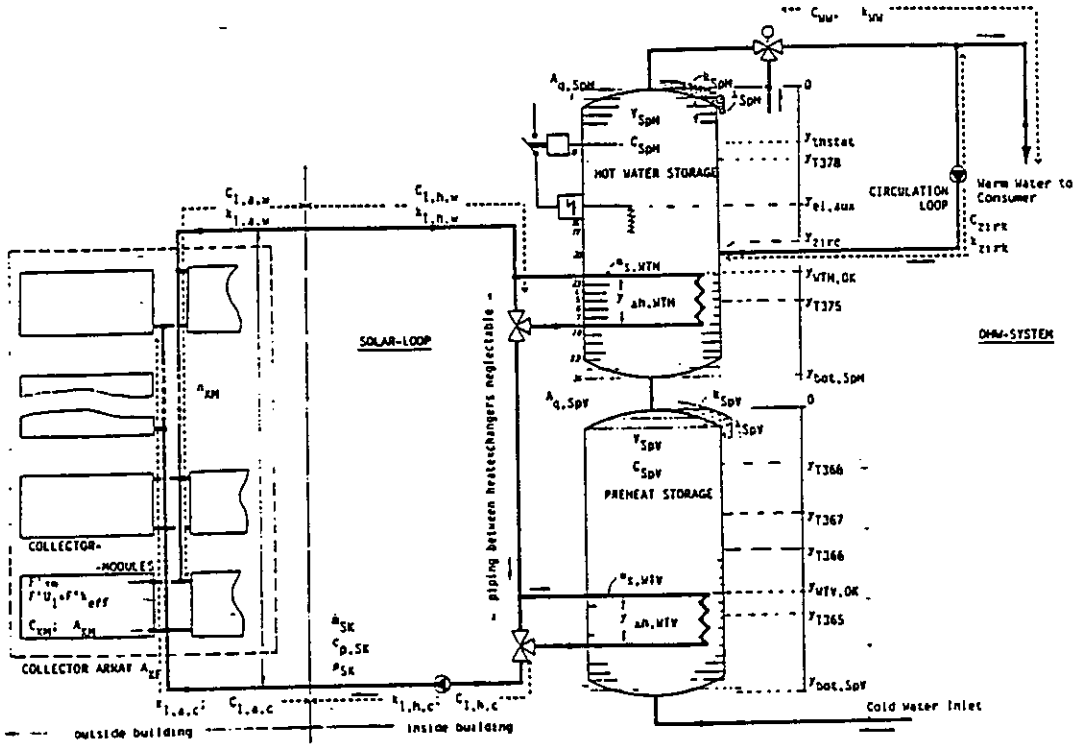

Figure 3.5.3 - Solarhaus Freiburg DHW - System Component parameters

Table 3.5.1 - Component Parameters of the SOLARHAUS FREIBURG DHW-System

Parameters of the Corning Glass Collector-Module and Collector-Array

$F'\tau\alpha$	65.9	%	Transmission-Absorption Coefficient
$F'k_{eff}$	1.37	W/m2K	Heat-Loss Coefficient
C_{KM}	3.39	kJ/K/m2	Heat-Capacity per Unit of Aperture Area (incl. heat-transfer medium)
A_{KM}	1.39	m2	Module Aperture - Area
A_{KF}	33.3	m2	Array Aperture - Area (= 24 Modules)
$\dot{m}_{SK}$	1600	Liter/hour	Volumetric Flow-Rate of heat transfer fluid
$\dot{\rho}_{SK}$	1.0245	kg/Liter	density of heat transfer fluid at 40 deg C
$c_{p,SK}$	3817.6	J/kg/K	specific heat of heat transfer fluid at 40 deg C
H_{min}	130	W/m2	radiation threshold for start of Collector-Operation
$t_{off,SK}$	5	min	delay-time for stop of Collector-Operation

Parameters of the Piping of the Solar-Loop

$k_{l,a,w}$	6	W/K	piping heat-loss parameter Collector-Modules to T101
$C_{l,a,w}$	87.5	kJ/K	piping capacity Collector-Modules to T101
$k_{l,h,w}$	8.2	W/K	piping heat-loss parameter T101 to preheat- and DHW-Storage heat-exchangers
$C_{l,h,w}$	267	kJ/K	piping capacity T101 to preheat- and DHW-Storage heat-exchangers
$k_{l,h,c}$	8.2	W/K	piping heat-loss parameter Storage Tank heat-exchanger to T100
$C_{l,h,c}$	267	kJ/K	piping capacity Storage Tank heat-exchanger to T100
$k_{l,a,c}$	6	W/K	piping heat-loss parameter T100 to Collector-Modules
$C_{l,a,c}$	119	kJ/K	piping capacity T100 to Collector-Modules

Parameters of Heat-Exchangers and Storage Tanks.

Preheat-Storage		DHW-Storage			
$\alpha_{s,WTV}$	1000	$\alpha_{s,WTH}$	1000	W/K	specific heat exchange rate
$y_{\Delta h,WTV}$	0.25	$y_{\Delta h,WTH}$	0.25	m	vertical extension
V_{SpV}	1500	V_{SpH}	1000	Liter	Storage Volume
C_{SpV}	6596	C_{SpH}	4450	kJ/K	Storage Capacity
k_{SpV}	9	k_{SpH}	5.9	W/K	heat-loss parameter
$\lambda_{SpV,eff}$	1.45	$\lambda_{SpH,eff}$	0.85	W/m/K	effective vertical heat conduction
$A_{q,SpV}$	0.95	$A_{q,SpH}$	0.64	m2	Cross-sectional Area
		E735	12	kW	Power of electrical heating resistance
		$\vartheta_{BW,soll}$	46	°C	DHW-Temperature Set-point
		$\Delta x_{sd,BW}$	5.6	K	Dead-Band of the electrical heating thermostat

Parameters of the DHW-Distribution System and Circulation-Loop

C_{WW}	62	kJ/K	Thermal Capacity of DHW-Distribution Piping
k_{WW}	6	W/K	Heat-loss parameter of DHW-Distribution Piping
C_{zirk}	127	kJ/K	Thermal Capacity of Circulation Piping
k_{zirk}	10	W/K	Heat-loss parameter of Circulation Piping
$t_{on,zirc}$	06:00	local Time	Start of Circulation-Loop operation
$t_{off,zirc}$	23:00	local Time	Stop of Circulation-Loop operation

yields a RMS error of ±20 W/m^2. This remaining uncertainty could probably be resolved by considering an incidence angle dependent $F'\tau\alpha$ coefficient. While comparing the energies Q112 and Q200, it is also demonstrated that the power fluctuations at the collector array are much more pronounced both in the measurements and in the simulation than they are at the storage heat exchanger. This is another proof for the validity of the selected representation of the components in the solar circuit.

The close correspondence of the measured and simulated energies under dynamic conditions shows that the steady Hottel-Whillier-Bliss collector representation has successfully been expanded to a simple one-capacity collector model.

For applications with higher operating temperatures, a second order heat-loss term may easily be integrated into this model.

Results of a continuous 43 day-long simulation period are presented in Figure 3.5.5 in the form of an autocorrelation diagram for the solar energy at the collector array Q112, with measured and calculated daily totals given on the x- and y-axis respectively. The average prediction error was -0.4% for Q112, and -1.3% for Q200. These daily results are in good agreement with the detailed comparison in Figure 3.5.4.

The linear correlation coefficients for both energies are higher than 0.99. The average daily deviation and RMS error are for Q112 - 0.1 ± 1.1 kWh/d, and for Q200 - 0.4 ± 1.5 kWh/d.

A statistical analysis of the daily scatter is shown in the error-histogram in Figure 3.5.6. The relative distribution of the energy from the collector array Q112 is plotted with respect to the daily percent prediction error (measured-predicted), which is partitioned in error bins of 1%.

From the small average daily deviation, it can be concluded that the gain and loss mechanisms in the solar loop are correctly modelled. The symmetrical profile of the error histogram shows that the prediction errors are randomly distributed. This indicates, that there are no essential systematic errors in the solar loop part of the component model.

Validation of the Temperature Profiles in Storage Tanks

The comparison of measured and simulated temperature profiles in storage tanks is the most severe check for the consistency of a simulation model. In the absence of daily temperature-corrective control strategies, long term accumulation effects may be detected by this means.

During the development phase of the model, the storage tank was first partitioned in 4 horizontal layers in order to describe the vertical temperature stratification. The first comparisons of the measured and simulated temperature profiles showed nearly identical values when the

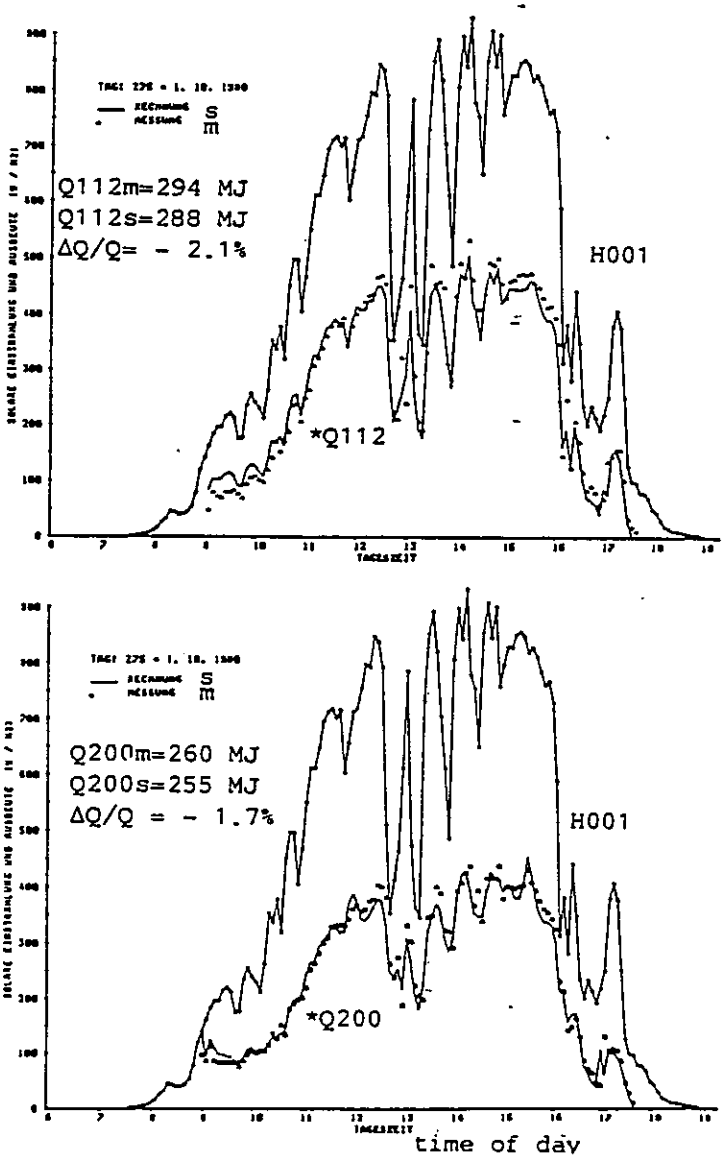

Figure 3.5.4 - Measured and Simulated Solar-Energy in the Collector Loop

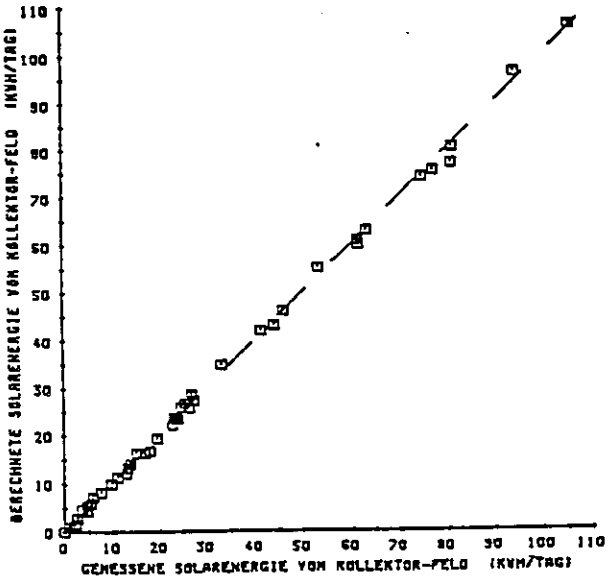

Figure 3.5.5 - Autocorrelation of measured (x) and simulated (y) $Q112$ for 43 days

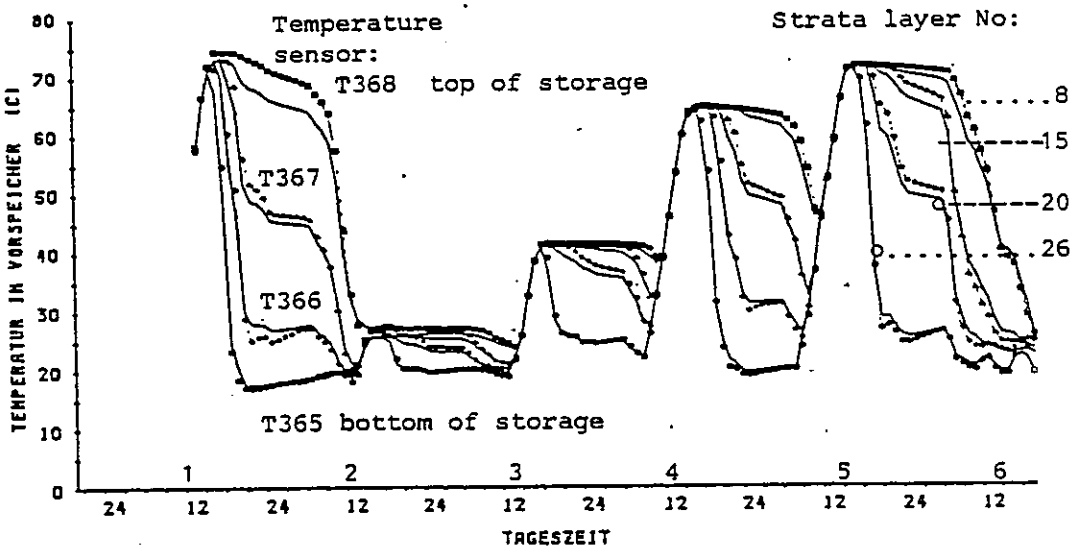

Figure 3.5.6 - Measured and Calculated Pre-heat Storage Tank Temperature Evolution during 6 consecutive days in 4 characteristic layers using a model with 34 horizontal layers

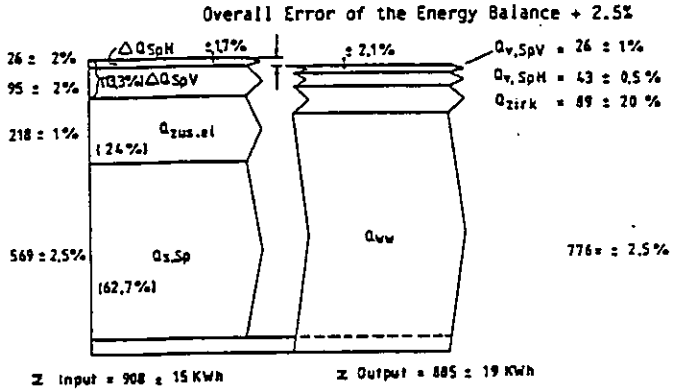

Figure 3.5.7 - Measured Energy Balance

storage tank was heated to a uniform temperature distribution, which was in good agreement with the accurate closure of the storage energy balance. However, temperature deviations of up to 30K were observed while discharging the storage tank. The reason for this observation was, that the step-function-like temperature profile, which is measured by a discrete temperature sensor must not be compared with the average temperature of a relatively large part of the storage (1/4 of the storage) which is determined by the differential equation. It was concluded from this experience, that the correct simulation of the energy balance of a storage tank does not imply the accurate representation of its temperature profile. Therefore, the number of temperature nodes in a tank model has to be defined in relation to the application of the model.

One of the important applications of this model is the simulation of control-strategies in solar systems. Of course, the realistic simulation of control-decisions requires the temperature in the vicinity of the appropriate temperature sensors. This requirement has been met by partitioning the storage tank into 34 horizontal layers, each represented by a temperature node. The model then accounts for the energy balance of each tank layer, including the heat conduction to and from adjacent layers.

The results of a typical, continuous validation period of 6 consecutive days are shown in Figure 3.5.6 for the preheat-storage tank. The simulation begins at about 12:00 on the first day when all 34 temperature nodes are initialized with the measured, uniform storage temperature. The plot shows the four measured temperatures (T365,...,T368, see Figure 3.5.1) and the calculated temperatures of the corresponding position inside the tank.

The measured and calculated temperature evolution shows a close agreement of the daily variation of the storage temperature in four characteristic layers, which is caused by the daily consumption of warm water and the varying delivered solar energy. During the charging mode, the compact, immersed heat exchanger supplies solar energy first to the lower storage layers in its local vicinity, while the upper layers are heated by means of convective heat transfer. The discharging mode is characterised by the inflow of cold water into the lowest tank, which creates a pronounced temperature stratification with a temperature difference from top to bottom of up to 50K.

Thus it can be concluded from the comparison of the measured and simulated temperatures, that the model simulates accurately the two basic operating modes of the storage. It has to be pointed out, that measured and calculated temperatures differ by less than 1K with a RMS error of 1.0 to 1.7K. Furthermore, the scatter remains constant with time, indicating that there are no accumulation errors in the model components describing the dynamic behaviour of the solar and DHW circuit.

Comparison of the Measured and Simulated Energy Balance and System Performance Parameters

A redundancy check of the simulation model has been performed by a comparison of the measured and calculated energy balance of the DHW-System. The inflow of energy into the system is composed of solar and auxiliary energy and the change in internal energy stored in the storage tanks (which has to be counted as positive input if the storage temperature decreased during the test period). The outflow of energy from the system consists of the energy supplied to meet the net warm water load plus the losses of the circulation loop and the hot water and preheat storages.

Figure 3.5.7 presents the measured energy balance for two continuous data periods of a total of 16 days. The specified experimental error ranges are related to the measurement uncertainties of the individual sensors and add up to an input-error of ±1.7% and to an output error of ±2.1%.

A simulated energy balance is shown for the same period in Figure 3.5.8. The individual measured and simulated energy flows differ less than their corresponding measurement accuracies. The comparison shows, that the described component model is able to calculate all energy flows in the DHW-System within the 1.5 - 2.5% accuracy of the experimental analysis.

The following table gives a comparison of measured and predicted key performance parameters required for the analysis of a system like the DHW-System:

	Measured	Predicted
Collector Array Efficiency:	47.0%	46.2%
System Efficiency:	43.4%	42.2%
Percent Solar Fraction:	62.7%	62.1%

The good agreement between theory and experiment shows that the model developed ca be applied for the precise calculation of performance parameters, which are required for the assessment of a solar system.

3.5.3 Discussion and Conclusions

The comparison of the measured and simulated energies and temperatures both in detailed resolution and over longer periods demonstrate the high level of accuracy and the internal consistency of the component model. The deviations between measurements and calculations are for all energy quantities in the range of the experimental error of 1.5 to 2.5%.

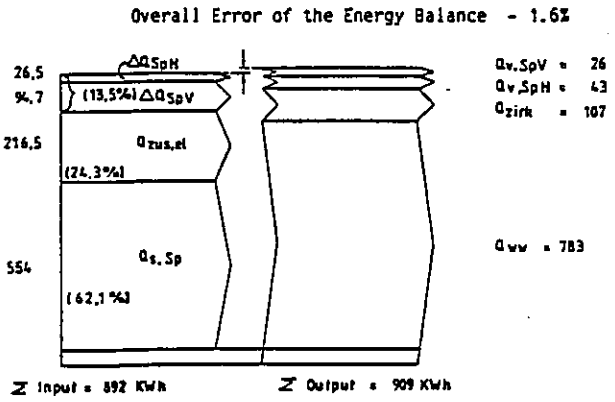

Figure 3.5.8 - Simulated Energy Balance

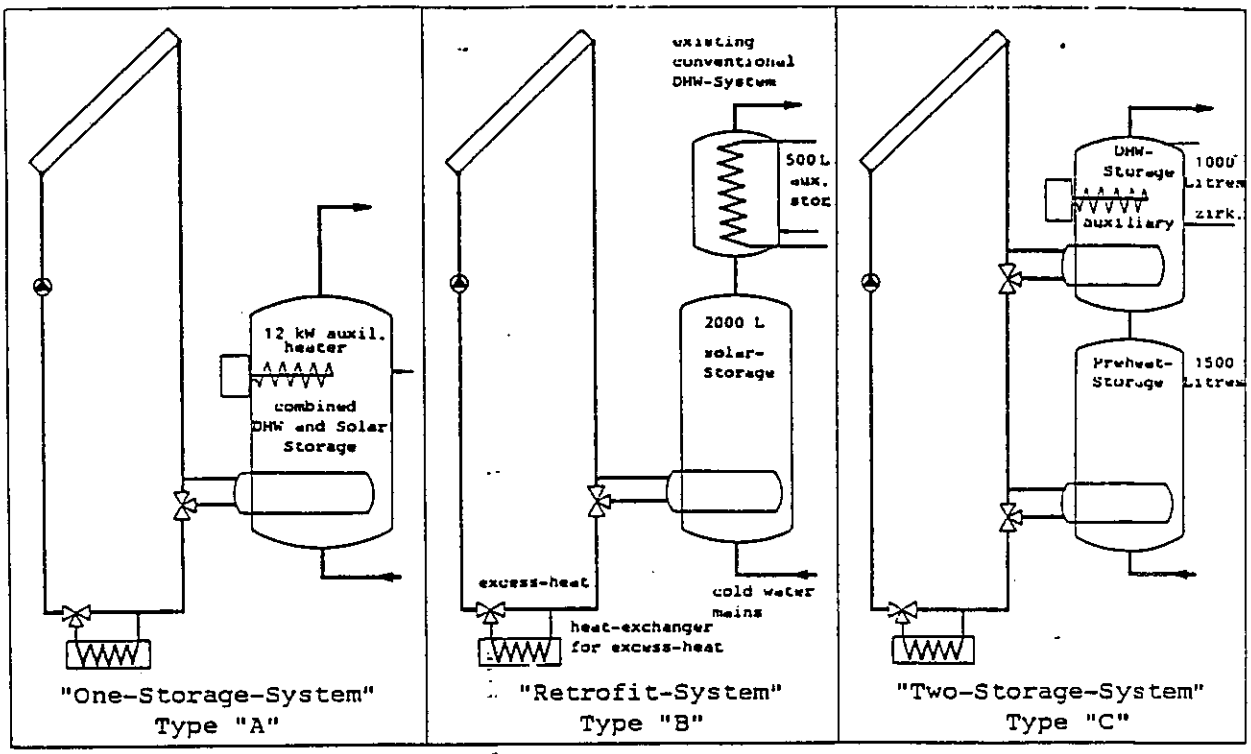

Figure 4.5.1 - Types of Solar DHW-System Investigated

The theoretical background of the model is based only on fundamental physical principles and experimentally determined component parameters. Thus, the model may be applied to the extrapolation of the experience gained in the SOLARHAUS FREIBURG DHW-System to systems with modified system configurations, other component parameters or different climate and/or load conditions.

4.0 SENSITIVITY ANALYSES

Four of the IEA member countries used the detailed models they developed to perform sensitivity studies. The topics covered were mentioned in the Introduction to this report and are treated in this chapter for each country.

4.1 Australia

In order to evaluate the importance of the various effects discussed earlier on the performance of the Sydney University Evacuated Tubular Collector on a long-term basis, 36 monthly simulations were run. Two different months were selected, a winter month (June) and a summer month (January) and collector performance was modelled for 3 different collector inlet temperatures, 50°C, 80°C and 120°C. The three groups were chosen as being fairly representative for average daily collector inlet temperatures in a domestic hot water system, a solar air conditioning or low temperature industrial heat application ($T_{min} \approx 75°C$) and a high temperature industrial process heat system.

A base case was selected for comparisons. The model of the base case incorporates all the effects which influence the performance of the S.U. Evacuated Tubular Collector, except intra array pipe losses which were neglected because they depend on specific system designs (array size, collector layout, collector mounting restriction, etc.). The features of the base case are listed below:

Base Case
- model of S.U. Evacuated Tubular Collector incorporating a copper U-tube manifold with Al-fin as described in equation (2.1.2);
- incidence angle modifier applied to beam component of radiation only;
- collector capacitance correction;
- no intra array pipe losses.

A base case with an inlet temperature of 50°C reflects closely measured conditions during June 1984 with predicted and measured daily collector outputs of 4.13MJ/m2 and 4.24MJ/m2, respectively. Measured January 1985 conditions are closer to the base case with an inlet temperature of 80°C (73°C with 9% performance difference). Five other cases were compared with

the base case. The specific features of these models are given below:

Case 1: - identical to base case, but no incidence angle modifier;

Case 2: - identical to base case, but no capacitance correction;

Case 3: - identical to base case, and incidence angle modifier applied to both beam and diffuse radiation;

Case 4: - HWB model including capacitance correction, but no incidence angle modifier;

Case 5: - HWB model, no capacitance correction, no incidence angle modifier;

4.1.1 Results

Performance predictions using Sydney weather data for June 1984 and January 1985 are summarised in Table 4.1.1 and Table 4.1.2. The two tables state predicted collector output for three different collector inlet temperatures as well as percentage deviations from the base case. Large deviations for the winter data at high inlet temperature are due to very small collector output (0.35 MJ/m^2-day). They may be somewhat misleading since these energy quantities have a minimal effect on overall yearly performance.

The effects of the various model features on predicted collector performance can be summarised as follows:

Case 1: Incidence Angle Modifier

Neglecting incidence angle modifier effects in the prediction of useful collector output of the S.U. Evacuated Tubular Collector leads to a significant underprediction of its performance. This underprediction is moderate at low to medium collector inlet temperatures (T_{ci} = 50°C: -10.95%; T_{ci} = 80°C: -16.9%) during June and becomes significant at high operating temperatures (T_{ci} = 120°C: -79.2%).

The magnitude of the deviation from the base case (which includes incidence angle modifier effects) further depends on the time of the year. For a summer month, the omission of incidence angle modifier effects are slightly smaller.

Table 4.1.1 - Predicted Collector Output of S.U. Evacuated Tubular Collector for Different Collector Model Assumptions (June 1984)

Inlet Temp.		BASE CASE	CASE 1	CASE 2	CASE 3	CASE 4	CASE 5
50 °C	Collector Output (MJ/m^2d)	4.13	3.68	4.79	4.16	3.51	4.11
	Deviation from Base Case (%)	----	-10.95	+15.94	+0.69	-15.10	-0.53
80 °C	Collector Output (MJ/m^2d)	2.37	1.97	3.37	2.37	1.96	2.86
	Deviation from Base Case (%)	----	-16.86	+42.36	+0.25	-17.17	+20.86
120 °C	Collector Output (MJ/m^2d)	0.35	0.07	1.59	0.35	0.38	1.61
	Deviation from Base Case (%)	----	-79.17	+351.33	-0.76	+8.52	+356.0

Table 4.1.2 - Predicted Collector Output of S.U. Evacuated Tubular Collector for Different Collector Model Assumptions (January 1985)

Inlet Temp.		BASE CASE	CASE 1	CASE 2	CASE 3	CASE 4	CASE 5
50 °C	Collector Output (MJ/m^2d)	11.46	10.49	12.03	11.56	10.30	10.85
	Deviation from Base Case (%)	-----	-8.50	+4.96	+0.90	-10.13	-5.37
80 °C	Collector Output (MJ/m^2d)	8.94	8.01	9.88	8.99	7.98	8.87
	Deviation from Base Case (%)	-----	-10.34	+10.57	+0.61	-10.72	-0.77
120 °C	Collector Output (MJ/m^2d)	5.54	4.73	6.90	5.60	5.32	6.63
	Deviation from Base Case (%)	-----	-14.66	+24.49	+1.12	-3.95	+19.62

Case 2: Capacitance Effects

Inclusion of capacitance effects in the prediction of solar collector performance is important, especially during months with low incident solar radiation and/or high collector operating temperatures. Table 4.1.1 shows that during winter at a low collector inlet temperature of 50°C, the predicted collector output is 16% higher. This error increases with higher collector operating temperatures and reaches 42% and 351% at 80°C and 120°C collector inlet temperature respectively. In summer (January) the overprediction is not as severe. The deviations from the base case vary between 5% and 24.5% depending on collector inlet conditions.

Case 3: Incidence Angle Modifier Applied to Beam and Diffuse Radiation

As mentioned above the incidence angle modifier should be applied to the beam component of total radiation only. Applying the incidence angle modifier to both components results in an error. Tables 4.1.1 and 4.1.2 however show that incorrect treatment of radiation with respect to incidence angle modifier effects only has a minor influence on the predictions. The error is around the 1% mark and is only slightly influenced by collector operating temperatures and/or season.

Case 4: Hottel-Whillier-Bliss (HWB) Approximation Incorporating Capacitance Correction but No Incidence Angle Modifier

A HWB model which includes capacitance effects but no incidence angle modifier effects generally underpredicts performance by 10-20% except at high collector temperatures. At a collector inlet temperature of 120°C the effect of overestimating the performance due to incorrectly describing the non-linear thermal behaviour of the collector begins to show. Table 4.1.1 indicates that during June, the non-linear thermal effects have a stronger influence on the result than the optical effects. Instead of underpredicting performance an overprediction of 8.5% results. This trend is not quite as strong during January. With generally much better solar radiation conditions the deviations of the HWB model from the effective thermal characteristics of the collector are much smaller. The predicted value for useful energy collected is approximately 4% below the base case value.

Case 5: Standard Hottel-Whillier-Bliss Approximation (no corrections)

A collector approximation as commonly used for the prediction of flat-plate collector performance (no incidence angle modifier, no capacitance correction) leads to discrepancies from the base case which are significantly influenced by the season and collector operating conditions. At low collector temperatures (T_{ci} = 50°C) in June, the HWB approximation yields reasonable

results.

At an elevated collector inlet temperature of 80°C the error becomes marked (+20.9%) and at 120°C the HWB-model overpredicts performance slightly up to a collector inlet temperature of approximately 85°C. At high operating temperatures the overprediction becomes again significant. At 80°C temperatures the error is much less than for the equivalent Case 2 results using the non-linear thermal model and at 120°C, Case 2 and Case 5 results are about the same. Case 5 is better overall (40% error) than Case 2 (44% error).

4.1.2 Conclusions

A validated model of the S.U. Evacuated Tubular Collector formed the basis of a study of factors which affect the performance of this type of collector on a short-term and long-term basis.

Most of the factors examined by the study (non-linear thermal losses, incidence angle modifier effects, array thermal capacitance, array pipe losses) were found to have a non-trivial effect on array performance. Others such as choice of differential temperature controller set-point (collector pump cycling) and different response (optically) of the collector to beam and diffuse radiation did not affect performance significantly. The results of the sensitivity analysis are summarized as follows:

- In an evacuated tubular collector with a curved absorbing surface, incidence angle modifier effects are important. A model which does not include such effects underpredicts performance by typically 10-20% at low to moderate collector operating temperatures. At high collector temperatures (≥100°C) and low solar radiation intensities the underprediction becomes worse;
- Applying the incidence angle modifier to both beam and diffuse radiation results in a relatively small error of approximately 1%. The extra complexity of treating beam and diffuse radiation components separately is not warranted.
- Inclusion of collector capacitance effects in an accurate model of collector performance is necessary. Predictions which do not include capacitance effects overpredict collector output typically by 5-25% during summer. During winter the overprediction is more severe and strongly depends on collector inlet temperatures.
- The standard Hottel-Whillier-Bliss appears to underpredict collector performance slightly at low to moderate collector temperatures and more so at higher temperatures. If no correction is made for thermal capacitance however the H-W-B characterization is clearly superior.

4.2 Canada

4.2.0 System Configurations and Parameter Values

The four systems selected are shown in Figure 4.2.1(a) to (d) in order of increasing complexity and consist of:

System A	-	Low temperature IPH
System B	-	Single tank DHW
System C	-	Double tank DHW
System D	-	Medium temperature IPH

System A is a 1/24 scale model of a system used in preheating river water for pulp and paper processes. A heat exchanger transfers energy from river water to a glycol collector loop which ranges in temperature from just above freezing to about 23°C in the summer. The river water is then boosted to the required temperature of 75°C by an auxiliary heater.

System B is a single tank DHW configuration. Water from the collector loop enters the solar tank where a volume in the top portion of the tank is heated to the required temperature of 50°C by an auxiliary heater if necessary whereas water passing to the load is tempered by mains water if it is hotter than 50°C. Tank water passing to the load is made up by mains water which varies in temperature from 10°C to 18°C during the year. Losses from pipes and tank are accounted for.

System C is the same as system B except that it has a preheat tank and a second tank. In this system the auxiliary heater is in the second tank and as with system B, the volume of water heated at the top of the tank is approximately the same as the maximum hourly load.

System D is a solar assisted bottle washing facility which uses a caustic soda solution in a long, low vat-type tank which has a large uncontrolled heat loss factor (13 W/m^2 - C). The caustic solution in the *soaker* (auxiliary) tank is kept at a minimum of 65°C during load periods by an auxiliary heater upstream from the soaker tank with pre-heating beginning about three hours before the load period. When water is available from the *accumulator* (preheat) tank at a temperature which exceeds the temperature of the caustic fluid by 3°C, the exchanger pump is turned on. The system has a drain back collector and a large piping system with pronounced capacitance effects (13 KJ/m^2 - C). As with the other systems, pipe losses and capacitance are accounted for.

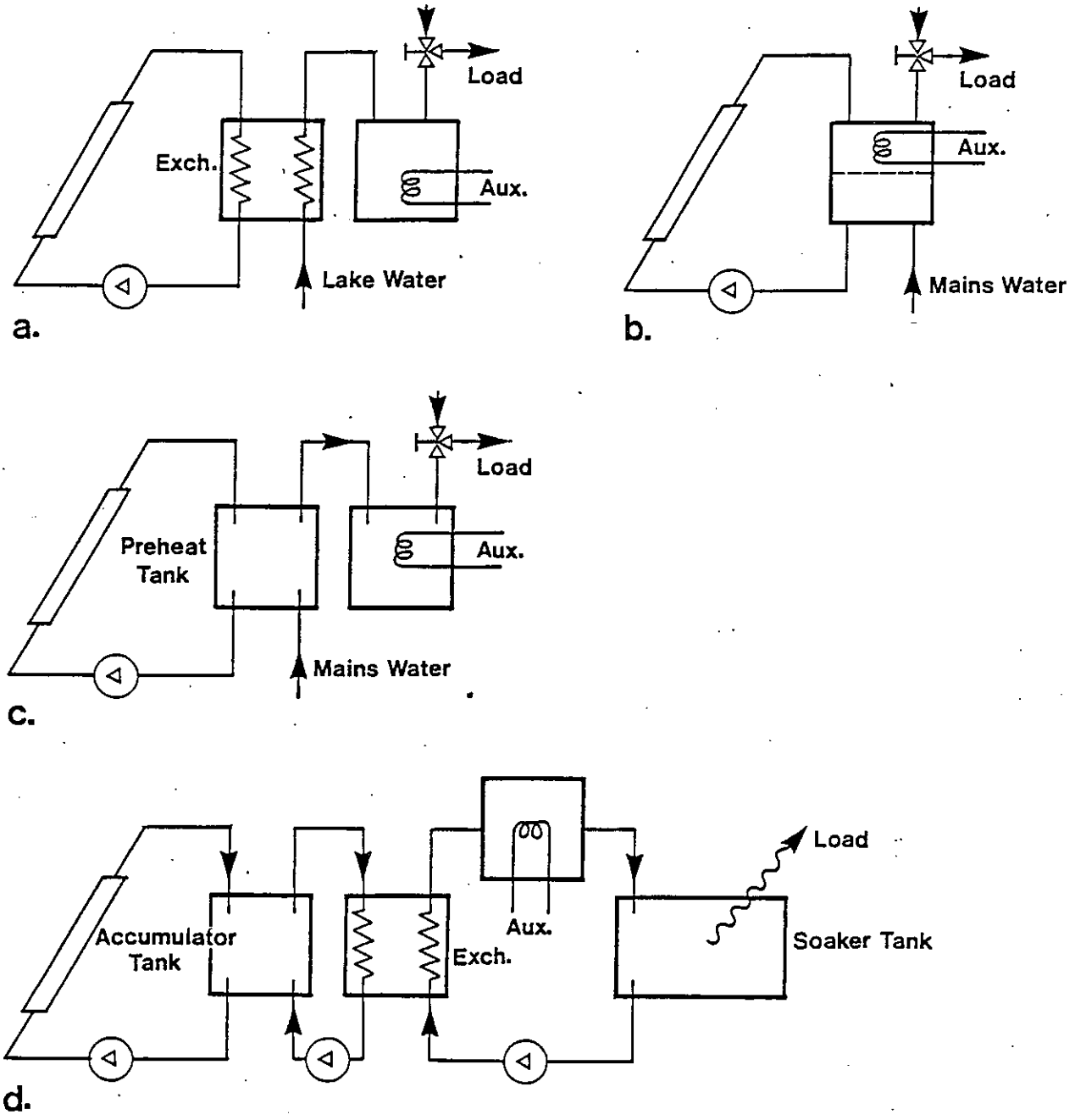

Figure 4.2.1 - System Configurations

Load volumes for the systems are as follows:

System A has a total daily load of 19,200 liters evenly distributed over the day;

System B and C have a load of 275 liters/day with peaks at 10 a.m. and 6 p.m.;

System D has no load flow but energy supplied to the bottle load is about 2.8 GJ/day which is relatively uniform from 6 a.m. to 3 p.m. (Assuming a flow of water heated from room temperature to the load temperature this translates to an equivalent flow of about 18,000 liters/day.) There is no load on the weekends for System D.

Table 4.2.1 summarizes the system parameters. In this table, there are two values given for the collector heat loss factor $F_R U_L$ since the heat removal factor F_R is dependent on the collector mass flow rate.

Meteorological input to the program involves historical radiation levels and ambient temperatures on an hourly basis for the location being considered. In this case the data used were for a typical meteorological year (TMY) [2.5]. The radiation data are for the horizontal plane and are processed [2.6] for conversion to the tilted collector plane.

A total of 80 simulations were run for a one year simulation period each. A breakdown of these simulations can be given as follows:

$$\left[(3\,\text{Sys} \times 3\text{Str}) + 1\,\text{Sys}\right] \times 2\,\text{Loc} \times 2\,\text{Col} \times 2\,\text{Fl} = 80$$

The abbreviations used are:

Sys	:	system configurations	-	(systems A to D)
Str	:	preheat tank stratification schemes (systems A to C)	-	(T-E independent, fully mixed, T-E dependent)
Loc	:	geographical location	-	(Ottawa, Vancouver)
Col	:	collector type	-	(FPC, ETC)
Fl	:	collector flow rate	-	(nominal, 1/4 nominal)

4.2.1 Results of the Sensitivity Analysis

ETC vs FPC

The results are presented in Figures 4.2.2 to 4.2.4 and consist of

Table 4.2.1 - System Parameters

System	Collector Area (m^2)	Collector Capacitance (W/m^2-^oC)	$F_R\tau\alpha$ F_RUL (W/m^2-^oC)	Pump Power (W/m^2)	Pipe Heat Loss (W/m^2-^oC)	Pipe Capacitance (KJ/m^2-^oC)	Exchanger Effectiveness	Storage Preheat (m^3)	Volume Auxilliary (m^3)	Set Point Temp. (^oC)	Daily Load (L)
System A	89.34	40.2	FPC: .75 5.0 ETC: .65 1.0	16.0	0.13	9.9	0.95	(1001)	-	75	19200
		10.05	FPC: .75 4.14 ETC: .65 0.963	4.0				($0W/m^2-C$)			
System B	5.0	42.0	FPC: .75 5.0 ETC: .65 1.0	5.0	1.0	1.0	-	1.0	-	50	275
		10.5	FPC: .75 4.17 ETC: .65 0.965	1.25				($0.5W/m^2-C$)			
System C	5.0	42.0	FPC: .75 5.0 ETC: .65 1.0	5.0	1.0	1.0	-	1.0	0.27	50	275
		10.5	FPC: .75 4.17 ETC: .65 0.965	1.25				($0.5W/m^2-C$)	($0.8W/m^2-C$)		
System D	281.6	28.4	FPC: .75 5.0 ETC: .65 1.0	6.0	20.0	12.8	0.65	4.2	14.8	65 (Load Period Only)	(2.8GJ)
		7.1	FPC: .75 3.83 ETC: .65 0.949	1.5				($1.2W/m^2-C$)	($12.6W/m^2C$)		(18,000)

(a) Input/Output Diagram giving Monthly Energy Collected vs Energy Incident;

(b) Annual Energy Collected per Unit Area vs Operating Temperature Difference; and

(c) Percent Energy Collected vs Normalized Temperature Difference.

The normalized temperature difference is defined as the difference between the collector plate temperature and ambient temperature divided by incident radiation (x-axis of efficiency plots). Figure 4.2.4 also includes FPC and ETC efficiency curves.

With reference to Figures 4.2.2 and 4.2.3 it can be stated that systems with lower operating temperature differences between collector and ambient have a higher rate of energy collection. The low temperature IPH system and DHW systems with T-E dependent preheat tank operate at low temperatures and for these systems both collector types show similar performance. At higher temperature differences ETC arrays outperform FPC arrays by as much as 70%. In one notable exception Ottawa System D ETC's showed slightly better (0.5%) efficiences than their Vancouver counterparts which operated at lower (by 5.5°C) temperatures. The reason for this anomaly was probably reduced operating time at the Vancouver location caused by intermittent insolation.

The seasonally dependent curve representing the System A flat plate collectors in Figure 4.2.3 is due to the temperature difference between river water and ambient. The collector behaves as a heat exchanger in the months around the Spring season when ambient temperatures are higher and this biases the results due to the relatively high flat plate $F_R U_L$. The dropoff at the upper end of the curve representing system B with fully mixed tank and ETC is due to overheat shutdowns of the collector system during summer months.

The effect of operating temperature differences is best illustrated by using the normalized temperature difference which is directly related to collector efficiency via the well-known Hottel-Whillier-Bliss equation. Figures 4.2.4(a) to (c) show the distribution of annual collected energy with respect to normalized temperature difference for systems A,C and D respectively. The mean normalized temperature for each distribution of collected energy tends to intercept the appropriate collector efficiency curve at a point which indicates the collector efficiency for that system. Figure 4.2.4(d) shows predicted collector efficiencies for a variety of systems plotted against mean normalized temperature in a bar chart format.

Table 4.2.2 provides an annual summary of the system efficiency, fraction solar, collection efficiency and energy collected, average inlet and ambient temperatures and the ratio of incident energy with collectors operating (H101) to the total incident energy (H100). The fraction solar is lower for the IPH systems due to the relatively large loads. The collection efficiencies are closely related to operating temperature difference as explained above. The normalized

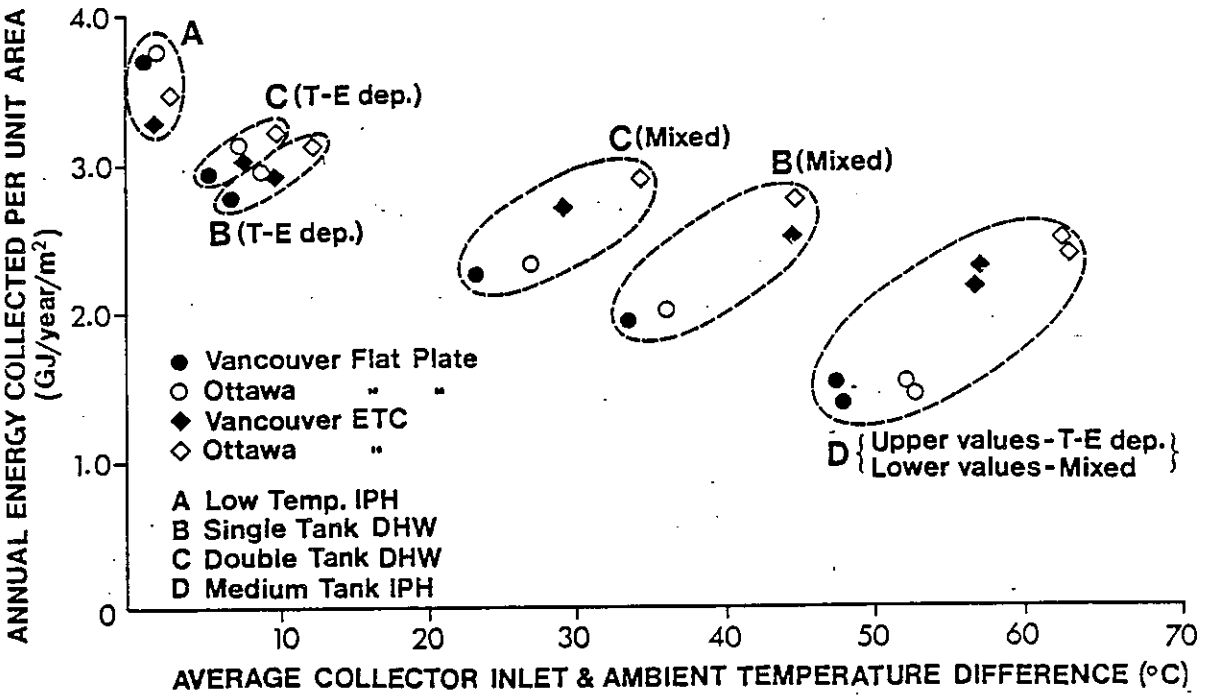

Figure 4.2.2 - Annual Energy Collected Versus Temperature Difference

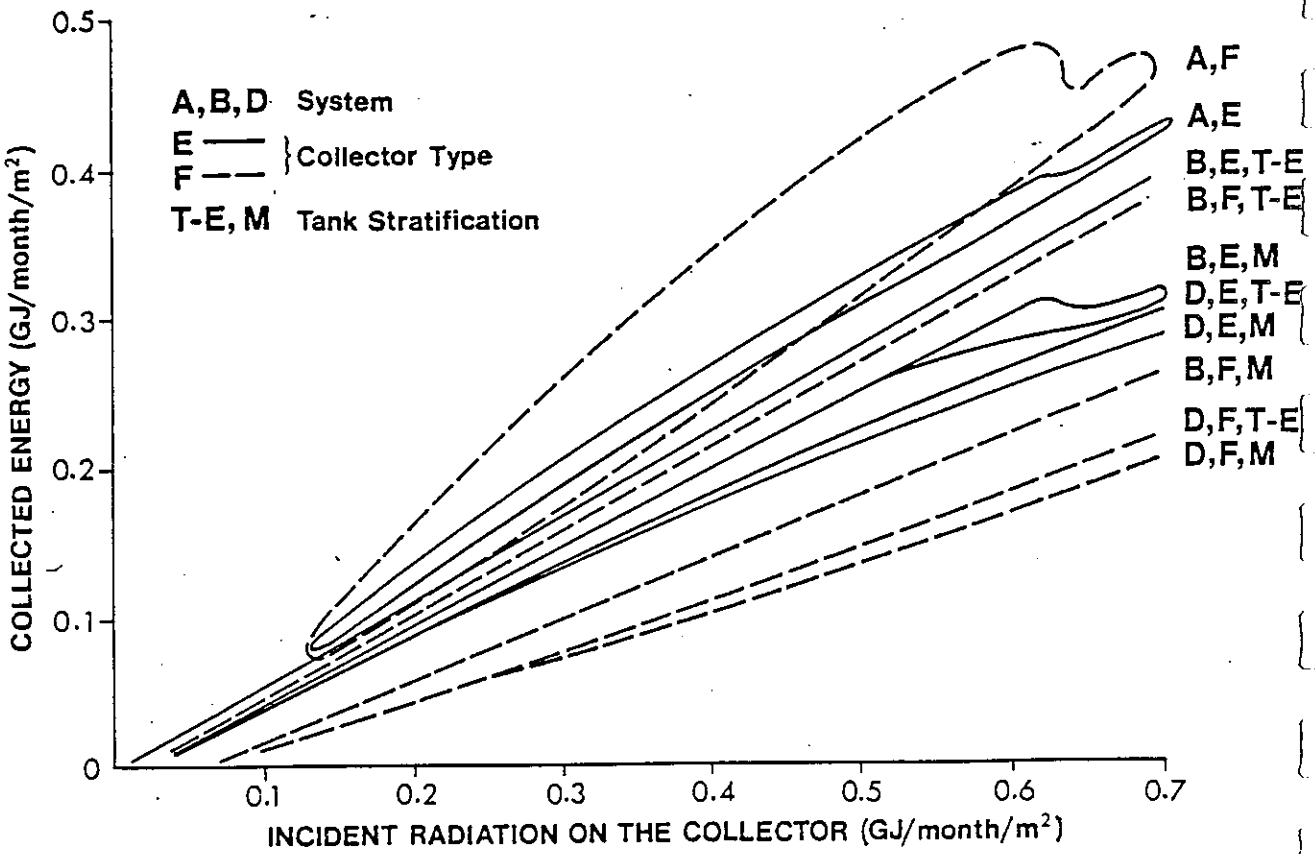

Figure 4.2.3 - Input/Output Diagram

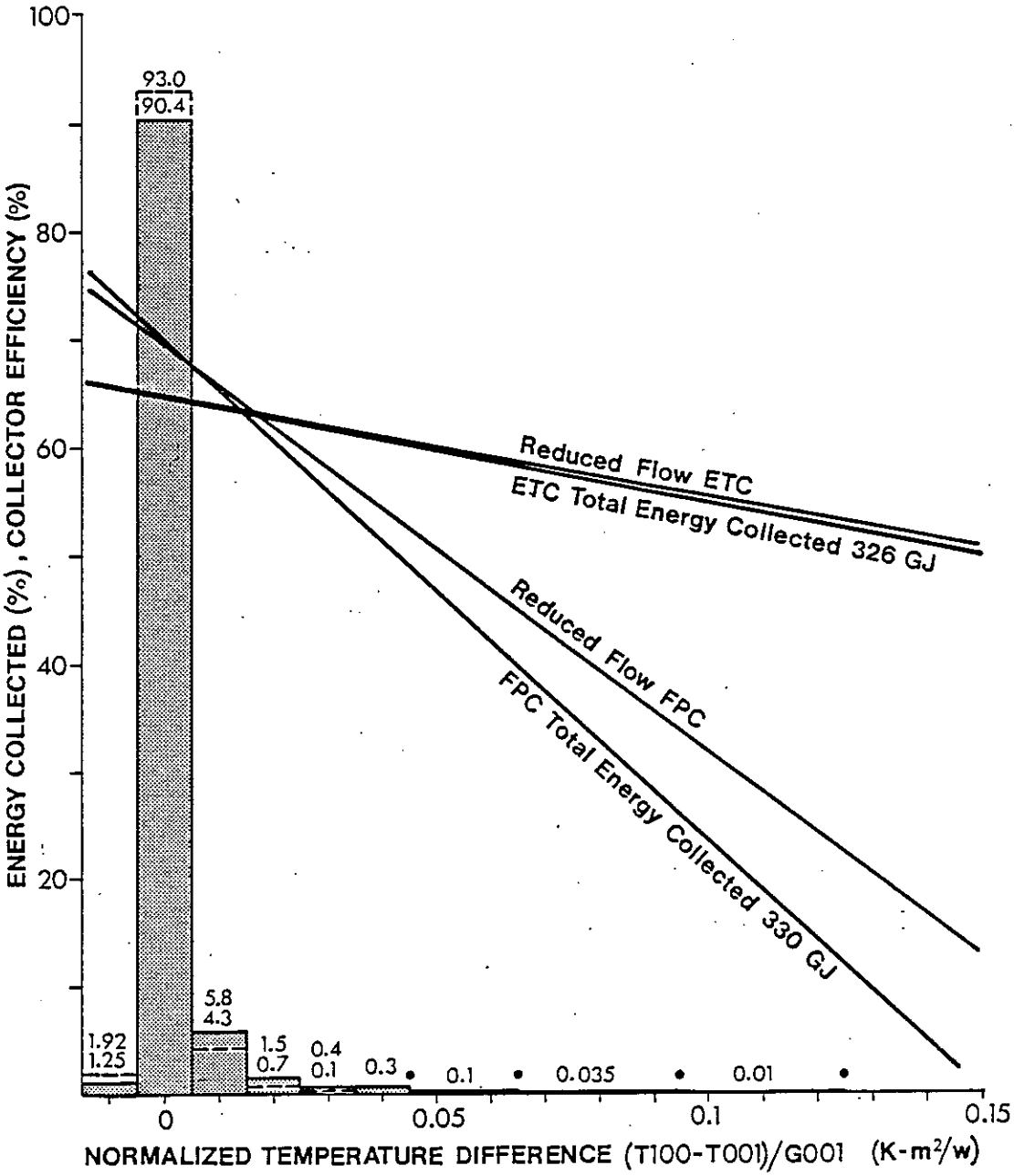

Figure 4.2.4(a) - System A in Ottawa - Nominal Flow

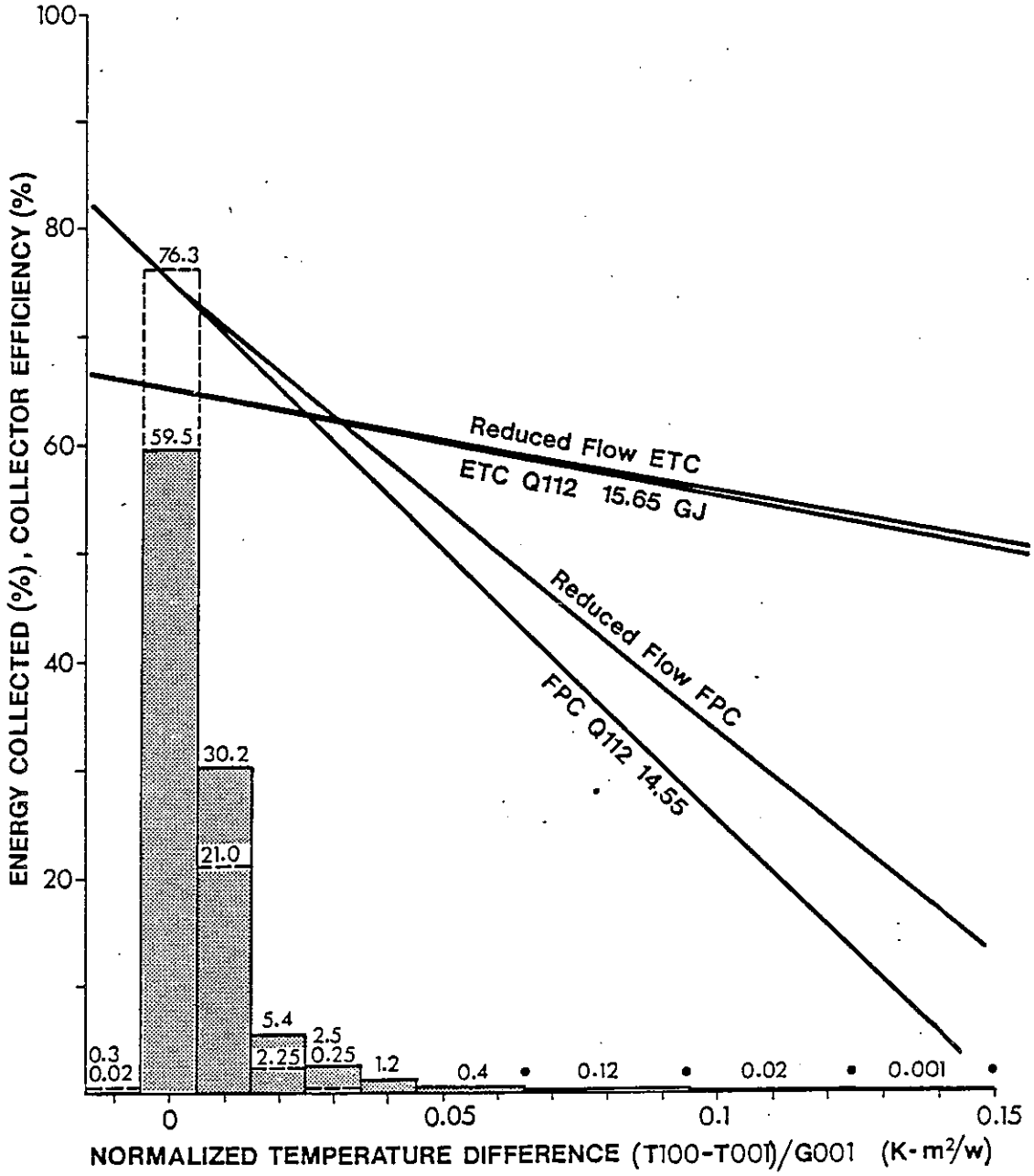

Figure 4.2.4(b) - System B in Ottawa - Nominal Flow

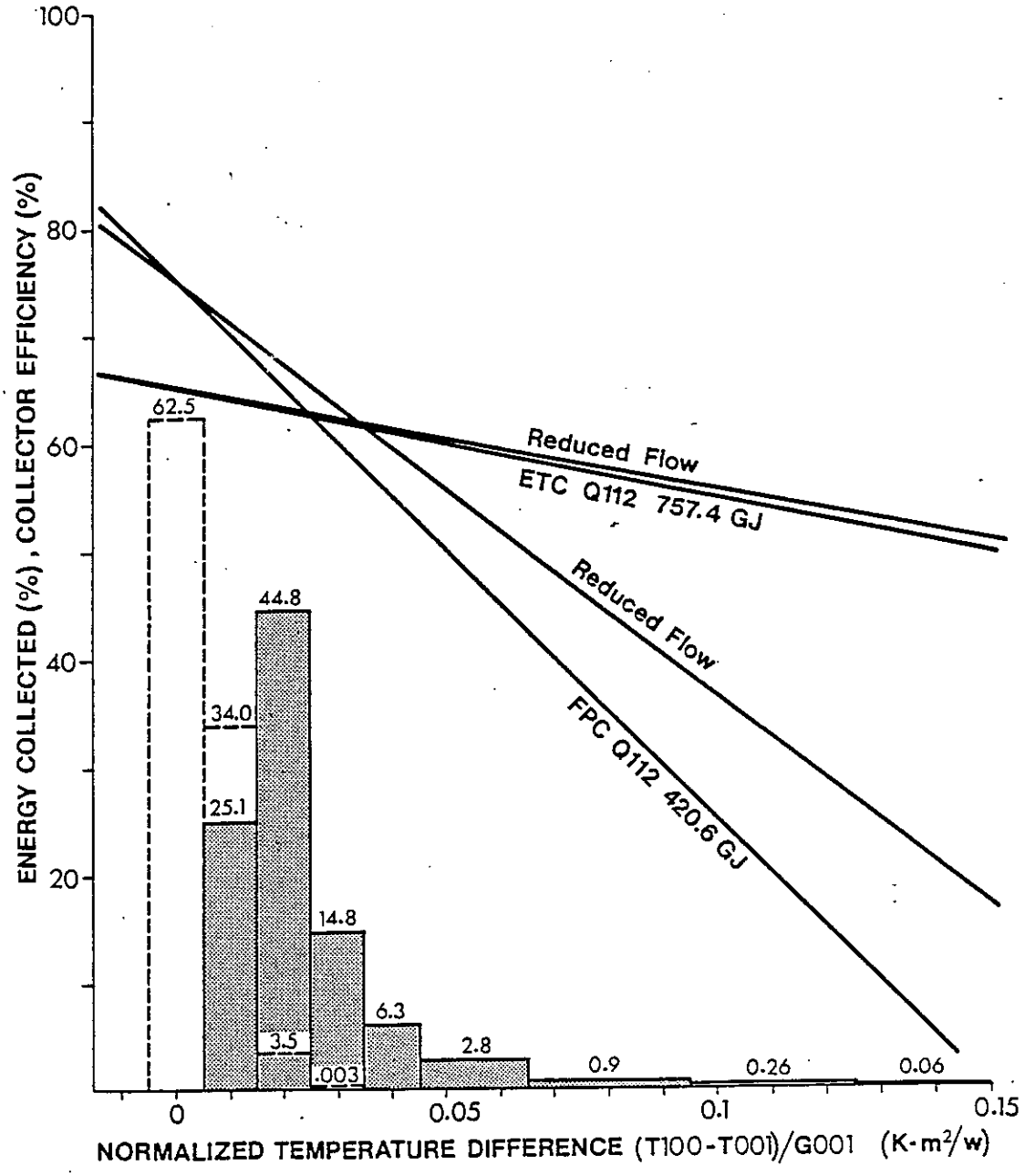

Figure 4.2.4(c) - System D in Ottawa - Nominal Flow

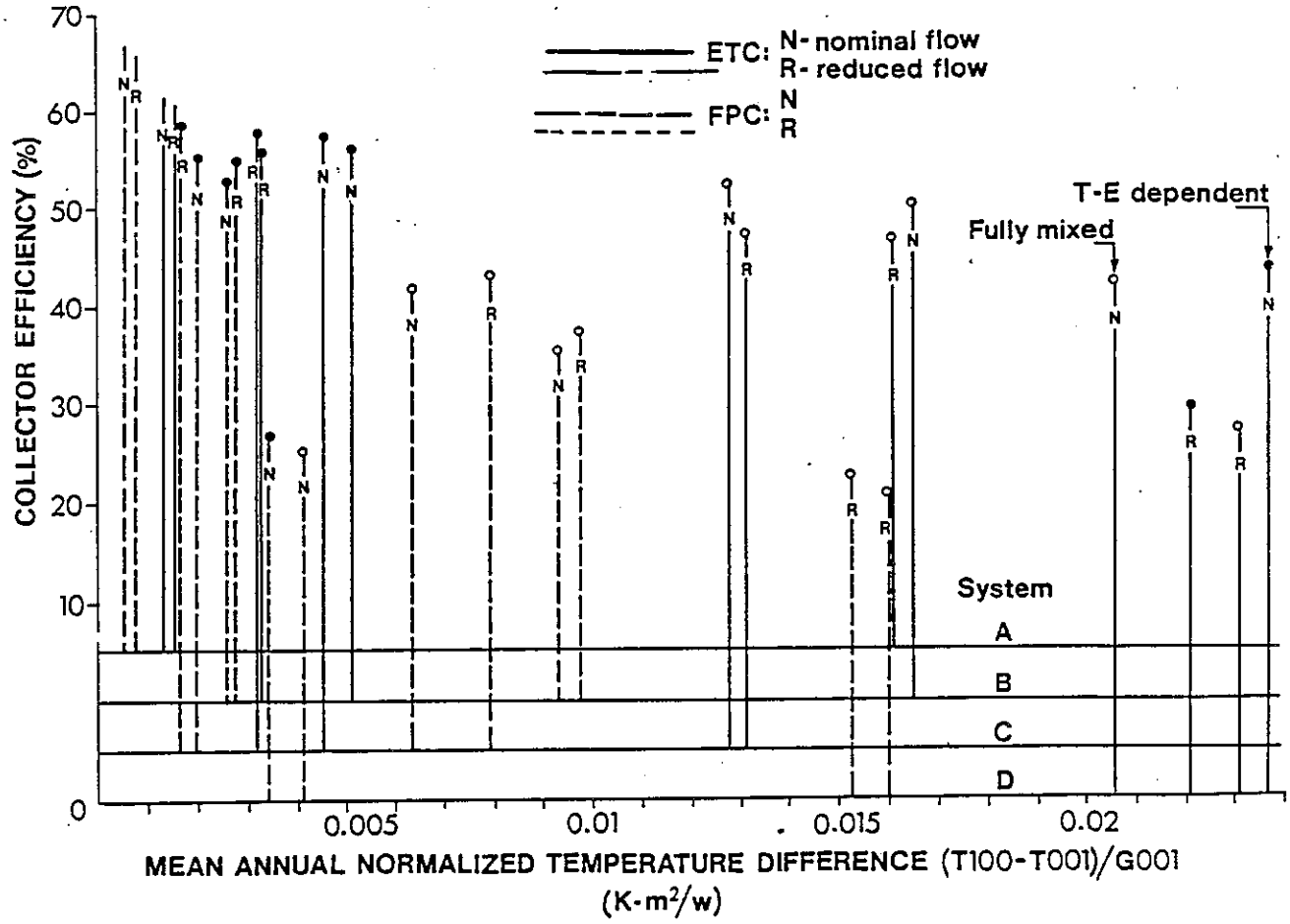

Figure 4.2.4(d) - Collector Efficiencies for 4 Systems versus Mean Annual Normalized Temperature Difference

temperature difference at which a given collector operates is much higher for ETC's which perform well at lower radiation and ambient temperature levels. The increased operating time for ETC's is evident from a comparison of H101/H100 ratios for the two collector types, particularly as the collector inlet temperature increases.

Tank Stratification

Several observations can be made regarding the simulations involving the T-E independent strategy for preheat tank stratification. In almost all of the cases, energy collected and stored in the preheat tank was highest for the T-E independent case and lowest for the fully mixed case. Table 4.2.3 shows the degree to which tank mixing has impaired collector and system performance. The numbers, expressed as percentages, represent the ratio of energy results for the T-E dependent (upper value in each set) and mixed cases (lower values) to the T-E independent case and are averaged for the Ottawa and Vancouver locations. The results are largely as expected except for the full flow DHW systems using ETC's.

In the fully mixed case for these sytems, higher collector (inlet) temperatures meant that the fluid at the top of the preheat tank was warmer than with the other stratification strategies and consequently required less auxiliary energy to boost the water to its required temperature. The extra auxiliary energy led to a corresponding decrease in system efficiency for the T-E independent case as well as the T-E dependent case since some of the source fluid was injected above the elevation of the auxiliary heater (or exited to the auxiliary tank where it was heated as in the case of System C). This effect disappears with the elevated collector outlet temperatures resulting from reduced flow. We note that this effect is absent from the results of system D because the auxiliary heater is *uncoupled* from the preheat tank by the heat exchanger and it is less evident for the FPC systems because of reduced operating time at low collector inlet temperatures..

Reduced Flow

With regard to the reduced flow simulations, the general effect was a slight reduction in collector efficiency for systems A and B (fully mixed, FPC was slightly better) and a large reduction for system D (35% for ETC, 15% for FPC). System C showed slightly improved collector efficiences for T-E independent ETC's (1-2%) and all FPC's (5-10%). Collector efficiencies for fully mixed ETC's were reduced by 4 to 6% due to higher collector inlet temperature.

System efficiencies were improved for all DHW systems except for the fully mixed ETC's which were unchanged. The increases ranged from 150% to 200% for the T-E dependent ETC and FPC single tank systems respectively and this was due to the complications arising from DHW in-tank auxiliary heaters as mentioned earlier. The results for the reduced flow

Table 4.2.2 - Annual Performance Indices

		Flat Plate*							ETC**						
	City	ηsystem (%)	Solar Frac.(%)	ηcoll. (%)	Qcoll. (GJ/M^2)	Tin (^{0}C)	Ta (^{0}C)	$\frac{H^{101}}{H^{100}}$	ηsystem (%)	Solar Frac.(%)	ηcoll. (%)	Qcall. (GJ/M^2)	Tin (^{0}C)	Ta (%)	$\frac{H^{101}}{H^{100}}$
System A	Vancouver	0.37	0.37	71.5	3.70	12.4	10.9	.987	0.31	0.31	62.5	3.23	12.4	10.6	.998
	Ottawa	0.38	0.38	67.1	3.75	12.4	10.5	.981	0.34	0.34	61.5	3.45	12.4	9.8	.997
System B	Vancouver	18.0** 33.7	25.0 47.8	53.8 37.0	2.78 1.91	19.5 47.4	12.9 13.8	.951 .843	22.0 43.8	30.6 62.2	56.3 47.7	2.92 2.48	21.5 56.9	12.1 12.5	.987 .942
	Ottawa	14.7 32.4	21.1 50.1	52.7 35.6	2.94 1.99	19.8 46.8	10.9 10.8	.938 .831	18.7 45.7	27.4 72.2	56.1 49.6	3.14 2.78	21.9 53.1	9.8 8.8	.985 .950
System C	Vancouver	29.6 39.1	46.2 59.6	56.4 43.0	2.92 2.22	18.4 36.2	12.8 13.1	.956 .887	32.5 48.4	50.4 69.1	57.4 52.3	2.98 2.70	19.9 41.3	12.0 12.1	.990 .956
	Ottawa	27.4 34.9	46.3 62.6	55.2 41.5	3.10 2.32	18.5 37.0	10.9 10.0	.946 .878	30.7 48.0	51.1 76.1	57.2 51.9	3.20 2.90	19.9 43.0	12.8 8.7	.988 .959
System D	Vancouver	23.6 21.1	7.5 3.2	28.4 26.9	1.47 1.39	61.5 61.8	13.9 13.9	.774 .771	38.8 36.2	30.0 26.6	43.7 42.2	2.26 2.18	69.6 69.4	12.7 12.7	.940 .940
	Ottawa	22.1 19.6	7.8 3.1	26.7 25.3	1.50 1.42	62.7 63.0	10.7 10.7	.760 .756	39.3 36.5	35.4 31.3	44.3 42.6	2.48 2.38	71.5 71.6	8.9 8.9	.945 .946

*$F_R\tau\alpha$ = 0.75 F_RU_L = 5.0 W/m^2-^{0}C

**$F_R\tau\alpha$ = 0.65 F_RU_L = 1.0 W/m^2-^{0}C

*** Numbers shown in sets of two per category represent stratification cases
(Upper value is for Tempi-Elevation dependent, lower for fully mixed)

Table 4.2.3 - Reduction in Efficiency due to Tank Mixing

Collector Type	ETC				FPC			
Flow	Full		Reduced		Full		Reduced	
Efficiency	Collector	System	Collector	System	Collector	System	Collector	System
System	96.8%	48.4$	98.3%	89.1%	93.1%	39.7%	97.6%	88.9%
B	84.0%	106.6%	81.0%	87.2%	63.5%	80.3%	67.4%	73.0%
System	98.1%	73.6%	96.9%	90.7%	97.7%	67.6%	93.3%	86.5%
C	88.9%	111.6%	82.8%	83.6%	73.7%	87.5%	69.9%	67.8%
System	100%	99.5%	96.6%	95.9%	100%	99.2%	94.9%	93.9%
D	96.2%	92.4%	89.5%	87.6%	94.6%	83.3%	86.3%	85.0%

Table 4.2.4 - Performance Change due to Reduced Flow

	ETC		FPC	
	Collector	System	Collector	System
System A	-1.0	(-1.0)	-2.2	(-2.2)
System B	-2.7	+122.8	+2.0	+176.1
	-7.6	-1.6	+3.3	+11.0
	-4.2	+20.2	-2.7	+22.1
System C	+0.6	+65.4	+6.0	86.9
	-5.0	+0.3	+5.3	13.4
	+1.9	+34.0	+11.0	
System D	-34.2	-28.0	-18.2	-5.7
	-36.6	-29.2	-21.4	-5.0
	-35.4	-25.3	-13.8	-0.4

simulations are summarized in Table 4.2.4 which shows performance change with respect to the nominal flow case expressed as the percentage difference in collected and stored energy. The numbers are given in sets of three, representing the three mixing cases (ordered T-E dependent, fully mixed and T-E independent).

4.2.2 Conclusions

Detailed hour-by-hour simulations were essential for investigating effects of several factors including storage stratification, meteorological conditions and operating strategy on the long term performance of the four generically different types of systems studied. For example, there is no method aside from using a detailed simulation, whereby the mean annual normalized temperature difference (which is useful in characterizing mean annual performance) can be determined . The ETC's operate over a larger range of the collector performance curve than do FPC's due to the lower overall collector loss factor associated with the ETC's. The actual operating time however depends on many other factors, including meteorological data and the operating strategy.

The energy collected (GJ/m^2 - year) ranged from 2.2 to 2.5 for ETC's at higher operating temperature differences (System D) while the FPC arrays collected only 1.45. For the low temperature system collected energy was 3.75 GJ/m^2 - year for the FPC's versus 3.23 to 3.45 for the ETC's (System A).

System effects including tank stratification and flow rates were found to have a significant influence on collector efficiencies and particularly on system efficiencies. In general, loss of tank stratification due to mixing led to reduced system efficiencies but certain combinations involving the system configuration and operating strategy produced unexpected results. As shown in Table 3.2.3 for ETCs with full flow, the collector efficiency decreased due to mixing by 4 to 16% points with respect to the fully stratified case (T-E independent); for FPCs, the numbers were 5 to 36%.

4.3 Netherlands

4.3.0 System Configuration

The configuration is given schematically in Figure 4.3.1. The load consists of a typical well-insulated a house with a yearly heating load of 28.2 GJ and hot water load of 13.1 GJ. The solar system consists of 25 m^2 of collectors and a water storage of 2m^3, insulated with 1m mineral wool. The maximum temperature in the storage is 80°C and 95°C for the series auxiliary heater.

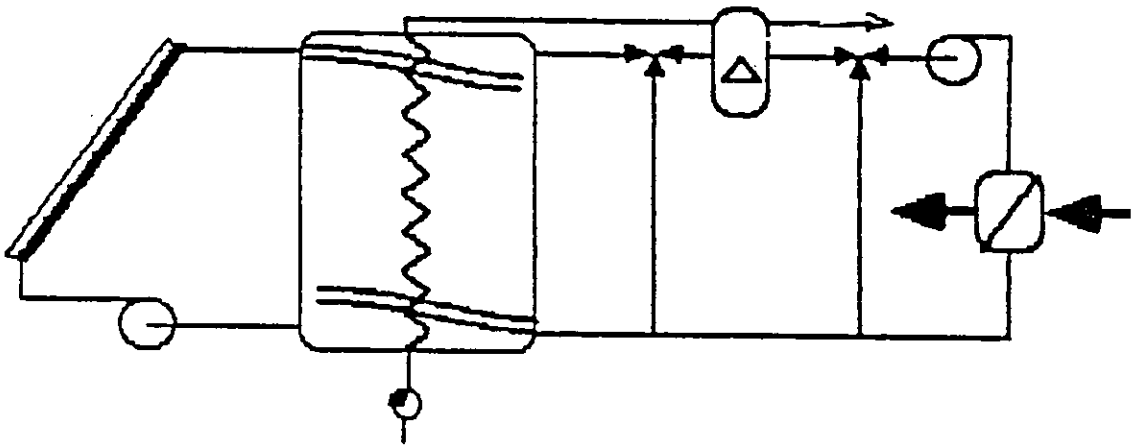

Figure 4.3.1 - Schematic of the System

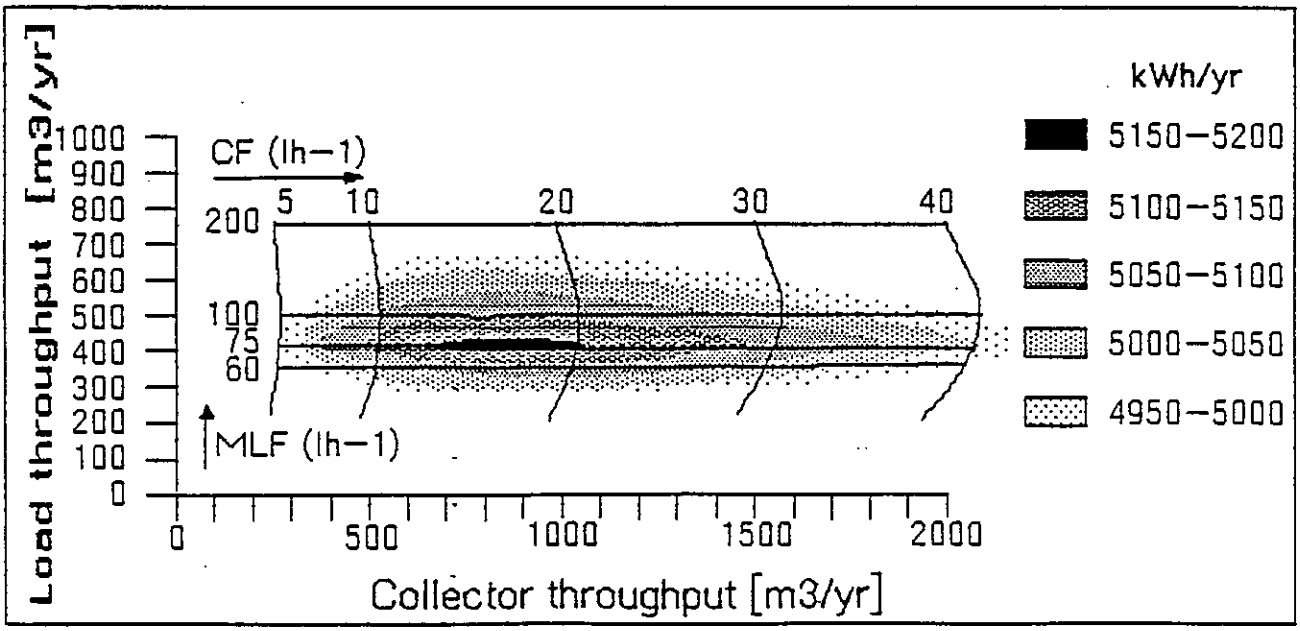

Figure 4.3.2 - Contours of constant displaced energy for a system with evacuated collector and uniform storage. Vertical curves refer to constant collector flow CF in $lm^{-2}h^{-1}$, horizontal curves to maximum load flow MLF in lh^{-1}.

The heat exchanging capacity of both the air heater and the hot water coil is 100 WK^{-1}. Two collector types are considered, a spectral selective flat plate collector of moderate quality and an evacuated tube collector (resp. $U_L = 6.2$ and $1.8\, Wm^{-2}K^{-1}$, transmittance-absorptance = .76 and .67, $F' = .96$).

For both the collector and the load circuit, a low power pump of 25 W in primary energy was selected at a flow rate of .375 m^3h^{-1} (1 W for a collector flow of .015 $m^3h^{-1}m^{-2}$). Because the layout will be adapted when the flow rate changes, the pumping power was assumed to be proportional to the flow rate to the power 7/4.

In the simulation part, three mutually linked controls are investigated.

Control I, the load flow is fixed if auxiliary heating is needed and supplied if the stored heat is sufficient to cover the heat demand. In the former case the temperature at the outlet of the series auxiliary heater follows the heat demand.

Control II, the temperature at the outlet of the series auxiliary heater is controlled by the temperature difference between room set temperature and ambient temperature. The load flow is controlled by the heat demand.

Control III, the temperature at the outlet of the series auxiliary heater is fixed, and the flow is controlled by the heat demand.

The optimum setting of the flows is assessed by a straight-forward simulation of the system for a range of flow values. The optimum flow settings are then determined as the ones which yields the maximum yearly heat gain for a given system and control strategy.

4.3.1.1 Effect of Flow Rates Using Various Controls

Mixed Tank Results

The optimum heat gain for the uniform temperature storage system is 19.1 GJ and is obtained with Control I for a yearly collector throughput beyond 3220 m^3 and a load throughput of 300 m^3 (collector flow > 60 $lm^{-2}h^{-1}$, maximum load flow 80 lh^{-1}). The load throughput includes the amount of hot water of 80 m^3, so as to obtain the complete load throughput. The maximum heat gain for Control II (weather dependent) is 18.3 GJ and for Control III (constant temperature auxiliary) 17.6 GJ. Usual practice of applying a high load flow rate (beyond 200 lh^{-1}), reduces the heat gain from 19.1 to 18.2 GJ, i.e., 5% or more.

Figure 4.3.2 shows the contours of constant displaced energy (pump included) for a mixed tank system using Control I. The optimum displaced energy amounts to 18.6 GJ at a collector flow of 15 $lm^{-2}h^{-1}$ and a maximum load flow of 85 lh^{-1}. For the usual high flow rates the

displaced energy is less than 16.7 GJ.

Stratified Tank Results

The optimum useful heat gain for a perfectly stratified storage, say with floating inlets is 20.1 GJ at a collector throughput of 790 m^3 and a load throughput of 280 m^3 (collector flow 12 $lm^{-2}h^{-1}$, maximum load flow 75 lh^{-1}). The maximum heat gain for Control II is 19.7 GJ and 19.1 GJ for Control III. As compared with the high flow rates, stratification and a good control of both flows increases the performance from 18.2 to 20.1 GJ or by 10%.

In Figure 4.3.3 the contours of constant displaced energy are given for a perfectly stratified storage using Control I. The optimum energy displaced is 20 GJ (collector flow 8.5 $lm^{-2}h^{-1}$, load flow $75lh^{-1}$).

4.3.1.2 Conclusions

The optimum is rather flat with respect to the collector flow. Changing the collector flow from 6 to 16 $lm^{-2}h^{-1}$ doesn't cost more thatn 1% of the energy displaced. The optimum with respect to the load flow is more pronounced, but still the load flow can be changed by 30% without losing more than 1% of the energy displaced. The gain in displaced energy obtained by using a perfectly stratified storage, Control I and the optimum flow settings as compared with the usual high flow rates, fully mixed storage and Control II (weather dependent) is at least 3.6 GJ or 22% for a system with evacuated collectors.

4.3.2.1 Effect of Flow Rates Using ETC & FPC Collectors

Comparing the flat plate collector and the evacuated tube collector, it is seen that the optimum flow for the evacuated collector and the gain by better flow control is substantially lower than with the flat plate collector. The benefits of proper flow control and stratification in terms of displaced energy are summarized in Table 4.3.1.

To get an idea of the causes of the losses in a solar heating system, a comparison of several systems with a (hypothetical) loss-free collector gives us the limits (see Figure 4.3.4). If the collector has zero losses, any control of the flows and any grade of stratification will lead to the same yearly heat gain, as long as temperature limits are not surpassed. A system with evacuated collectors, optimum control and perfectly stratified storage apparently loses only 10% as compared to a system with the loss-free collector. A system with simple flat plate collectors, optimum control and perfectly stratified storage looses 20% and a system with a fully mixed storage and the usual high flow rates the system looses 39% as compared to the loss-free collector.

Table 4.3.1
Displaced Energy due to Flow Control and Stratification

Collector Type	Tank Type	Flow Rate Strategy	Displaced Energy (GJ/yr)	Collector Flow Rate ($lm^{-2}h^{-1}$)	Load Flow Rate (lh^{-1})
FPC	Mixed	high flow	13.7	60	200
FPC	Mixed	optimum	15.4	25	70
FPC	Stratified	optimum	18.0	13.5	75
ETC	Mixed	high flow	16.4	60	200
ETC	Mixed	optimum	18.6	15	85
ETC	Stratified	optimum	20.0	8.5	75

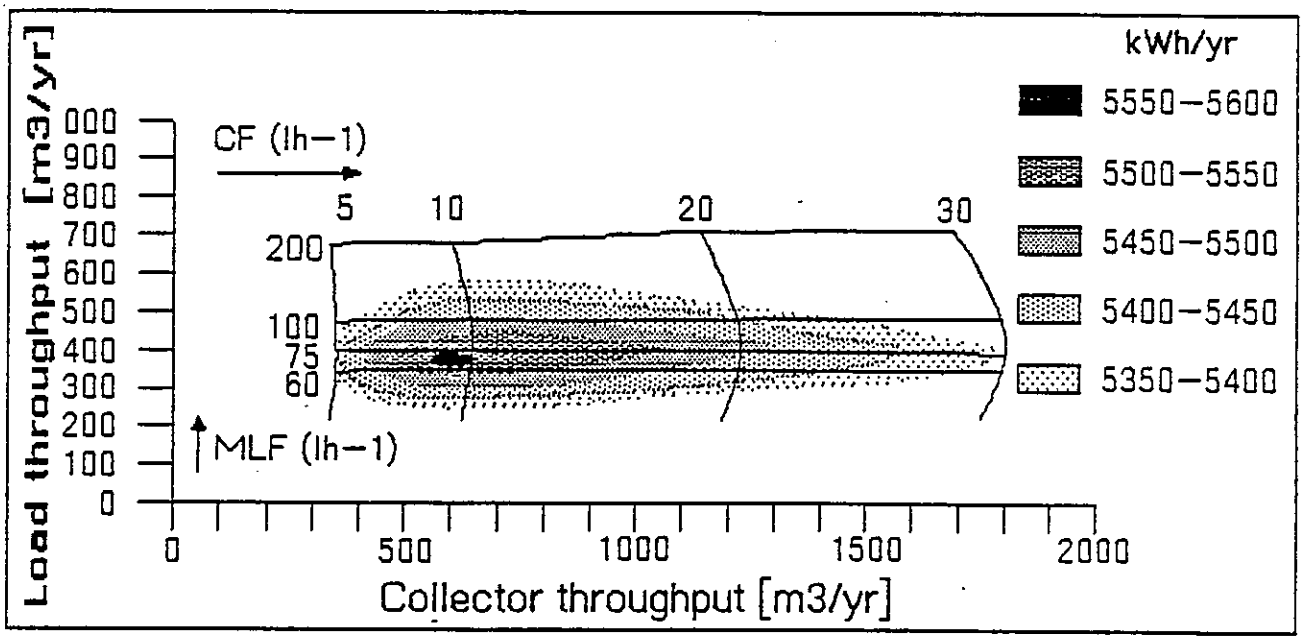

Figure 4.3.3 - Contours of constant displaced energy for Control I system with evacuated collector and stratified storage. Vertical curves refer to constant collector flow CF in $lm^{-2}h^{-1}$, horizontal curves to maximum load flow MLF in lh^{-1}.

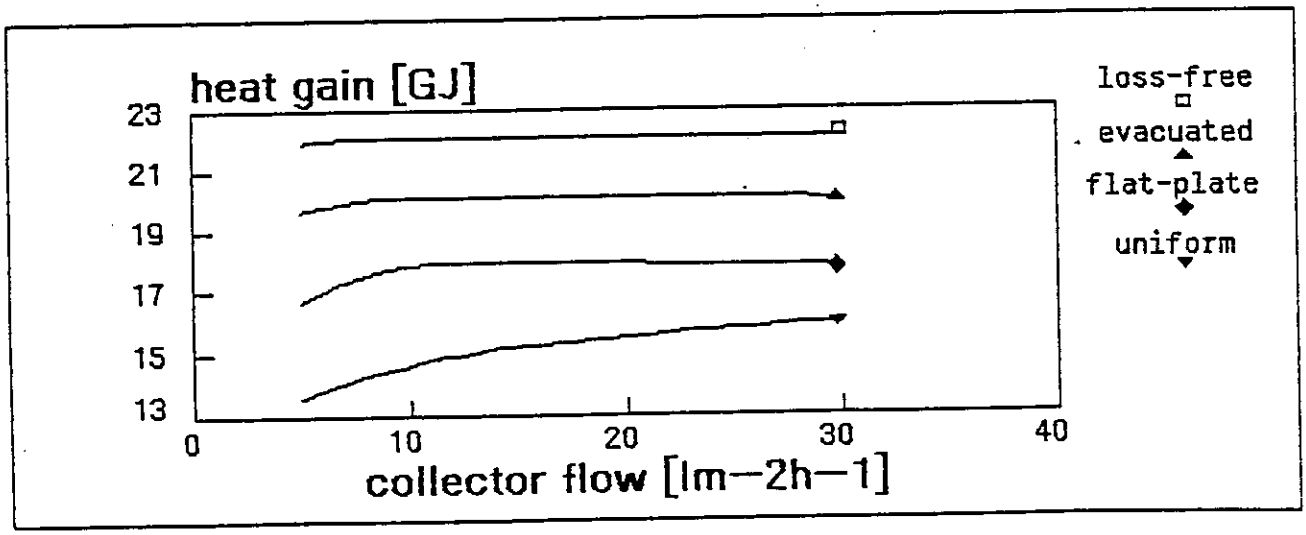

Figure 4.3.4 - Causes of losses in a system, comparison to loss-free collector.

4.3.2.2 Conclusions

A solar heating and hot water system behaves non-linearly as regards the flow through the collector and the flow through the heating system. Therefore a well thought-out control strategy for the flows is necessary to maximize the heat gain or, better, minimize the auxiliary energy needed. Such an optimum control strategy requires stratified storage, equal daily capacitance throughputs of collector and load circuit, variable flow rates and reliable weather forecasting. A practical approximation of the optimum control strategy, by using on-off control and fixed flows leads to a decrease of the performance of only about 1%, if the yearly collector throughput be somewhat higher than the yearly load throughput. This result is virtually independent of the system parameters. The optimum control strategy leads to much lower flow rates throughout the system than commonly applied. From a comparison of the displaced energies it appears that the low flow strategy combined with stratified storage brings with it improvements of up to 20% for evacuated collectors and 35% for flat place collectors.

4.5 West Germany

4.5.0 System Configurations and Collector Types

With the validated component-model described in Section 3.5, 16 new solar systems with modified configuration and control strategy have been analysed.

The three system types shown in Figure 4.5.1 of different levels of complexity have been investigated.

Type A: *Simplified One-Storage Systems*, with only one stratified, combined DHW storage for solar and auxiliary energy. Solar energy is delivered by an integrated high performance tubular heat exchanger at the bottom (cold end) of the storage, and auxiliary energy is delivered by an immersed 12 kW electric heater, heating the upper 500ℓ volume. The storage volume has been varied from 2500 to 1000 litres in steps of 500ℓ.

Type B: *Simplified Retrofit-Systems* with a 2000ℓ solar storage (new) and an (existing) 500ℓ auxiliary storage. Investigations of size and efficiency of the heat exchanger, of collector loop flow rates, and pump operating time were made.

Type C: *Two-Storage Systems*, with a 1500ℓ preheat and a 1000ℓ DHW and auxiliary storage. Solar energy at radiation densities above a threshold-value (variable) is delivered to the DHW storage until it reaches its maximum temperature of 60°C. Solar at lower intensities is used in the preheat storage. The radiation threshold was varied from 100-1000 W/m^2. The details of the control strategies are explained in [5.5,5.6].

In order to investigate the mutual interaction between collector performance and the complexity of both system configuration and control strategy, the specified system types and their variations have been simulated with both a high performance ETC and a non-selective double glazed FPC collector with the following specifications:

Evacuated tubular collector: Area = $33\,m^2$; $F'\tau\alpha = 60\%$; $F'U_l = 1.0\,W/m^2K$,

Flat plate collector: Area = $65\,m^2$; $F'U_1 = 6.2\,W/m^2K$.

The two collector types were sized in order to obtain two reference systems with similar values of used solar energy (142 MJ/day), auxiliary energy (72 MJ/day) and solar fractions (62.8%) thus giving comparable operational conditions and system temperatures.

Figure 4.5.2 presents an overview of the ETC- and FPC-systems performance, showing the radiation incident on the aperture area of 33 and 65 m^2 and the energy output of the collector array Q112 as well as the corresponding collector array efficiency.

It becomes apparent from Figure 4.5.2, that the FPC system operates at about half the system efficiency of the ETC system. This is a direct consequence of the larger collector array of the FPC system, which is needed to produce the same amount of useful solar input to the preheat storage.

The *Retrofit-System* Type B1 was selected as "Reference System". The solar loop of this system is analysed in a day by day sequence, showing the input to the preheat tank in Figure 4.5.3 and the losses of the solar loop in Figure 4.5.4, both for the ETC and FPC systems.

Although the ETC and FPC collector areas were designed to deliver in the case of the "Reference System B1" the same amount of solar input into the preheat storage (Q200) over the simulation period, there are considerable differences in the daily values. A detailed investigation of this situation yielded the result, that the FPC produces more energy than the ETC when the daily radiation level is high and the differences between the storage and the loop temperatures are low; on the opposite, the ETC produces more with higher operating temperatures and under less favourable radiation conditions. An analysis of the daily operating temperatures was obtained by studying the piping losses of the solar loop in Figure 4.5.4. It is seen, that the ETC system operates most of the time with higher operating temperatures than the FPC system. The reason for this behaviour is the low heat-loss factor of the ETC collector, enabling this collector to operate with an efficiency of about 45% at radiation levels of 100 - 200 W/m^2 and operating temperatures of 30 -40°C; comparing the operating conditions of the FPC from this situation, it can be observed that the ETC collector operates in the course of the day during longer periods at higher temperatures and with higher efficiencies, while the FPC collector compensates its relative deficiency especially under conditions of high incident radiation and because of its larger

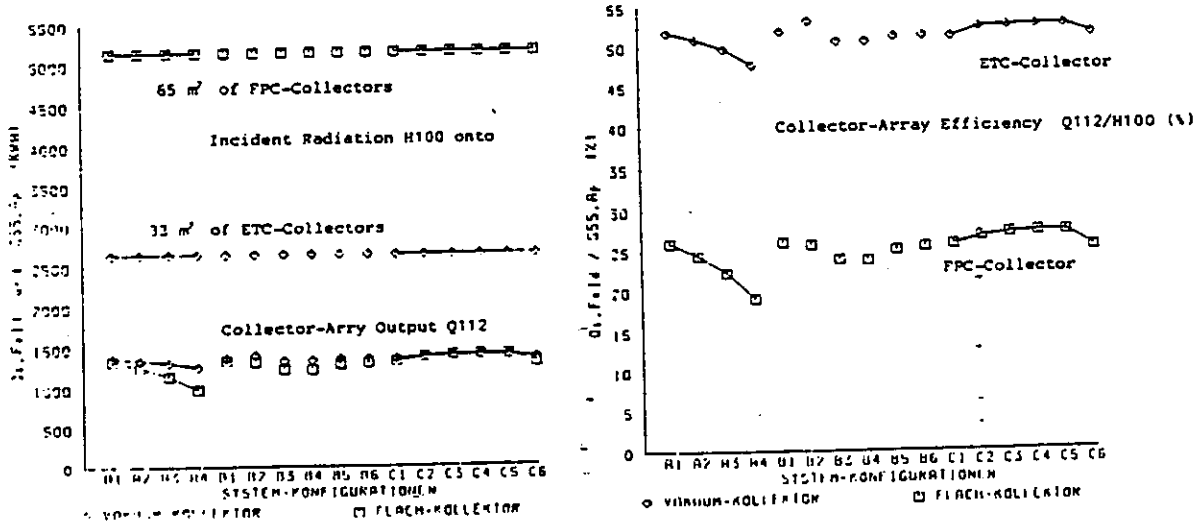

Figure 4.5.2 - Incident Radiation, Array Output and Collector Array Efficiency

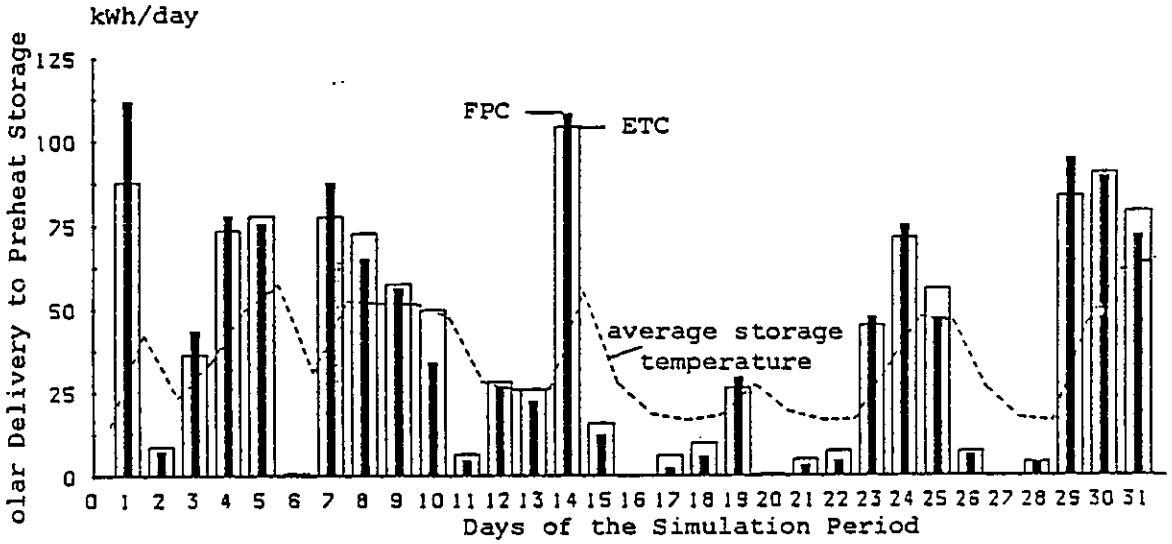

Figure 4.5.3 - Daily Re-heat Storage Input Q200 for ETC and FPC Systems

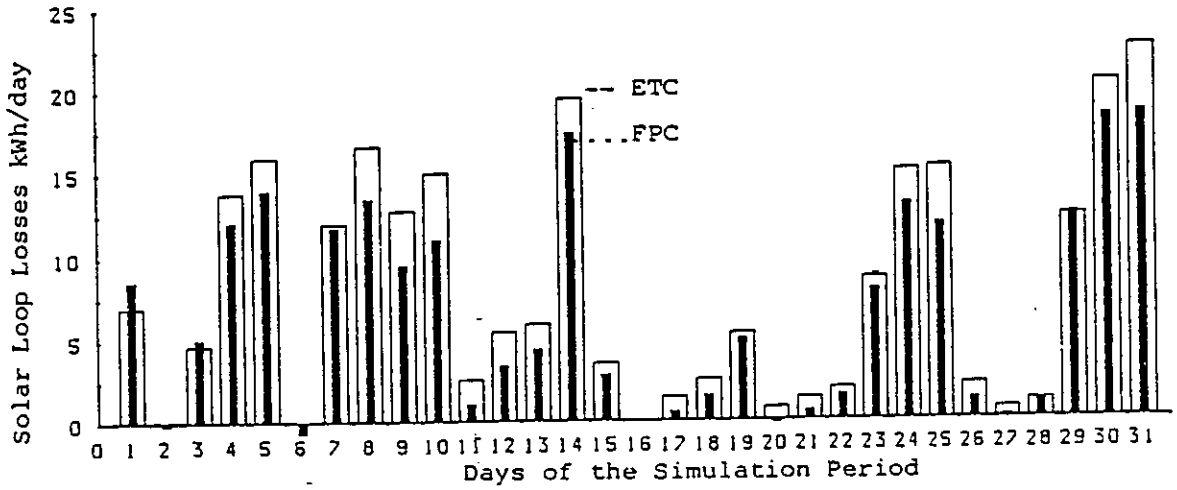

Figure 4.5.4 - Daily Solar Loop Losses Q112-Q200 for ETC and FPC Systems

area in a relatively short time.

An analysis of the daily collection efficiency is presented in Figure 4.5.5 in the form of an Input/Output diagram for both types of collectors; squares represent the FPC, diamonds the ETC collector. The daily collector output increases nearly linearly with the daily insolation total, and also with a decreasing operating collector to ambient temperature difference. However, it is remarkable that the FPC collector shows a much larger scatter in the daily output for identical values of daily insolation, which is a direct consequence of its higher heat-loss parameter. Moreover, it is observed that the value of the correlation does not directly depend on the $F'\tau\alpha$ value, but is a combined function of several interacting parameters including $F'\tau\alpha$, $F'U_L$, collector-array capacity, piping insulation and operational temperature difference.

Representative Climate and Load Period for the Sensitivity Analysis

In order to perform realistic simulations of alternative control strategies with different levels of complexity, measured data in 5-minute time steps of the radiation and the warm water flow rate were taken from the SOLARHAUS FREIBURG project. The following table compares the average annual data with values of the *representative* period used in this analysis:

			annual average	analysis period
ambient temperature	T001	°C	9.5	9.9
tilted global radiation	H001	kWh/m^2/day	2.6-3.3	2.6
room temperature	T606	°C	26.	26.
warm water consumption	F430	litre/day	1230.	1210.

The hourly profile of the tilted global radiation H001 and of the warm water consumption F430 are shown in Figures 4.5.6 and 4.5.7 respectively.

It is demonstrated in these figures, that the representative period is composed of a typical sequence in days with high, medium and low insolation levels and daily warm water consumption. However, a comparison of the radiation profile with 5-minute-resolution in Figure 3.5.4 together with the 1-hour-resolution profile of the same day (5th day in Figure 4.5.6) shows the high level of real dynamics in the data used.

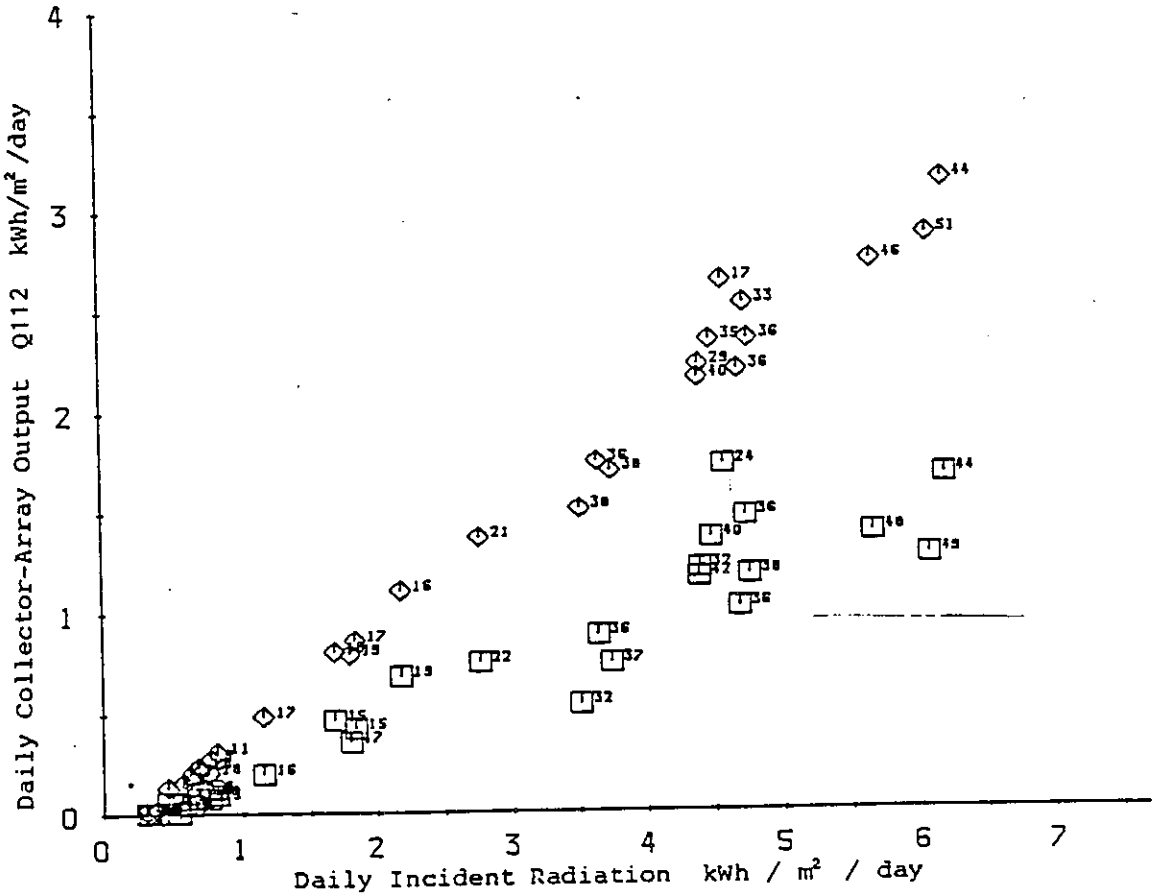

Figure 4.5.5 - Dialy Input/Output Diagram for ETC and FPC Collectors

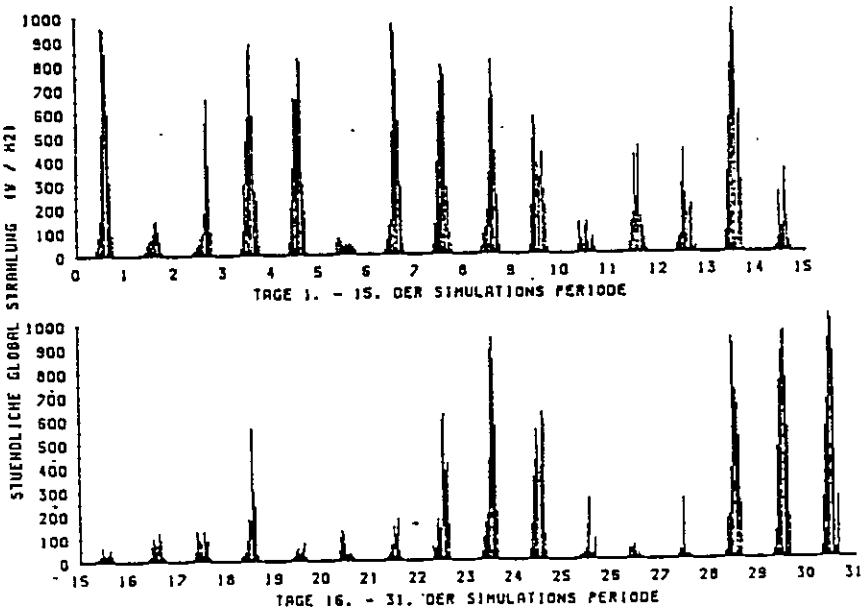

Figure 4.5.6 - Hourly Profile of the tilted global radiation H001

Abb. 9-6 Stündliche Einstrahlung der 31-tägigen Untersuchungs-Periode

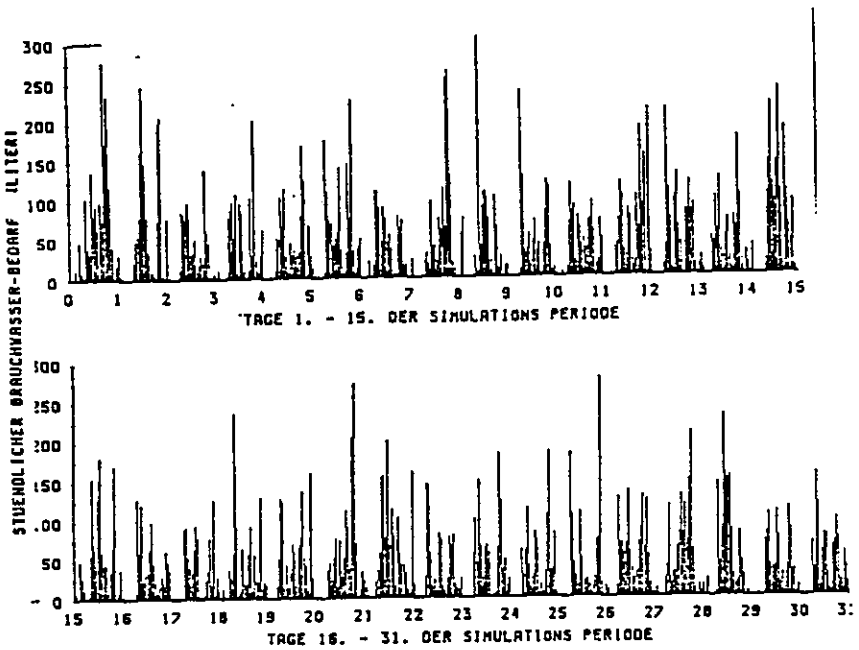

Figure 4.5.7 - Hourly Profile of the Warm Water Consumption F430

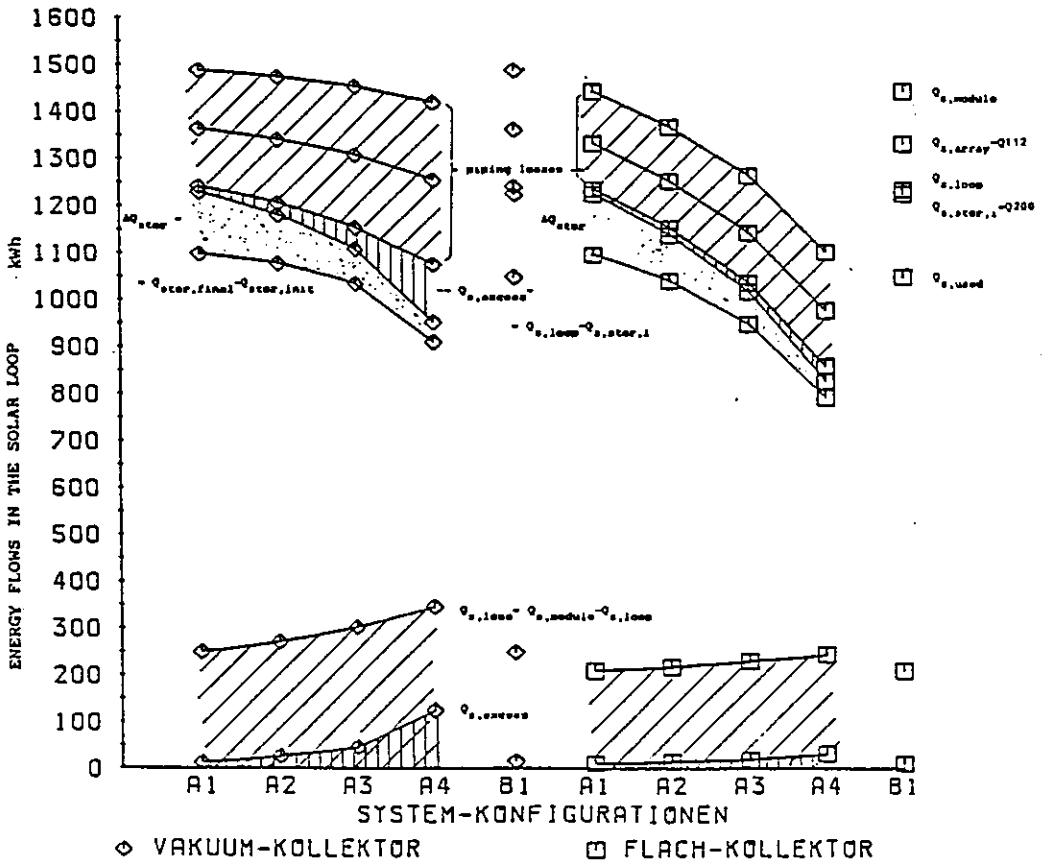

Figure 4.5.8 - Effect of Storage Volume Reduction on Solar Loop Energy Flows

4.5.1 ONE-Storage Tank System, Type A

4.5.1.0 Variation of DHW-Storage Tank Parameters

The storage volume of system A1 of 2500 litres corresponds to the design conditions in the SOLARHAUS FREIBURG installation; it is reduced in steps of 500 litres up to a value of 1000 litres in system A4. The storage volume heated by auxiliary energy is held on a constant value of 500ℓ by adjusting the associated geometry parameters. Thus similar conventional operating conditions are maintained for the analysis.

4.5.1.1 Results of Sensitivity Analysis for System A

Figure 4.5.8 demonstrates in a side-by-side comparison, how the performance of the collectors is affected by the gradually reduced storage volume. It shows the changing energy flows in the solar loop between collector module and the storage. The storage volume reduction results in a decreased energy delivery from the collector modules of - 1%, -2.4%, -5% in the case of th ETC collector, and in the case of the FPC collector -5.3%, -12.4% and -24%, the values being relative to the respective reference system B1. The difference in the behaviour is explained by the different heat-loss parameters of the ETC and FPC Collectors. A comparison of the piping-losses shows that the ETC collector operated on the average at higher system temperatures than the FPC collector, a fact already discussed for the reference system B1 together with Figures 4.5.3 and 4.5.4. It is observed, however, that the piping-losses of the ETC systems increase more with the reduced storage volume than do the FPC system. This can be explained by the higher operating temperatures associated with the production of excess heat at 100°C, which occurs when the storage tank has reached its maximum temperature. It is interesting to note that the FPC collector produces only a negligible amount of excess heat.

The change in stored energy is given by energy delivered minus energy extracted from the storage tank between the final and initial state of the storage temperature profile; this energy decreases linearly with the storage volume, as the ΔT did not change in the analysis period.

The solar fraction is influenced in the same way as the collector output, although it is made more uniform by the different loss mechanisms in the solar loop. Relative to the solar fraction of the system A1 of 64.5%, the reduction of the storage volume causes the ETC solar fraction to be reduced by -2%, -5.8% and -17%, whereas the FPC solar fraction is reduced by -5.2%, -13.5% and -28%.

4.5.1.2 Conclusions for System A

Solar DHW Systems with high quality ETC collectors give a high solar fraction of 65% and a system efficiency of 42%; the same solar fraction requires about two times as much area of simple conventional collectors, yielding a system efficiency of 21%. A reduction in storage tank volume reduces the efficiency of both the ETC and the FPC systems but the magnitude of the reduction is about two times larger in the case of the FPC system. The relative insensitivity of the ETC collector to high operating temperatures leads to a considerable production of excess heat, when the storage volume is not sufficient.

4.5.2 Retrofit System Type B

4.5.2.0 Variation of Preheat-Storage Parameters

The Reference system **B1** is characterized by a 2000 litre storage tank with a compact, 950 W/K heat exchanger located in the lower storage part. The collector pump operates at radiation levels higher than a threshold value of 100 W/m^2 and stops 10 minutes after the radiation has fallen below it. The mass flow rate in the solar loop is about 1700 litres/hour.

System **B2** is essentially identical to system **B1** and differs only in the pump control radiation threhold value, which was reduced to 50 W/m^2 in order to investigate the sensitivity of the COP on pump control.

In systems **B3** and **B4** the specific exchange rate of the heat exchanger was reduced to 50% of the reference case (i.e. 425 W/K); in system **B3** an additional 50% reduction of the solar loop flow rate was made.

In systems **B5** and **B6** a *double-shell*-type heat exchanger, which uses the cylindrical part of the storage tank as heat exchange surface, was used instead of a compact boiler tube type exchanger. Because of its vertical extension, such a heat exchanger may destroy the stratified storge temperature profile to a certain degree. The position of the temperature sensor inside the storage was placed at the lower storage part in system **B5** and in the centre of the heat exchanger in system **B6**.

4.5.2.1 Results of Sensitivity Analysis for System B

Figure 4.5.9 shows for the *Retrofit*-type system **B** the output of the collector array, Q112 and the input into the preheat-storage, Q200 both for the ETC and FPC systems.

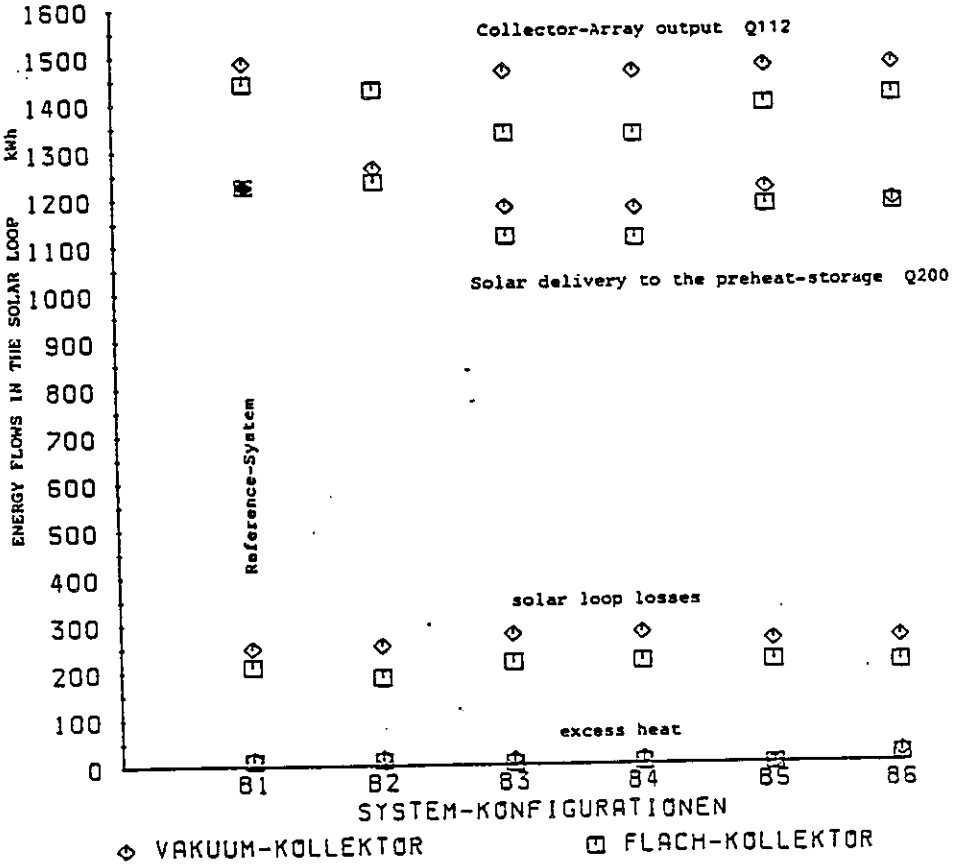

Figure 4.5.9 - Solar Loop Analysis for the "Retrofit-Type" System

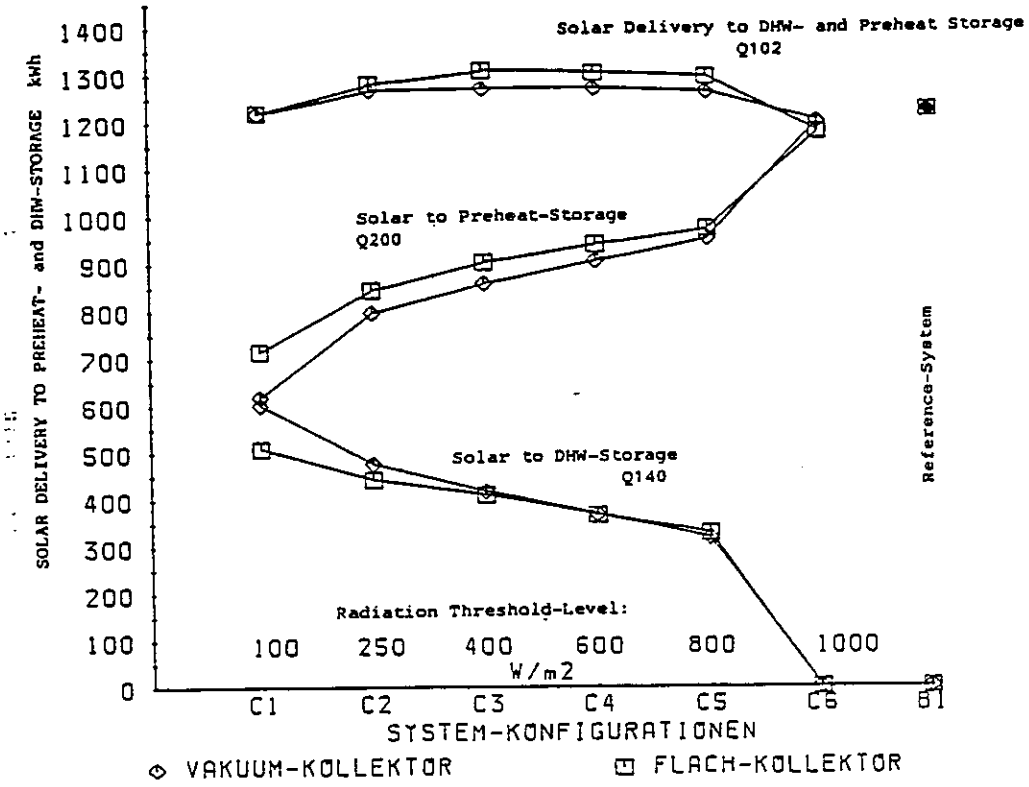

Figure 4.5.10 - Analysis of the "Two-Storage-Tank" - System Type "C"

The performance of the reference system **B1** has already been discussed in Section 4.5.0 together with the characteristics of the different collectors. During the 31-day analysis period, a total of 4406 MJ has been delivered by each of the collector loops to the preheat storage, corresponding to an effective ETC system efficiency of 40% and a FPC system efficiency of 20.4%.

The reduction of the radiation threshold-level of the collector pump control to 50 W/m^2 caused both collector types to operate 40% longer than in system **B1** with a threshold-level of 100 W/m^2; the additional 18.5 kWh pumping energy required reduced the COP of FPC system to 17.4, and that of ETC system to 17.8 as compared to the reference COP of 23.5 for both collectors. This shows that both collector types react in a different way: the FPC-collector module output was reduced by 1%; the output of the ETC modules was increased by 2.8%; the storage input was increased by 0.6% for the FPC system, and by 3% for the ETC system. Electric auxiliary energy was reduced by 30 kWh in the case of the ETC system, and by 6 kWh in the case of the FPC system. Adding up the total amount of electric energy, the ETC system needs 12 kWh less electric energy and the FPC system requires 13 kWh more electric energy as compared to the reference system. Although the change of the pump-control parameter results in a rather small difference of the electric energy requirement, the analysis shows that solar loop control decisions must be taken with respect to the collector performance parameters.

The operation of systems **B3** and **B4** with the heat exchange rate reduced by 50% results in higher system temperatures; the module output of the FPC is reduced by -8%, the output of the ETC modules is reduced by 1.5%; because of higher piping losses, the storage input of the ETC system is further reduced to -3.5%. The auxiliary energy of the FPC system is increased by 14%, but is only increased by 7% in the ETC system.

The system **B5** and **B6** with a double-shell heat exchanger operate less efficiently than the reference system **B1**; auxiliary energy consumption is increased in the FPC system by 7% (sensor low) and 3% (sensor in the centre); the ETC system requires 2% and 1% more auxiliary energy respectively. Thus, the sensor position in the centre of the heat exchanger is less disadvantageous.

4.5.2.2 Conclusions for System B

The investigated design variations of the *Retrofit* systems tend to simplify the overall system design. All simplifications result in a higher average solar loop temperature, which causes both ETC and FPC systems to operate with reduced efficiency. However, the reduction of the FPC system performance in all the systems is about twice as high as in the case of the ETC system.

4.5.3 TWO-Storage Tank System Type C

4.5.3.0 Radiation-dependent Charging of the Preheat- and DHW-Storage

The basic goal of the Two-Storage Tank system type is the separation of solar energy utilization with respect to low-temperature and higher-temperature levels. One way of realizing this separation, as investigated experimentally in the SOLARHAUS FREIBURG DHW-System is by means of the radiation-dependent two-storage tank control strategy; however, the stochastical nature of the climate and the non-reproducibility of the warm water consumption made an accurate comparison of different experimental periods impossible.

The concept was that useful solar energy originating from *low-level radiation* was delivered to the preheat-storage, whereas solar energy from *high-level radiation* was delivered into the DHW-storage until it reached its maximum temperature. Thus, the total available radiation is separated by a radiation-threshold value.

In order to analyze the performance of the Two-Storage-Tank System C under operation with the appropriate radiation-control-strategy, it was simulated for the representative climate and load period. The sensitivity analysis included the following radiation-threshold values: 100, 250, 400, 600, 800, to 1000 W/m^2.

Figure 4.5.10 shows the total solar energy delivery to the two storage tanks, Q102 which is subdivided into the energy flow to the preheat storage, Q200 and the energy flow to the DHW storage, Q140. At a radiation threshold level of 100 W/m^2, solar delivery to the DHW storage is of highest priority until this storage reaches its maximum temperature of 60°C. On the other hand, at a radiation-threshold level of 1000 W/m^2, solar energy is delivered only to the preheat storage.

4.5.3.1 Results of Sensitivity Analysis for System C

The solar energy flows in Figure 4.5.10 show a broad optimum of solar energy delivery to the storage tanks with a maximum at a radiation-threshold value of about 400 W/m^2. Near the maximum, (System C3), the total solar input into the storages for the FPC system is 7%, and for ETC system 4% greater than for the reference system **B1**. As compared to the reference system **B1**, the solar fraction is increased by 8% for FPC and by 6% for ETC systems. Thus, two-storage control strategy results in a performance improvement, which is slightly greater in the case of the FPC system. The reason for this behaviour is the two-storage control strategy, which promotes better utilization of solar energy at an appropriate temperature. This leads to a more frequent replacement of electric auxiliary energy by solar energy as well as better operation of the preheat storage tank. The average operating temperatures of the storages, and therefore also

the solar loop, are reduced. This result has been proven by the numerical simulations, which showed a reduction of the piping losses of 14%, or a contribution to the storage input of 2.5 - 3%. Furthermore, the calculations show an increase in collector efficiency of 4% for the FPC collector and of 1% for the ETC collector, which is another indication of the reduction of the solar loop temperature.

4.5.3.2 Conclusions for System C

The analysis of the two-storage system operating with a highly sophisticated control strategy leads to an increase in FPC system efficiency of 11% and an 8% increase in ETC system efficiency. The overall improvement in system performance is nevertheless relatively small, especially if it is related to the additional complexity and investment required for this type of installation. However, if the required storage capacity must be subdivided in several units, there might be some justification for a radiation-dependent storage control.

4.5.4 Conclusions for the Three Systems

In order to compare the performance of the 16 different systems, their solar fractions normalized to the value of the reference system **B1**, which is set to 100, are shown in Figure 4.5.11.

First, it has to be pointed out that DHW systems with ETC collectors operate in Central European climate with system efficiences about two times as high as standard flat plate collectors (see also [5.1]). Further it has been demonstrated that improvement due to sophisticated control strategies for DHW sytems (radiation-dependent control with hot water and preheat storage tanks, configuration type C) is relatively small as compared with the simpler system Types A and B, especially if the associated investment costs are considered.

A comparison of configuration type A and B both with storage volumes of 250ℓ shows that type A systems have higher solar fractions with the same values of used solar energy used; the difference is explained by the reduction of storage losses. If the storage size is reduced, ETC systems show a much less pronounced decrease of solar fraction than the FPC collector systems. The same tendency is observed with less efficient or reduced heat exchangers.

Generally, DHW systems with ETC are less sensitive to simplifications in system configuration and control strategy than those with conventional FPC. In larger systems, (e.g., for industrial process heat generation) control problems have to be further analyzed, especially if load profiles may be adapted to the solar energy delivery. The analysis shows that system simplications may be realized with minor reductions in efficiency, thus improving the overall cost effectiveness and reliability of solar installations.

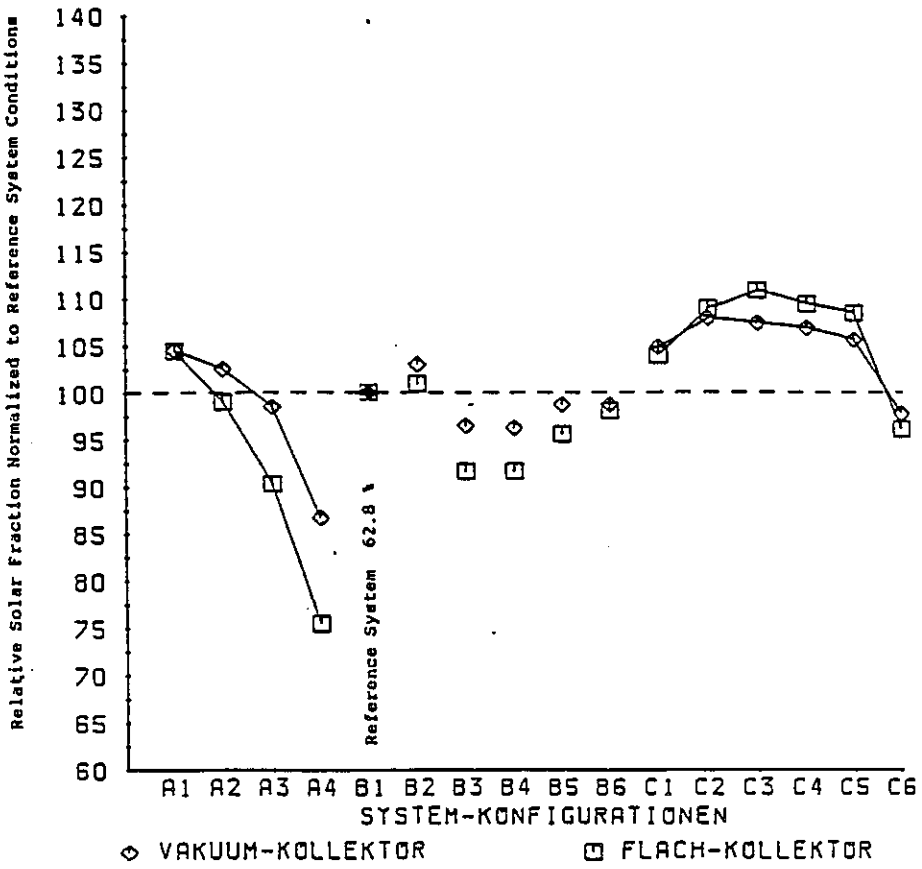

Figure 4.5.11 - Normalized Solar Fraction of investigated Systems

5.0 General Conclusions

The detailed models described in this report have been shown to perform well within the expected limits of prediction accuracy. Perfect agreement with measured results is not possible due to a variety of factors including measurement error and approximations in characterizing the driving functions and the physical behaviour of a given system. The important consideration here is the level of confidence which can be applied to the simulation results when no independent confirmation is available and the validation studies have shown that in all cases predictions within 5 to 10% of measured energy flows can be expected. Those models which also compared temperature profiles illustrate graphically how well a detailed model can perform.

Three methods of solution were used for the models. The Australian and Canadian models were quasi-steady state with sequentially computed values whereas the Netherlands and West Germany solved differential equations using numerical integration methods. The U.S.A. employed a novel approach using analytical solutions to the differential equations. Although models based on differential equations seem to provide somewhat better accuracy by accounting for transients, all of the models performed well.

The results of the sensitivity studies were sometimes as expected, giving confirmation to and quantifying the underlying theory which is an effective means of promoting better utilization of available resources. For example, it is well known that loss of tank stratification impairs system performance, but to see this effect operating under a variety of conditions is to come to grips with the problem and begin to offer concrete methods for dealing with it. The ability to test a hypothesis using a detailed simulation gives the analyst quick and effective means of discarding, implementing or improving it. The sensitivity studies in this report offer several instances in which a proposed improvement was found to be unattractive or in which valuable insights were gained by unexpectedly poor results.

There seems to be no consensus as to what the ideal detailed model should incorporate or indeed if any detailed model could constitute an ideal. The priorities of the individual members have largely dictated the direction of development. With Australia for instance, the focus of research was on collector behaviour so there was no need to create a general purpose simulation program. The Netherlands on the other hand found that only the specialized software associated with stratified storage needed to be developed since this could be used with an existing simulation program. The Canadian situation is very similar in as much as WATSUN was developed some time ago and components are added to it or changed as required for the particular system being considered. West Germany developed its own program based on existing methods and structured the program strictly as a model of Solarhaus Freiburg and intended only for research of that facility. It is not clear how easily or how thoroughly it could be adapted for other systems

or what parts of the program are transportable.

The American DAYSIM program is a radical departure from traditional simulation methods and is designed to provide very fast execution times. The functional representation of driving forces may be a drawback in some applications but the basic approach is attractive and promising. If it can be developed as a general simulation tool with broad capabilities, it may well be the wave of the future.

It would seem that currently, prospective users of detailed simulation models for energy systems are not sufficiently aware of the uses to which these models can be put. In addition to the studies given in this report which are largely research oriented, detailed simulations can be used for diagnoses of system operation and detection of data acquisition and control faults. This trouble-shooting and maintenance role has been either unknown or largely ignored. The most important roles, however, remain in the field of sizing and designing/optimizing of systems where simplified methods have not as yet been adequate and possibly never will be.

Assuming that potential users of detailed simulation programs can be convinced of their value, it still remains to provide them with suitable tools. The criterion should be; ease of use, which implies a minimum of programming and simple problem set-up for a broad variety of systems; implementation on a micro-computer, which will require a relatively small program size and fast execution times; provision of a data base for standard component parameters and weather data for a variety of climates; complete and meaningful simulation statistics including temperatures, energy flows and performance indicators and; a reasonable cost for the entire package.

If an when the above is accomplished and potential users informed, the detailed simulation should become more widely accepted as a beneficial tool.

Appendix A

The flow adjustment factor $\beta(0<\beta<1)$ is applied to the mass flow rate of fluid passing through the collectors in order to increase the simulated collector outlet temperature for a given rate of energy collection, Q_c. The method is valid for systems in which the collector mass flow rate is high relative to the mass of fluid in the collector loop (MC_p) so that fluid may pass through the collectors several times in the interval chosen for a single simulation time step.

In the derivation we will assume that the energy collected over an interval Δt is given by

$$Q_c = \Delta t\,[AI - B\,(T_i - T_a)] \tag{A.1}$$

which is simply the Hottel-Whillier-Bliss equation. At the end of the interval the new collector outlet temperature is

$$T_o^+ = T_i + Q_c/\beta\,\dot{m}\,C_p \tag{A.2}$$

and β is included since we are assuming that a given fluid element has passed through the collectors several times during the interval (over which the radiation, I and ambient temperature, T_a are assumed constant).

Some fraction, α of the collected energy is extracted via a heat exchanger and this is given by

$$\alpha Q_c = \Delta t\,[E\dot{m}C_p(T_0 - T_s)] \tag{A.3}$$

where E and T_s are exchanger effectiveness and cold inlet temperature (constant over Δt). The exchanger hot outlet temperature is the new collector inlet temperature given by

$$T_i^+ = T_o - \alpha Q_c/\dot{m}C_p \tag{A.4}$$

The energy change in the collector loop fluid is

$$\begin{aligned}\Delta T/\Delta t &= [(T_o^+ - T_o) + (T_i^+ - T_i)]/2\Delta t \\ &= (1-\alpha)Q_c/MC_p\end{aligned} \tag{A.5}$$

Substituting (A.2) and (A.4) into (A.5) gives

$$MC_p\,[(1/\beta) - \alpha] = \dot{m}C_p\,(1-\alpha)2\Delta t$$

or

$$\beta = MC_p/[MC_p + \dot{m}C_p(1-\alpha)2\Delta t] \tag{A.6}$$

where

$$\alpha = E\dot{m}C_p(T_0 - T_s)/[A\,1 - B\,(T_i - T_a)]$$

Obviously, β is constant only for constant α which is true for small Δt or where T_s changes slowly. A more comprehensive derivation incorporating changes in T_s and a loadside MC_p and $\dot{m}C_p$ is possible but this will be left to the reader.

Appendix B
Basic Component Equations

Collector

For a collector characterized by $F_R U_L$ and $F_R(\tau\alpha)$, the Hottel-Whillier-Bliss equation may be used.

$$Q_u = A_c F_R [H_T(\tau\alpha) - U_L(T_i - T_a)] \tag{B.1}$$

A corrected heat removal factor F_R' may be used to modify Equation (B.1) to account for the heat exchanger.

$$F_R' = F_R \left[1 + \left[\frac{F_R U_L A_c}{(\dot{m}C_p)_c} \right] \left[\frac{(\dot{m}C_p)_c}{\varepsilon_c (\dot{m}C_p)_{\min}} - 1 \right] \right]^{-1} \tag{B.2}$$

and $Q_{u_c} = A_c F_R' [H_T(\tau\alpha) - U_L (T_s - T_a)]$. Pipe losses are assumd to occur only outside the house, and are calculated on the basis of an average fluid temperature.

$$T_{av} = \frac{T_0 + T_s}{2} \tag{B.3}$$

$$\text{Pipe losses} = (UA)_{\text{pipe}}(T_{av} - T_a). \tag{B.4}$$

Combining equations (B.1), (B.2) and (B.4) gives energy collected that is delivered to the tank.

$$Q_u = A_c F_R' [H_T(\tau\alpha) - U_L(T_s - T_a)] - \text{pipe losses} \tag{B.5}$$

If the conductance between the absorber plate and fluid is not a constant, then this ΔT is given by

$$\Delta T_{a-f} = I_T / G_1$$

where G_1 is input for each particular collector. $(W/m^2 \cdot K)$ and I_T is irrandiance (W/m^2). The temperature from which collector losses occur is then modified.

Storage Tank

Calculation of storage tank temperature depends on the mode of operation of the heating and cooling systems, and on whether the collector is on or off. The storage is currently a single fully-mixed tank. Losses occur to the conditioned space and are based on a UA factor input by the user.

$$\text{storage losses} = (UA)_s(T_s - T_r) \tag{B.6}$$

For space heating, when these storage losses are greater than the load from the building, no heating is required and

$$\frac{dT_s}{dt} = \frac{Q_u - \text{storage losses}}{(MC_p)_s} \tag{B.7}$$

Q_u will be zero in Equation (B.7) when the collector is off.

When space heating is required, since losses are assumed to occur inside the conditioned space,

$$\text{load}_{act} = \text{load}_{calc} - \text{storage losses} \tag{B.8}$$

Then

$$\frac{dT_s}{dt} = \frac{Q_u - \text{load}_{act}}{(MC_p)_s}$$

Again, $Q_u = 0$ when the collector is off.

For space cooling, storage tank losses are added to the load.

Method of Solution

The functional form of the variable inputs allows for mathematical solution of the equations over large time steps. In DAYSIM the full set of non-linear differential equations is solved exactly. This approach gives more accuracy than the use of approximations which would simplify the solution. These approximations might include linerization of the storage temperature or weather data over a time-step.

Since load and weather characteristics are in a functional form it is only necessary to calculate T_s from Equation (B.8), then all parameters which determine system performance are specified. In Equation (B.8)

$$Q_u = f(H_T, T_a)$$

H_T and T_a are both in cosine form. When cosine terms and constants are grouped together

$$\frac{dT_s}{dt} + \alpha T_s = \beta + \gamma \cos\left[\frac{\pi}{12}t + \theta\right] \tag{B.9}$$

where α, β, θ, and γ are constants. This may be solved directly as

$$T_{s.} = T_s + B_s \cos\left[\frac{\pi}{12}t + \rho_s\right] + C_s e^{D,t} + E_s t \tag{B.10}$$

where A_s, T_s, C_s, D_s and E_s are all constants.

Since the initial form of the equation changes with each time-step, Q_u, storage withdrawal, storage losses, and storage temperature expressions must change also. These changes determine the beginning of a new time-step with a new equation for the storage temperature. Thus time-steps are determined by the following events: DHW withdrawal, collector pump turn on and off, end or beginning of a load period, or a switch from solar to auxiliary or auxiliary to solar. All events except DHW withdrawal must be calculated.

In determining collector pump turn-on time, first the average fluid temperature in the collector loop, T_c, is determined.

$$M_c C_{p_c} = \frac{dT_c}{dt} = A F_R \left[H_T(t) \cdot (\tau\alpha) - U_L(T_c - T_a(t))\right] \tag{B.11}$$

The collector will turn on when

$$T_c = T_s + \Delta T_c, \text{ on} \tag{B.12}$$

where ΔT_c, is input by the user.

The collector will turn off when $Q_u = 0$.

$$H_T(t) \cdot (\tau\alpha) - U_L(T_s - T_a) - \text{pipe losses} = 0 \tag{B.13}$$

A change from solar to auxiliary or auxiliary to solar usage will occur when the storage temperature reaches a control reference temperature $T_{s,\text{ref}}$. $T_{s,\text{ref}}$ is input by the user and may be different when switching from solar to auxiliary than when switching from auxiliary to solar. Care should be taken in choosing the reference temperatures. The dead band should be large enough to avoid cycling.

The need for heating or cooling will change if the value of load_{act} (Equation (B.8)) changes sign.

The equations for collector pumb turn-on time, change in heating mode, and change in load are all of the form.

$$A + B\cos\left[\frac{\pi}{12}t + \rho\right] + Ce^{DT} + Et = 0 \qquad \text{(B.14)}$$

These are solved using the second order Newton's method.

Once the beginning and the end of the various time steps are determined, energy flows may be directly integrated over the time periods and accumulated over the day.

$$\int_{H_1}^{H_2} \text{load}_{act}\, dt \qquad \text{for heating}$$

$$\int_{H_1}^{H_2} \text{load}_{act}/COP\ dt \quad \text{for cooling}$$

Energy collected:

$$Q_u = \int_{H_1}^{H_2} \left[A_c F_R'(H_T(t)\cdot(\tau\alpha) - U_L(T_s(t) - T_a(t)) - \text{pipeloss}\right]dt$$

Tank Losses:

$$\text{storage losses} = \int_{H_1}^{H_2} (UA)_s(T_s - T_r)dt$$

and so on for the other energies.

These energies are accumulated daily, monthly, and over the entire simulation period, and results for any of these products may be easily obtained.

Nomenclature for Appendix B

Variables

A	area
COP	coefficient of performance
C_p	specific heat
F	collector heat removal factor
$F_R^{'}$	modified heat removal factor
H_1	time at beginning of time-step
H_2	time at end of time-step
H_T	total radiation per unit are on the collector surface
M	mass
m	mass flow rate
Q_u	rate of energy gain
T	temperature
t	time
UA	loss coefficient to surroundings
U_L	collector heat transfer coefficient for losses from the plate
ε	efficiency
$(\tau\alpha)$	transmittance-absorptance product

Subscripts

a	ambient
act	actual
av	average
c	collector
$calc$	calculated
i	inlet fluid
min	minimum
o	outlet fluid
r	room
s	storage

References

1. Australia

[1] W. S. Duff et al, Experimental Results from Eleven Evacuated Collector Installations, IEA Report No. IEA-SHAC-TV1-4, Colorado State University (Nov. 1986).

[2] G. L. Hardin and T. T. Moon, Calorimetric Measurement of the Absorptance and Emittance of the Sydney University Evacuated Collector, *Solar Energy*, Vol. 26, pp. 281-285 (1981).

[3] S. P. Chow et al, Effect of Collector Components on the Collection Efficiency of Tubular Evacuated Collectors with Diffuse Reflectors, *Solar Energy*, Vol. 32, pp. 251-262 (1984).

[4] Window, B., Zybert, J., Optical Collection Efficiencies of Arrays of Tubular Collectors with Diffuse Reflectors, *Solar Energy*, Vol. 26, pp. 325-331 (1981).

[5] G. L. Harding, et al, Heat Extraction Efficiency of a Concentric Glass Tubular Evacuated Collector, *Solar Energy*, Vol. 35, No. 1 (1985).

[6] S. Harrison, Address given at IEA Task VI meeting, Studsvik, Sweden (September 1984).

[7] O. Guisan, A. Mermoud, B. Lachal and O. Rudaz, Characterization of Evacuated Collectors, Arrays and Collection Subsystems, IEA-SHAC-TVI-3, June 1986.

2. Canada

[1] WATSUN User Service, University of Waterloo, Waterloo, Ontario, Canada, N2l, 3G1.

[2] M. Chandrashekar, N. T. Le, H. F. Sullivan, K. G. T. Hollands, A Comparative study of solar assisted heat pump systems for Canadian locations, *Solar Energy*, Vol. 28, pp. 217-226, 1982.

[3] W. S. Duff et al, Experimental Results from Eleven Evacuated Collector Installations, IEA Report No. IEA-SHAC-TV1-4, Colorado State University (Nov. 1986).

[4] TRNSYS version 11.1, Users Manual, University of Wisconsin, Madison, Wisconsin.

[5] J. A. Duffie and W. A. Beckman, Solar Engineering of Thermal Processes, Wylie & Sons, 1980, page 85.

3. Netherlands

[1] Veltkamp, W. B., van Koppen, C. W. J., (1981). Optimisation of the mass flow in the heat distribution circuit of a solar heating system with a stratified storage. In D.O. Hall (Ed.,), *Solar World Forum.* Pergamon, Oxford, Vol. 2, Chap. 2, pp. 286-290.

[2] Veltkamp, W. B., van Koppen, C. W. J., (1982). *Optimisation of the flows in a solar energy system.* Report Eindhoven University of Technology, WPS3-82.09 R335.

[3] Klein, S. A., Fanney, A. H. (1985). Thermal performance comparisons for solar hot water systems subjected to various collector array flow rates. In Proceedings ISES Congress Montreal, Pergamon (to be published shortly).

[4] Morrison, G. L., Braun, J. E. (1985). System modelling and opertion characterisitcs of thermoshyphon solar water heaters. *Solar Energy*, 34, 389-405.

[5] Veltkamp, W. B., van Koppen, C. W. J., (1983). A two level simulation model for combined active and passive solar space heating, S. V. Szokolay (Ed.), *Solar World Congress,* Pergamon, Oxford, Vol. 2, part II, pp. 939-943.

4. U.S.A.

[1] *TRNSYS, A Transient System Simulation Program*, Engineering Experiment Station Report 38, Solar Energy Laboratory, University of Wisconsin-Madison, June 1979.

[2] Monaghan, P. F., *Efficient Analysis of Long-Term Performance of Solar Heating Systems,* Proceedings of NELP/UNESCO International Solar Building Technology Conference, London, 1976.

[3] Bruno, R. and Kersten, R., *Models for the Analysis of Solar Energy System,* AIM Conference on Solar Heating of Buildins, Liege, Belgium, 1977.

[4] Bruno, R., *Weather Data Compression,* Publikation Nr. 10/76, philips GmbH Forschungslaboratorium Aachen, July 1976.

[5] Haslet, J. and Monaghan, P., *Mathematical Modelling of the Use of Solar Energy in Buildings*, Operations Research Laboratory, Trinity College, Dublin, November 1977.

[6] DenBraven, K. R., Duff, W. S., and Favard, G. J., *An Event Time Simulation of Residential Solar Heating*, Proceedings of Energex '82, The Solar Energy Society of Canada, Inc., Regina, Saskatchewan, August 1982.

5. West Germany

[1] Schreitmüller, Vanoli, Solarhouse Freiburg: *Performance and Limitations of Evacuated Tubular Collectors in Domestic Hot Water Spce Heating Systems within Central Europe*, ISES Solar World Forum, Perth 1983.

[2] Turrent, et al., *Solar Water Heating, An analysis of design and performance date from 28 systems*, Commission of the European Communities, ES-A-P009-UK(N), December 1981.

[3] Peuser et al, *General Experience from the Measurementsof Solar Systems within the Future Investment Program*, Proc. 5 Int. Solar Forum, DGS, Berlin 1984.

[4] Schreitmüller, Vanoli, *Modelling the SOLARHAUS FREIBURG DHW-System*, Proc. IEA Task VI Meeting, Kobe Japan, Dec. 80.

[5] Vanoli, Schreitmüller, Solarhaus Freiburg: Performance of Evacuated Tubular Solar Collectors in DHW and Heating Systems. Proc. IEA Task VI Meeting, Kobe Japan, Dec. 80.

[6] Vanoli, Schreitmüller, Systems Design and Experimental Perforamance of Two Types of Evacuated Tubular Solar Collectors in Residential DHW and HTG Systems. 1st Energietechnik GmbH, May 1982.